Technische Universität München

Lehrstuhl für Energiesysteme

CO_2 separation by calcium looping from full and partial fuel oxidation processes

Senthoorselvan Sivalingam

Vollständiger Abdruck der von der Fakultät für Maschinenwesen der Technischen Universität München zur Erlangung des akademischen Grades eines

Doktor-Ingenieurs

genehmigten Dissertation.

Vorsitzender: Univ.-Prof. Wolfgang Polifke, Ph.D.

Prüfer der Dissertation:

1. Univ.-Prof. Dr.-Ing. Hartmut Spliethoff
2. Univ.-Prof. Dr. techn. Günter Scheffknecht, Universität Stuttgart

Die Dissertation wurde am 12.11.2012 bei der Technischen Universität München eingereicht und durch die Fakultät für Maschinenwesen am 05.06.2013 angenommen.

Summary

This thesis work deals with the research & development of calcium looping process for CO_2 separation from full and partial fuel oxidation based power generation systems.

CO_2 is the main greenhouse gas and undoubtedly a major contributor to the global warming. It is estimated that more than one third of the total anthropogenic CO_2 emissions come from fossil fuel based heat and power generation. Moreover, fossil fuels are unlikely to be phased out rapidly, since developing alternative energy sources not only take time but also require huge investments and infrastructure. An alternative way to reduce emissions in a medium term is to capture the CO_2 from fossil fueled power plants and store it away from the atmosphere. This process system combining a bunch of technologies is called carbon capture and storage (CCS). CO_2 capture is an important & costly part of CCS and an array of technologies is considered for this. Calcium looping (CaL) is one of such and seems to offer effective and efficient CO_2 separation from fuel oxidation processes.

CaL process involves separation of CO_2 at high temperatures (600-700°C) by calcium sorbents (CaO). CO_2 reacts with CaO in a carbonation process and produces $CaCO_3$. In a subsequent thermal regeneration (>850°C) called calcination, the CO_2 is released from $CaCO_3$. By alternating carbonations and calcinations over multiple cycles, CO_2 is separated from a gas stream. Moreover, the CaL is realised in industrial scale with dual fluidised bed reactors for CO_2 capture (the carbonator) and sorbent regeneration (the calciner). As a process in the development, research is still required in many aspects from thermodynamic modeling to experimental studies. Research works have been carried out in process simulations, sorbent reactivity & optimisation studies in a controlled reactor environment and process parametric studies in a semi-pilot scale CaL test facility.

ASPEN Plus power plant simulations integrating the CaL based CO_2 capture processes were performed and compared with other important competing CO_2 capture technologies. The efficiency penalties for CaL looping are less than that of the Amine based process, oxyfuel process and IGCC.

Sorbent reactivity studies were the main focus of this work. A wide range of sorbent samples have been studied in several experimental setups. Sorbents decay coefficients and the carbonation and calcination reaction rate coefficients were determined and compared for each of the samples. Experiments have been performed to identify the CaL process parameters that influence the sorbent deactivation. For a given sorbent with a particular number of carbonation and calcination reactions(CCR) cycles, it was found that the calcination temperature is the parameter that directly affects the reactivity. Moreover, the

higher the calcination temperature the higher is the sorbent decay. In an effort to minimise the sorbent decay, a calciner design was proposed to lower the calciner temperature.

A parametric study has been carried out at a semi pilot scale dual fluidised bed(DFB) CaL test facility that belongs to the Institut für Feuerungs- und Kraftwerkstechnik(IFK), at the Universität Stuttgart. A crucial parameter which defines the CO_2 capture efficiency of a particular CaL reactor system was determined by analysing the sorbent samples in a Thermogravimetric Analyser(TGA), collected at steady state operation. A specific TGA experimental procedure was applied for this parametric study. In a separate study, reactivities of DFB samples and fresh ones were analysed in a TGA and compared. A successful method has been tested to substantially restore the lost CO_2 capture capacity of spent sorbents from this test facility. Based on the experimental results, a partial hydration of sorbent stream was proposed to sustain the reactivity of the carbonator. Further TGA studies on simultaneous carbonation and sulfation have been performed to optimise the CO_2 capture in presence of SO_2. Carbonation to sulfation ratio was compared against the residence time and it provided clear indication to minimise the adverse effect of sulfation on CO_2 separation.

Moreover, pressurised TGA experiments in the context of CaL for partial oxidation processes have been carried out with synthetic syngas. Sorbent behavior under varying temperatures and CO_2 concentrations have been studied. Under these conditions, neither the reducing atmosphere nor the presence of H_2 and CH_4 have a negative influence on the reactivity of CO_2 and CaO. In a separate study, sorbent decay due to high temperature sintering have been experimentally determined & discussed. Further on, incomplete(partial) carbonation experiments showed improved sorbent reactivity with number of CCR cycles when compared to that of the same number of complete CCR cycles.

Zusammenfassung

Im Rahmen dieser Doktorarbeit wird die Forschung und Entwicklung von Calcium Looping Verfahren zur CO_2-Abtrennung aus vollständigen und teilweise oxidierten Brennstoffen in Kraftwerksprozessen behandelt.

CO_2 ist das wichtigste Treibhausgas und zweifellos ein wesentlicher Faktor für die globale Erderwärmung. Es wird geschätzt, dass mehr als ein Drittel der gesamten anthropogenen CO_2-Emissionen aus auf fossilen Brennstoffen basierender Wärme-und Stromerzeugung kommen. Zudem ist unwahrscheinlich, dass fossile Brennstoffe in naher Zukunft ersetzt werden können, da die Entwicklung alternativer Energiequellen nicht nur Zeit, sondern auch enorme Investitionen und neue Infrastruktur erfordern. Ein alternativer Weg, um die Emissionen in einem mittelfristigen Rahmen zu reduzieren, ist, CO_2 in fossil befeuerten Kraftwerken abzuscheiden, zu speichern und nicht in die Atmosphäre gelangen zu lassen. Die hierfür notwendige Prozesskette kombiniert eine Reihe von Technologien und wird Carbon Capture and Storage(CCS) genannt. Die CO_2-Abscheidung ist ein wichtiger und kostspieliger Teil von CCS und eine Reihe von Technologien kommt hierfür in Betracht. Calcium Looping(CAL) ist ein solcher und scheint eine effektive und effiziente CO_2-Abtrennung aus Verbrennungsprozessen zu ermöglichen.

Der CaL-Prozess umfasst die Abtrennung von CO_2 bei hohen Temperaturen (600-700°C) durch Kalzium-haltige Sorbentien (CaO). CO_2 reagiert mit CaO in einem Karbonisierungsprozess und produziert $CaCO_3$. In einer anschließenden thermischen Regeneration (>850°C), genannt Kalzinierung, wird das CO_2 aus $CaCO_3$ freigesetzt. Durch abwechselnde Karbonisierung und Kalzinierung über mehrere Zyklen wird CO_2 aus einem Gasstrom getrennt. Darüber hinaus wird CaL im industriellen Maßstab mit Hilfe von Zwillings-Wirbelschichtreaktoren zur CO_2-Abscheidung (Karbonator) und zur Sorbensregeneration (Kalzinator) realisiert. Da es sich um ein noch in der Entwicklung befindliches Verfahren handelt, ist noch Forschung hinsichtlich vieler Aspekte, von thermodynamischer Modellierung bis hin zu experimentelle Studien erforderlich. Forschungsarbeiten wurden im Bereich Prozess-Simulationen, Sorbensreaktivität und -optimierung, sowie in Laborversuchen durchgeführt. Zudem wurden bereits verfahrenstechnische Fragestellungen anhand einer kleinen CaL-Pilotanlage untersucht.

Im Rahmen von Systemsimulationen mit ASPEN Plus wurden CaL-basierte CO_2-Abscheidungsverfahren im Kraftwerksmaßstab untersucht und mit anderen wichtigen konkurrierenden Verfahren verglichen. Die inhärenten Effizienzverluste sind bei CaL-Verfahren geringer als bei Verfahren auf Aminbasis, Oxyfuelprozessen und IGCC-Kraftwerken.

Untersuchungen zur Sorbensreaktivität waren der Schwerpunkt dieser Arbeit. Eine

große Zahl von Sorbensproben wurde in verschiedenen Versuchsanordnungen untersucht. Zerfallskoeffizienten der Sorbentien und die Karbonisierungs, sowie Kalzinierungsraten wurden für jede der Proben bestimmt und verglichen. Es wurden Versuche durchgeführt, um die CaL-Prozessparameter, die die Sorbensdeaktivierung beeinflussen zu identifizieren. Für ein gegebenes Sorbens mit einer bestimmten Anzahl von Karbonisierungs- und Kalzinierungszyklen(CCR), wurde herausgefunden, dass die Kalzinierungstemperatur der entscheidende Parameter ist, der direkten Einfluss auf die Reaktivität hat. Außerdem nimmt die Geschwindigkeit des Sorbenszerfalls mit steigender Kalzinierungstemperatur zu. In dem Bemühen zur Minimierung des Sorbenszerfalls wurde ein alternatives Kalzinatordesign vorgeschlagen, um die Kalzinatortemperatur zu senken.

Eine parametrische Studie wurde an einer kleinen Zwillings-Wirbelschicht Pilotanlage (DFB) am Institut für Feuerungs-und Kraftwerkstechnik (IFK) der Universität Stuttgart durchgeführt. Ein für den CO_2-Abscheidegrad eines CaL Reaktorsystem entscheidender Parameter, die aktive Karbonator Raum-Zeit, wurde anhand von thermogravimetrischen Analysen von Sorbensproben bestimmt, die jeweils während des Regelbetriebs entnommen wurden. Eine spezifische TGA experimentelle Verfahren wurde für dieses parametrische Studie angewendet. In einer weiteren Studie wurden die Reaktivitäten von DFB-Proben mit ungenutzten Proben in einer Thermowaage analysiert und verglichen. Basierend auf diesen Ergebnissen wurde eine teilweise Hydrierung des Sorbensstroms vorgeschlagen, um die Reaktivität des Karbonators zu erhalten. Weitere TGA-Untersuchungen der Karbonisierung wurden bei Anwesenheit von SO_2 durchgeführt, um die CO_2-Abscheidung in Gegenwart von SO_2 zu optimieren. Das Karbonisierungs- zu Sulfatisierungsverhältnis wurde in Abhängigkeit der Aufenthaltsdauer verglichen und ergab eine klare Indikation zur Minimierung des Effekts der Sulfatisierung auf die CO_2-Abscheidung.

Weiterhin wurden TGA-Versuche hinsichtlich CaL für partielle Oxidation von synthetischen Prozessgasen unter Druck durchgeführt. Das Verhalten der Sorbentien bei variierenden Temperaturen und CO_2-Konzentrationen wurden dabei untersucht. Unter diesen Bedingungen hatten weder die reduzierende Atmosphäre, noch die Anwesenheit von H_2 und CH_4 einen negativen Einfluss auf die Reaktivität des CO_2 und des CaO. In einer weiteren Studie wurde der Zerfall der Sorbentien aufgrund von Hochtemperatursinterungsprozessen experimentell untersucht und diskutiert. Anschließend zeigten Experimente zur unvollständigen (Teil-)Karbonisierung eine verbesserte Sorbensreaktivität für eine gegebene Anzahl von CCR-Zyklen im Vergleich einer gleichhohen Zahl kompletter Zyklen.

Contents

List of Figures

List of Tables

Nomenclature

Abbreviations

AEGS Absorption Enhanced Gasification of Solids

ASU Air Separation Unit

BET Brunauer Emmett Teller

CaL Calcium Looping

CCR Carbonation Calcination Reaction

CFB Circulating Fluidised Bed

CLC Chemical Looping Combustion

CLP Chemical Looping Process

COP Coefficient of Performance

DFB Dual Fluidised Bed

DM Dolomite

DTA Differential Thermal Analyser

HP High Pressure

HRSG Heat Recovery Steam Generator

IFK Institut für Feuerungs- und Kraftwerkstechnik or Institute of Combustion and Power Plant Technology

IGCC Integrated Gasification Combined Cycle

IP Intermediate Pressure

LEGS Lime Enhanced Gasification of Solids

LES Lehrstuhl für Energiesysteme

LP Low Pressure

LS Limestone

MEA Monoethanolamine

PTGA Pressurized Thermogravimetric Analysis

SCL Syngas Chemical Looping

SEM Scanning Electron Microscopy

SMR Steam Methane Reforming

TGA Thermogravimetric Analysis

wt. Weight

Greek symbols

α fraction of reaction completed at time t $[-]$

ΔH reaction enthalpy $[kJ/reaction]$

λ CaO to $CaCO_3$ conversion $[\% - mol]$

τ Carbonator space time $[h]$

Indices

calc Calcination

carb Carbonation

eq Equilibrium

max maximum

n number of CCR cycles

r reaction order $[-]$

t time $[s]$

Latin symbols

e_0 Sorbent particle porosity

E_{CO_2} CO_2 capture efficiency $[\%]$

F_a Active CaO fraction $[\% - mol]$

F_{Ca} Calcium looping rate between reactors $[mol/h]$

F_{CO_2}	Incoming CO_2 to the carbonator	$[mol/h]$
F_{rest}	Flue gas flow except the CO_2	$[mol/h]$
K_s	Surface carbonation rate constant	$[m^4 mol/s]$
N_{Ca}	Amount of calcium in the carbonator	$[mol]$
S_0	Initial CaO surface area	$[m^2/cm^3]$
k	Coefficient of decay	
F_R	Amount of reactive CaO in a carbonator bed	$[mol]$
K	Reaction rate constant	$[s^{-1}]$
M	Molecular weight	$[g/mol]$
m	weight of the sample	$[mg]$
m$'$	TGA weight signal	$[mg]$
P	Pressure	$[bars]$
Y	Concentration of a gas species	$[mol/m^3]$

Chapter 1

Introduction

Growing global concern over unabated CO_2 emissions exerts pressure on conventional fossil fueled power generation to seek new technologies that mitigate carbon emissions. In this context carbon capture and storage (CCS) technology is considered as a feasible future option that contains CO_2 emissions to the atmosphere. CCS can be implemented in three steps of CO_2 separation, CO_2 transportation and safe CO_2 storage. A large portion of the total CCS cost is associated with the CO_2 separation itself when considering the current industrial separation technologies. However, Calcium looping(CaL) based CO_2 separation offers cost benefits by utilising naturally occurring carbonate sorbents and producing more power from capture components. Furthermore, the CaL system can not only be conveniently retrofitted into existing power plants but also in future power plants with full and partial oxidation reactors. Thus the CaL emerges as one of the promising processes for CO_2 separation from power generation.

Though the CaL process utilises naturally occurring and abundant carbonate sorbents, reducing sorbent reactivity with increasing number of capture and release cycles is a matter of great concern. Apart from that the presence of SO_2 also hinders the reactivity with CO_2. When it comes to the process design, physical attrition of sorbent particles and solids handling between reactors are posing a considerable challenge. However, ongoing research activities on sorbent reactivities and process design help to overcome the challenges and proceed towards pilot scale demonstrations.

1.1 Motivation and scope of the dissertation

Excessive presence of greenhouse gases in the earth atmosphere enhances the natural greenhouse effect and cause global warming. Governments and United Nations Framework Convention on Climate Change (UNCCC) have long been working together to control and reduce the global emissions. As a result, a protocol which set binding targets for 37 industrialised countries and the European community for reducing GHG emissions was adopted in Kyoto, Japan, on 11^{th} December 1997. The required reduction amounts, in average, five per cent of 1990 levels over the five year period between 2008 - 2012. At present, negotiations for a new binding agreement, intended to include the fast developing countries like Brazil, China and India are underway. The resulting agreement will replace

the Kyoto protocol when it expires in 2012. European governments are playing a leading role in GHG emission control by setting their own collective targets. One of the three important EU targets, established by law through an EU directive 2009/28/EC, demands 20% reduction in GHG emission by 2020 against the 1990 levels.

CO_2 is the main greenhouse gas and undoubtedly a major contributor to the global warming. Concentration of CO_2 in the atmosphere increased from 280 ppm of preindustrial era to about 380 ppm today. Unabated usage of fossil fuels for heat and power generation, industrial processes and transportation caused this sharp increase over a short period of time. It is however estimated that the heat and power generation alone contribute to more than one third of the total CO_2 emissions, Quadrelli and Peterson [2007]. On the other hand, the demand for heat and power raises with growing global population and improving living standards especially in developing countries, as such the emissions. Emissions from power generation can be lowered by a range of measures, such as enhancing energy efficiency and utilising alternative non fossil energy sources like solar, wind and nuclear. However, fossil fuels are unlikely to be phased out rapidly, since developing alternative energy sources not only take time but also require huge investments and infrastructure. An alternative way to reduce emissions is to capture the CO_2 from fossil fuel fired power plants and store it away from the atmosphere. As mentioned in the introduction, this scheme is called CCS. Timely implementation of the CCS will allow the use of fossil energy to continue, while providing time to develop alternative energy sources. The importance of CCS in Germany's perspective has been established in a recent work, Martinsen et al. [2007]. It is concluded that a significant contribution of CCS is inevitable to achieve a mitigation goal of 35% reduction against 1990 CO_2 levels in 2030. However it is estimated that more than 75% of the total CCS cost is associated with the CO_2 capture itself, Herzog [2001], Herzog [2011]. There is a need to reduce the CO_2 capture cost from the power generation which triggers the development of a number of technologies.

CO_2 capture technologies can be categorised into post-combustion capture, pre-combustion capture and oxy-fuel capture. Another set of capture technology is chemical looping where the oxygen is supplied through chemical means, i.e. by circulating solid oxygen carriers, making it, in a way, related to the oxy-fuel capture. There are a number of process schemes being developed in each of the categories. Calcium Looping (CaL) process scheme which utilises naturally occurring and abundant calcium sorbents, can be applied to both post and pre combustion CO_2 capture. One of the biggest problem in the CaL process is the diminishing sorbent reactivity with the increasing number of capture and release cycles which would increase the reactor size and the amount of solid handling. Furthermore the sorbent reactivity also depends on a number of parameters such as its geographical origin, calcination temperature & duration, carbonation temperature etc. Apart from that, the presence of SO_2 in the flue gas hinders the CO_2 capture efficiency of the CaL process.

A three way approach namely process modeling, sorbent reactivity & optimisation in a controlled reactor environment and process parametric studies in a pilot scale reactor

would be appropriate to analyse, develop and optimise the CaL process. The scope of this PhD work is to contribute in all three aspects of the CaL process development with more focus on sorbent reactivity and optimisation studies.

1.2 Carbon capture from power generation

Power generation from fossil fuels produces more than one third of the global anthropogenic CO_2 emissions to the atmosphere, Quadrelli and Peterson [2007]. However, in today's context of growing energy demand, mainly driven by the emerging economies, fossil fuels will remain the dominant energy source for the foreseeable future power generation, Spliethoff [2011]. Therefore, the carbon capture from power generation becomes inevitable to prevent the CO_2 from entering into the atmosphere. The purpose of CO_2 capture is to produce a concentrated CO_2 stream at high pressure suitable for transportation and storage. Although, in principle, the entire flue gas stream containing low concentrations of carbon dioxide could be transported and injected underground, energy costs and other associated costs generally make this approach impractical, Spliethoff [2010].

1.2.1 Classification of capture technologies

The CO_2 capture technologies are mainly classified into post-combustion capture, pre-combustion capture and oxy-fuel capture. Figure 1.1 shows the fundamental process steps, including the CO_2 separation, in each classified group of technologies. Chemical looping is another set of emerging technology, in a way relevant to the oxy-fuel capture. The oxygen is supplied by a metal oxide loop rather than an air separation unit. However the two processes are fundamentally different in process design and reaction kinetics.

Post-combustion CO_2 capture

Post-combustion capture refers to the separation of CO_2 from flue gases produced by combustion of carboniferous fuels in air. The concentration of CO_2 in the flue gas lies between 3 - 15-vol%, depending on the fuel. The separation can be performed by following processes: absorption using solvents or solid sorbents, pressure and temperature swing adsorption using various solid sorbents, cryogenic distillation and membranes. At present, most mature and commercially available technologies are based on chemical solvents, especially using monoethanolamine(MEA). These mature technologies can conveniently be retrofitted into existing power plants since the capture unit can be added downstream of the boiler without any significant changes to the original plant, Davison [2007]. However, the demonstrated scale of operation is significantly smaller than the typical size of power plants and severe penalties to the plant efficiency exist. The anticipated drop in the net efficiency of the power plant is about 10-14% points, Toftegaard et al. [2010].

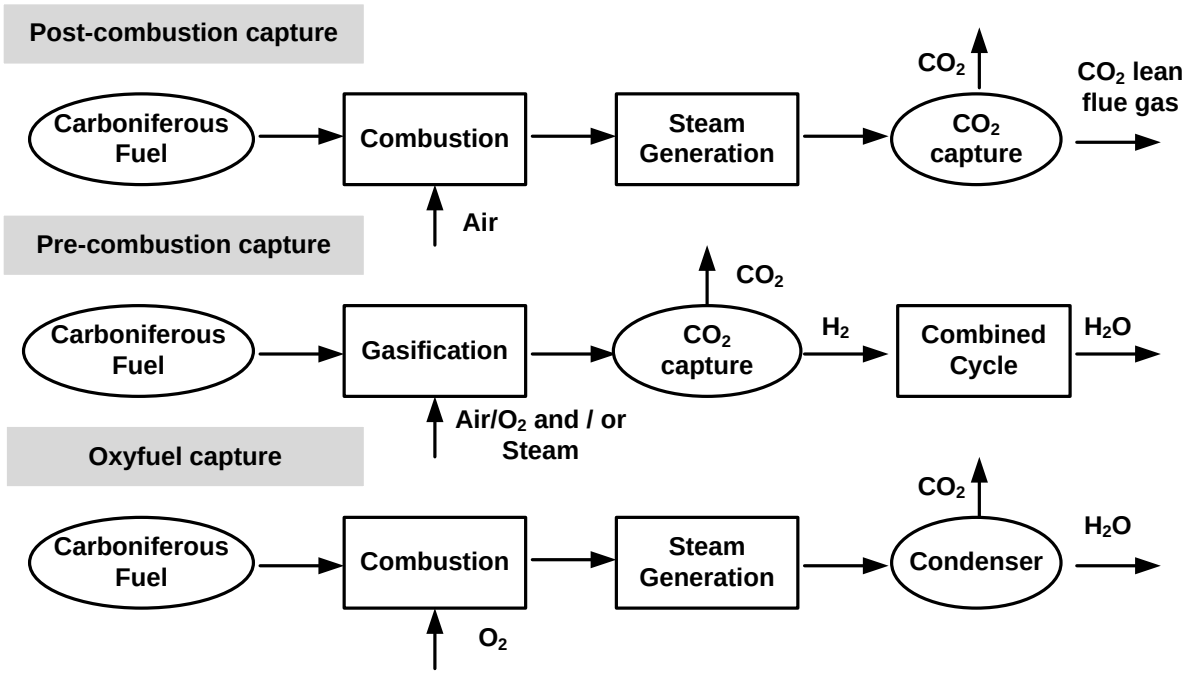

Figure 1.1: Classification of CO_2 capture technologies

Though the cryogenic separation produces high purity liquid CO_2 ready for sequestration, the extremely energy intensive nature of the process makes it ineffective. Membrane separation process is relatively simple. Nevertheless the main drawbacks of the membranes stem from either their poor selectivity or rather low permeability with respect to CO_2, Aaron and Tsouris [2005]. Thus the purity of the CO_2 produced and the capture efficiency are very low compared to other processes. There are many other sorbent based processes in various stages of development and one of them is the CaL.

Pre-combustion CO_2 capture

Pre-combustion CO_2 capture refers to the process of decarbonisation of a carboniferous fuel. It is achieved through partial oxidation of fuel followed by shift-reaction and CO_2 capture prior to the combustion in air. Two primary process technologies included in this category are integrated gasification combined cycle (IGCC) and lime enhanced gasification of solids (LEGS). Another process called steam methane reforming(SMR) is for methane decarbonisation. Techno-economic calculations of IGCC shows promising process economics, however high capital costs and the complicated nature of process are the two main hurdles for fast commercialisation, Damen et al. [2006], Toftegaard et al. [2010], Feron and Hendriks [2005]. On the other hand LEGS can be performed with reduced number of steps because of the in situ CO_2 separation by CaO. Nevertheless it suffers from low CaO reactivity and sorbent deactivation, Weimer et al. [2008] Pfeifer et al. [2007]. Despite this it is reported that a pressurised coal/CaO mixture with high pressure

steam produced about 85-vol% of H_2 in the product gas, Lin et al. [2002].

Oxy-fuel CO_2 capture

It generally refers to the combustion of carboniferous fuel in pure O_2 to produce a flue gas stream mainly composed of CO_2 and steam. A pure CO_2 stream can be obtained after the condensation of steam in the flue gases. The air nitrogen is excluded from the whole combustion process by supplying pure O_2. On the other hand the combustion in pure oxygen drastically increases the flame temperature and reduces the flue gas volume. The reduction in flue gas volume will have a negative impact on the temperature and heat flux profiles of a boiler. Oxy-fuel technology overcomes these problems by recycling the flue gas back into the furnace to reduces the flame temperature and to makeup the volume of the missing N_2. Literally the combustion takes place in O_2 & CO_2 mixture. An additional advantage of this process is that the NO_x emissions are substantially reduced, Buhre et al. [2005] Wall et al. [2009]. However a significant efficiency loss is caused by the cryogenic air separation unit which supplies the O_2. This unit consumes high amounts of energy in the form of electricity. It is reported that this operation alone requires about 60% of the power consumption for carbon capture and reduces the overall efficiency of the oxy-fuel power plant by about 7-9 percentage points, Toftegaard et al. [2010].

Chemical looping based CO_2 capture

It refers to the oxidation of carboniferous fuel by an oxygen carrier instead of directly by air/oxygen. The most investigated oxygen carrier particles are NiO, Fe_2O_3 and Mn_3O_4. This process technology is applicable to combustion (Chemical looping combustion, CLC) as well as gasification (Syngas chemical looping, SCL) and reforming processes. Chemical looping processes (CLP) inherently separate the CO_2 because the air-nitrogen is excluded by circulating the oxygen carriers between air and fuel reactors. This gives a possibility to increase the net power efficiency with carbon capture, Anheden and Svedberg [1998] McGlashan [2008]. CLP for fuel conversion is still in lab scale demonstration stage in many countries around the world. However, with a significant progress being made in oxygen carrier particle design and chemical looping reactor development, CLP can play a significant role in the future for processing carboniferous fuels, Fan [2010].

1.3 Calcium looping process for CO_2 capture

CaL process involves the separation of CO_2 at high temperatures (600-700°C) using carbonation reaction of CaO, according to the reaction equation 1.1. Once the CaO has reached its ultimate conversion to $CaCO_3$ by reacting with the CO_2, it can be thermally regenerated by heating beyond its calcination temperature (>850°C), according to the reaction equation 1.2. Pure CO_2 is released during the regeneration of CaO. The CaL

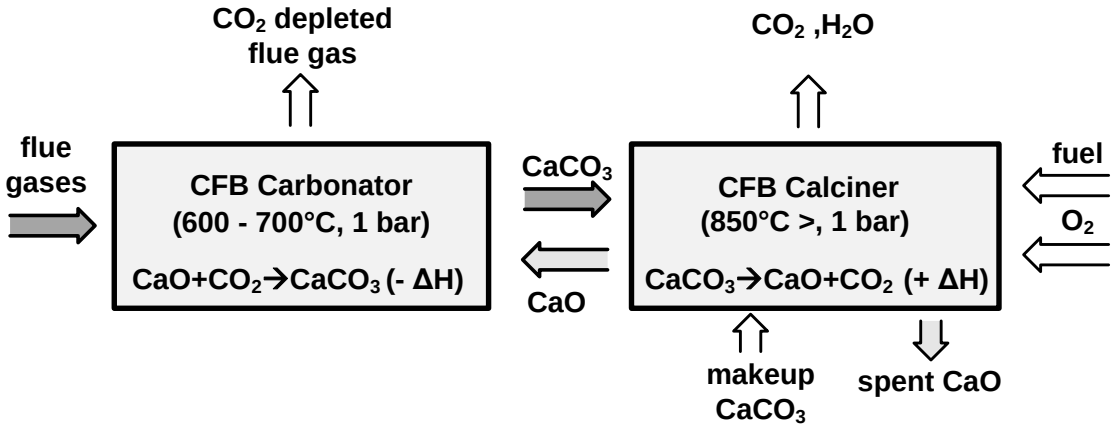

Figure 1.2: CaL process block diagram for post-combustion CO_2 capture

process alternates carbonations and calcinations over multiple cycles to capture CO_2 from gas streams.

$$Carbonation : CaO + CO_2 \rightarrow CaCO_3 \qquad \Delta H = -178\ kJ \tag{1.1}$$

$$Calcination : CaCO_3 \rightarrow CaO + CO_2 \qquad \Delta H = +178\ kJ \tag{1.2}$$

1.3.1 CaL process for post-combustion capture

Figure 1.2 shows the CaL process scheme for post-combustion CO_2 capture. Flue gases from a typical power plant boiler pass through a circulating fluidised bed (CFB) carbonator, where the CO_2 in the flue gases reacts with CaO and produces $CaCO_3$. Thus the CO_2 concentration in the flue gases is reduced to a very low level. CFB reactors are more suitable than the bubbling fluidised (BFB) beds since the CFBs have higher throughput than BFBs. The carbonated sorbent ($CaCO_3$) is then led to the CFB calciner, where it is thermally regenerated to CaO and CO_2. The required energy for the endothermic thermal regeneration process can be supplied directly from the combustion of the same fuel in pure oxygen. The reason for using oxygen instead of air is to produce a pure CO_2 stream without air N_2, at the exit of the calciner. The sorbent is circulated between the carbonator and calciner while adding makeup to replace deactivated sorbent.

1.3.2 CaL process for pre-combustion capture

As the figure 1.3 shows, the CaL process can also be applicable to pre-combustion CO_2 capture. Lime enhanced gasification of solids (LEGS) is a process combined with steam gasification and CO_2 capture by calcium sorbents. Hydrogen rich syngas is generated in this process from a carboniferous fuel. Gasification, CO shift and CO_2 capture take place in a single BFB reactor. BFBs are more suitable here as they give more residence time than

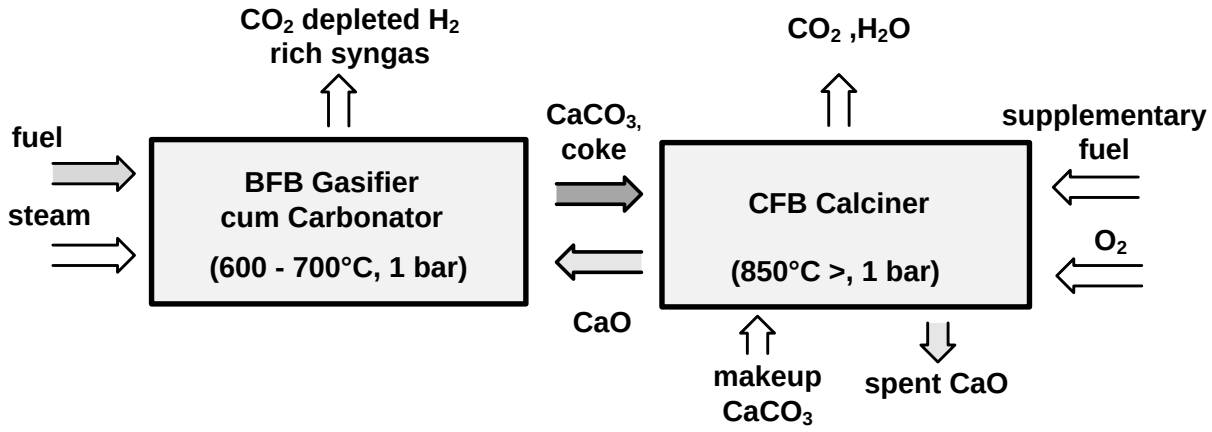

Figure 1.3: CaL process block diagram for pre-combustion CO_2 capture

the CFBs. Exothermic (carbonation and the CO shift) and endothermic (gasification) nature of these reactions help to minimise the energy losses within the reactor. Apart from the production of hydrogen rich syngas, a solid product consisting of $CaCO_3$, CaO, char, ash and CaS (in case of coal feed with sulfur content) is produced, Sivalingam et al. [2009]. This solid product is separated from the syngas and combusted along with the supplementary fuel to produce regeneration heat in the calciner, where the CO_2 laden sorbent is regenerated and a high purity CO_2 stream is produced. The sorbent is circulated back to the gasifier to complete the loop. Sorbents go through hundreds of cycles before being replaced by the makeup flow.

1.4 Development and challenges of the CaL process technology

Although CaO was used as early as in 1967 to aid the gasification of carbon, it was first outlined for high temperature 'CO_2 separation' during a process to produce hydrogen in 1995 by Silaben and Harison, Abanades and Alvarey [2003]. Moreover, a complete looping system for CO_2 capture from combustion processes was proposed by Shimizu et al. and a comprehensive conceptual assessment of the process was also presented in their study, Shimizu et al. [1999]. The CaL process research gathered momentum among the research groups around the world after the year 2000. The research works were directed in three categories as process modeling, sorbent particle research and lab scale dual fluidised bed experiments. However, many challenges remain particularly in the last two categories.

Process modeling approaches cover various process configurations with thermodynamic cycle calculations of power plants with CO_2 capture by CaL. A comparison of process efficiencies and CO_2 capture costs with other competing processes reveals the future potential of the CaL. Process modeling studies showed potentials for a step wise CO_2 capture costs

reductions by the CaL process scheme, Abanades et al. [2004], Davison [2007], Abanades et al. [2007], Hawthorne et al. [2009].

Sorbent particle study in controlled environments depicting the CaL process conditions is another key part of the process development. How fast and to what extent the carbonation and calcination reactions take place under these process conditions and how the reactivity varies with increasing number of cycles are main focus of these studies, Abanades and Alvarey [2003], Alvarez and Abanades [2005a], Sivalingam et al. [2011b]. Understanding the reaction and particle deactivation mechanisms is necessary to optimise process parameters to achieve high efficiencies. Apart from this, sustaining the sorbent reactivity by various means and enhancing the mechanical strength and the reactivity by particle synthesis are another part of particle research, Gupta and Fan [2002].

Lab scale dual fluidised bed (DFB) experiments are necessary to study the CaL process operating parameters. Hydrodynamically scaled cold models are used to study operating parameters such as the total solid inventory, riser superficial velocity, particle size etc., to fully characterise the DFB operation, Charitos et al. [2010b]. Charitos et al. have also studied carbonator space time, carbonator temperature and calcium looping ratio in a lab scale 10 kW_{th} DFB reactor and reported to have reached above 90% CO_2 capture efficiencies, Charitos et al. [2010a].

1.5 Research needs and goals of the thesis

CCS from fossil fuel power generation is an important part of collective measures that would mitigate global anthropogenic CO_2 emissions. CaL processes offer effective and efficient CO_2 separation for existing and future power generation. This work aims at contributing to a better understanding of CaL based pre- and post-combustion CO_2 capture processes by investigating and optimising the sorbents' performance under calciner, carbonator and gasifier operating conditions. In CaL processes, loss of sorbent reactivity would not only require large make up flows for restoring the CO_2 capture capacity but also needs large reactors to handle huge sorbent flows.

Since the process is largely in lab and semi-pilot scale developmental stage, there are many open research questions which have to be answered. These questions are related to both, the competitiveness of the CaL process with the more close to commercialisation technologies like pre-, post- and oxy-fuel CO_2 separation technologies and the sorbent reactivity with the flue gas from full and partial fuel oxidation processes under various operating conditions such as TGA and lab-scale DFB reactors. Therefore, to address these research requirements, the following goals were defined:

- Efficiency assessments of various CaL process configurations and their comparison with other emerging CO_2 capture technologies.
- Address the loss in reactivity of naturally occurring calcium sorbents under various controlled reactor environments. Find ways to reduce its impact on the overall process efficiency.
- Investigations to identify optimum values for the carbonator space time operating parameter for which the CO_2 capture efficiency is maximised. Find ways to restore the reactivity of the spent sorbents to levels comparable to fresh samples.
- Analyse the influence of SO_2 presence in the flue gases and its effect on the degree of CO_2 capture in a CaL process.

1.6 Methodology

Thermodynamic modeling approach

The objective of the thermodynamic modeling approach is to calculate the CaL process efficiencies and to provide a comparative overview of efficiency penalties associated with other competing CO_2 separation technologies. In this context, ASPEN plus process simulations of CaL based full and partial oxidation processes are carried out. Process efficiencies of oxy-fuel, amine based post-combustion and IGCC processes from the literature are summarised along with that of the CaL.

Experimental approach

Experimental activities at lab and semi pilot scales have been designed and carried out to study and improve sorbent particle reactivity that can help to enhance the CO_2 capture efficiency. A number of naturally occurring calcium sorbents from various geographical origins along with samples form a semi-pilot scale 10 kW_{th} DFB CaL test facility have been tested during the experiments.

Naturally occurring and geographically diversified limestone and dolomite samples serve as basis for this study.

- At lab scale:
  - The carbonate content of the samples is measured in a differential thermal analyser(DTA).
  - A parameter directly proportional to the reactivity, the specific surface area is measured by the Brunauer Emmett Teller(BET) method for the original samples and their derivatives.
  - Surface texture and pore structures of the calcined and carbonated samples are analysed in a scanning electron microscope (SEM).
  - CO_2 capture capacities and the reaction rates of the samples with widely varying process parameters, such as calcination and carbonation temperatures, CO_2 concentrations etc., are measured in a thermogravimetric analyser (TGA). Various process modifications are explored to enhance or sustain sorbent reactivity.
  - The influence of SO_2 on CO_2 capture is another important aspect investigated in TGA experiments.

- At semi pilot scale: experiments at a 10 kW_{th} DFB CaL test facility are carried out to study the process parameters such as the carbonator space time, carbonation temperature and the calcium looping ratio by the Institut für Feuerungs- und Kraftwerkstechnik (IFK) at the Universität Stuttgart. An important information to calculate the carbonator space time is the 'active CaO fraction' of the sorbents collected from the steady state carbonator. A custom designed TGA experimental procedure is used to obtain this information at the Lehrstuhl für Energiesysteme (LES). Spent samples from this test facility are studied in TGA to restore the reactivity to the extent of the fresh samples by means of hydration.

1.6.1 Summary on the benefits of this research

An urgent need persists to develop a cost effective and environmental friendly CO_2 separation technology applicable to power generation and industrial processes. The CaL technology evolves as one of such kind. This thesis is to contribute further into the development of the CaL process. Research works have been directed towards process

simulations, sorbent reactivity & optimisation experiments in a controlled reactor environment and process parameter studies in a semi-pilot scale CaL dual fluidised bed test facility.

Fundamental aspects along with detailed descriptions of the emerging CaL process for pre- and post-combustion CO_2 separation are highlighted. ASPEN plus power plant simulations integrating both of the CaL based CO_2 capture processes are performed and compared with other important competing CO_2 capture technologies.

Major focus is given to the sorbent reactivity studies. A wide range of sorbent samples have been studied in several experimental setups. The data gathered on these specific sets of limestone/dolomite samples and the correlation with the chemical theory will be very useful in future designs of real CaL processes. Furthermore, sorbent deactivation with increasing number of calcination and carbonation cycles impair the efficiency of the CaL process despite the fact that the sorbents are abundant and cheap. Several experiments have been carried out to identify the process parameters that influence the sorbent deactivation. One of which directly affects the sorbent reactivity is identified as the calcination temperature (calciner operating temperature in a CaL process). The higher the calcination temperature the higher the rate of deactivation. Specific surface area measurements and scanning electron microscopic analyses are performed to strengthen the finding. A process modification scheme aiming at reducing the sorbent deactivation is proposed by lowering the calciner operating temperature via steam injection.

In a collaborative work with the IFK, Universität Stuttgart, a parametric study has been carried out in a semi pilot scale 10 kW_{th} DFB CaL test facility. A crucial parameter 'active space time(τ_{active})' which defines the CO_2 capture efficiency of a particular CaL reactor system is determined by analysing the samples collected at steady state operation. A TGA experimental procedure is designed and applied for this parametric study. This test procedure can be used as a template to evaluate the performance of a real CaL process. Further on, a successful method has been found out to restore the lost CO_2 capture capacity of spent sorbents from this test facility.

The flue gas from a coal power plant would contain small amounts (ppm level) of SO_2 which can react with calcium sorbents in a CaL process conditions. Several experiments are carried out in a TGA to analyse the effect of SO_2 on CO_2 capture. Moreover, pressurised TGA experiments in the context of CaL for partial oxidation processes have been carried out with synthetic syngas. Sorbent behaviour under varying temperatures and CO_2 concentrations has been studied under these conditions. Effects of high temperature sintering and incomplete (partial) carbonations over the sorbent reactivity are experimentally studied in two separate cases and their implications on the CaL process are discussed.

1.7 Thesis outline

This thesis is divided into 7 chapters which are briefly described as follows:

Chapter 2 gives an overview of important CO_2 capture technologies. A detailed description of the CaL process along with its pre- and post-combustion configurations is presented. ASPEN plus thermodynamic cycle calculations of the CaL processes are also included in this chapter. Efficiency penalties of selected CO_2 capture technologies are compared.

Chapter 3 is based on the journal publication titled 'Cyclic Carbonation Calcination Studies of Limestone and Dolomite for CO_2 Separation From Combustion Flue Gases', Sivalingam et al. [2009]. Sorbent reactivity plays a vital role in achieving high efficiencies in any CaL based CO_2 capture system. Sorbent reactivity variations due to type & geographical origin of the sorbent, calcination temperature and the number of CCR cycles are experimentally determined in various tests, on different experimental setups. A calciner concept is outlined to reduce the sorbent deactivation.

Chapter 4 is based on two journal publications titled 'Parametric investigation of the calcium looping process for CO_2 capture in a 10 kW_{th} dual fluidized bed', Charitos et al. [2010a] and 'Analysis and Comparison of Reactivity and CO_2 Capture Capacity of Fresh Calcium-Based Sorbents and Samples From a Lab-Scale Dual Fluidized Bed Calcium Looping Facility', Sivalingam et al. [2011b]. A method for determining the active space time, a CaL carbonator operating parameter to characterise the CO_2 capture efficiency, is presented and discussed. In the second part, reactivities of spent samples are compared with the fresh ones. A successful reactivation of spent samples by hydration is presented and a carbonator design is outlined to sustain the reactivity.

Chapter 5 is based on peer reviewed conference proceedings titled 'Sorbent Reactivity Studies for CO_2 and SO_2 Co-capture by Calcium Looping Process', Sivalingam et al. [2011a]. Sulfations at calciner and carbonator conditions are performed in a TGA. Rates of CO_2 and SO_2 co-capture as a function of residence time and temperature are studied for optimising the CO_2 capture. Moreover, sulfation rates of limestone derivatives are determined and compared.

Chapter 6 reports pressurised TGA experiments with synthetic syngas mixture depicting partial oxidation processes(gasification). A number of operating parameters were studied at this conditions. A section is also dedicated to study the high temperature sintering often encountered in calciners and the last section investigates the effect of incomplete carbonations on the CO_2 capture capacity with number of CCR cycles.

Finally, **Chapter 7** contains the conclusions regarding all the experimental and process simulation studies. Furthermore, recommendations for future research are also presented.

Chapter 2

CO_2 capture technologies comparison

The fundamental aspects along with detailed descriptions of CaL process for pre- and post-combustion CO_2 separation are presented. ASPEN plus power plant simulations integrating both of the CaL based CO_2 capture processes are performed and compared. Important aspects of other competing CO_2 capture technologies namely solvents based post-combustion capture, oxy-fuel capture and pre-combustion capture with IGCC are discussed. A summary on various CO_2 capture schemes draws the conclusion of this chapter.

2.1 CaL process

A brief introduction of the calcium looping(CaL) process is given in chapter 1. A more detailed description including possible process configurations are discussed in this section. The CaL process can be used to decarbonate a fuel or a combustion flue gas stream by pre-combustion or post-combustion CO_2 capture.

2.1.1 Advantages of the calcium sorbents and the CaL process

- The sorption capacity of CaO is very high when compared to other processes. Under ideal conditions, the sorption capacities of monoethanolamine(MEA), silica gel and activated carbon are 60, 13.2 and 88 g of CO_2/kg of sorbent respectively. In contrast, CaO would capture 393 g of CO_2/kg of sorbent, assuming a 50% conversion of CaO over repeated cycles, Gupta and Fan [2002].

- The high availability of $CaCO_3$ in nature as limestone and dolomite, its well geographical distribution on earth and its low cost, Abanades et al. [2004] allow this capture process to be implemented all over the world including fast developing countries like China, Brazil and India.

- In a CaL process both the carbonation and the calcination reactions take place at high temperatures, essentially above 600°C, enabling the effective recovery of calcination energy (supplied to the calciner for the thermal regeneration) in the

carbonator. In contrast, at low temperature CO_2 capture systems, such as MEA, the heat delivered to the sorbent regeneration cannot be recovered in a steam cycle, Sivalingam et al. [2009].

- The $CaO/CaCO_3$ system does not require pressurised conditions unlike the other sorption processes that need high pressures and /or low temperatures to enhance the sorption efficiency. Further the carbonation temperature of CaO fits well in the domain of flue gas exit temperatures especially from that of the circulating fluidized bed based combustion systems. Moreover the fast reaction rate of CaO at temperatures above 600°C allows compact reactor designs, Abanades et al. [2005].
- The CaL process has got unique prospects for synergies with heavy-emitting industries, e.g., cement manufacturing. It uses mature large-scale equipment, which reduces scale-up risk, e.g., fluidised beds, Florin and Fennell [2010].

2.1.2 CaO-$CaCO_3$ equilibrium diagram

Figure 2.1 plots the partial pressure of CO_2 (P_{CO_2}) against the temperature of a $CaO/CaCO_3$ equilibrium system. It was calculated by HSC Chemistry 5.0 software from Outokumpu Research Oy, Finland. The equilibrium CO_2 concentration of the $CaO/CaCO_3$ system at a particular reaction temperature can also be calculated by a formula. Baker [1962] has proposed the formula 2.1 where $C_{CO_2,eq}$ refers to the equilibrium CO_2 concentration in [mol/m^3].

$$C_{CO_2,eq} = \frac{1.462 \times 10^{11}}{T_{carb}} exp\left(\frac{-19.13}{T_{carb}}\right) \tag{2.1}$$

As of the diagram, for a given CO_2 partial pressure, a temperature higher than the equilibrium temperature favours the calcination and a lower temperature favours carbonation. An equilibrium point indicated by the arrows in the diagram corresponds to $P_{CO_2,eq}$ = 0.2 bar and T_{eq} = 792°C. Hence, at P_{CO_2} = 0.2 bar, the calcination would be favoured at temperatures above 792°C. On the other hand the carbonation would be favoured at temperatures lower than 792°C. Moreover a carbonation can also be performed at the same temperature if the P_{CO_2} is increased to more than 0.2 bar, similarly the calcination at less than 0.2 bar. This data is important to optimise the operating temperatures of a calciner or a carbonator. It can be deduced from the diagram that the $CaO/CaCO_3$ equilibrium allows a CO_2 capture of more than 90% from a typical coal combustion flue gas (max 15%-vol) at atmospheric pressure conditions and temperatures around 650°C. Same applies for a pre combustion in-situ CO_2 capture where the CO_2 concentrations are much higher due to the water gas shift reaction 2.2 and the capture efficiencies would be even higher than 90%. However in reality the chemical reactor design plays a vital role in achieving these theoretical maximum efficiencies defined by the $CaO/CaCO_3$ equilibrium system.

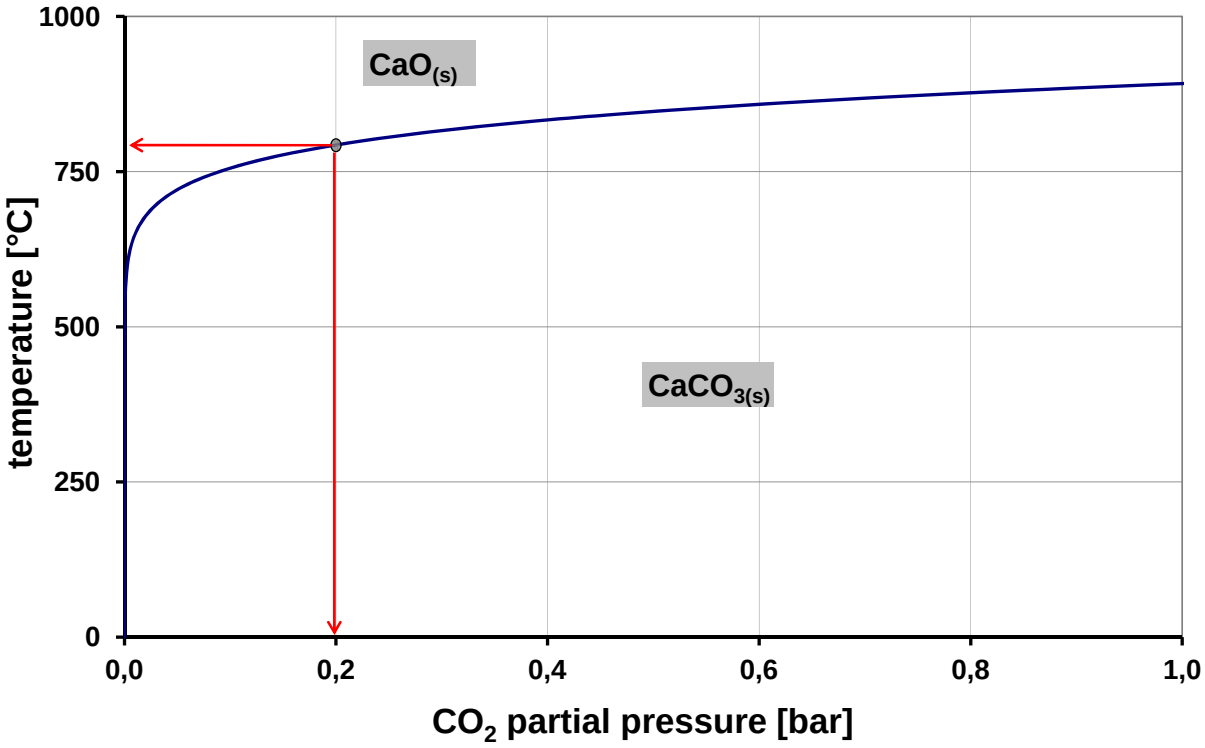

Figure 2.1: Partial pressure of CO_2 versus the temperature of the $CaO/CaCO_3$ equilibrium system

2.1.3 CaL for full oxidation process and its reactor configuration

The process is also referred to as CaL based post-combustion CO_2 capture. A looping reactor configuration would be required to circulate the calcium sorbents in a cyclic manner between the carbonator and calciner. When it comes to the question of suitable type of reactors for calciner and carbonator, the fluidised beds are the first choice not only because of the high reaction rate requirement and high enthalpy of the reactions involved but also due to the maturity of the fluidised bed technology. Moreover, circulating fluidised bed(CFB) reactors are more suitable for this purpose than the bubbling fluidised beds(BFB) since a huge volume of flue gases coming from a power plant with an air blown combustion are to be treated online. These two CFB reactors are connected by a solid looping system which transports the $CaO/CaCO_3$ mixture between them. Figure 2.2 shows a possible configuration of the CaL system for post-combustion CO_2 capture. In another configuration, the solid flow from the carbonator can be split with a predefined ratio from which one part goes to the calciner and the other is recirculated back to the carbonator. In this way the sorbents are allowed to spend more time in the carbonator and achieve more conversions. This mechanism will also limit the solid inflow to the calciner which operates at a higher (>900°C) temperature than the carbonator, thus reducing the heat load to the calciner. A more detailed design of solid split is presented in section 4.1.2.

The flue gas at around 650°C, passes through the CFB carbonator, where CO_2 gets

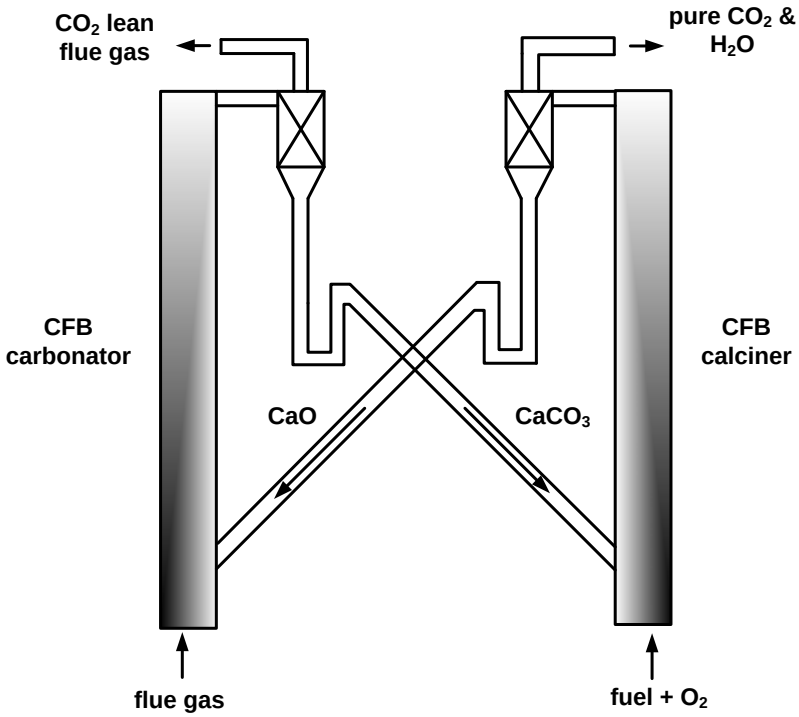

Figure 2.2: Schematics of the CaL based post-combustion CO_2 capture DFB configuration

reduced by reacting with CaO. Since the carbonation reaction is an exothermic one, a substantial portion of useful power can be produced in the carbonator. Energy balance calculations revealed that about 30% of total power could be extracted from the carbonator. The carbonated sorbent ($CaCO_3$) is then led to the CFB calciner, where it is thermally regenerated to CaO and CO_2 at around 900°C. The required thermal energy for the regeneration is supplied by the oxy-combustion of same fuel from which the flue gases originate. In such a way after condensing the steam, a pure CO_2 stream is produced in the calciner. The reaction equations for carbonator and the calciner are respectively given in equations 1.1 & 1.2.

2.1.4 CaL for partial oxidation process and its reactor configuration

It is also generally referred to as CaL based pre-combustion CO_2 capture. However in particular it is called Lime Enhanced Gasification of Solids(LEGS), a sub set of Absorption Enhanced Reforming(AER). Similar to the CaL based post-combustion CO_2 capture reactor configuration, the FB reactor technology is suitable for pre-combustion schemes too. In this process the carbonation and the gasification take place in the same reactor so that a BFB reactor which provides more residence time, will be the right reactor choice. However the calciner will be a CFB reactor as the calcination occurs in a couple of seconds at high temperatures. A sorbent particle circulating loop connects these two reactors. At

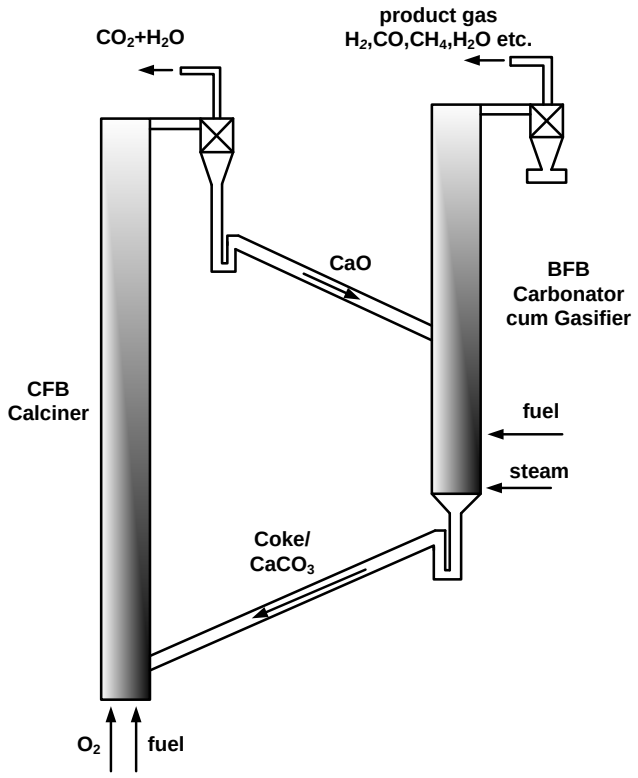

Figure 2.3: Schematics of the CaL based pre combustion CO_2 capture DFB configuration

atmospheric pressure conditions the carbonator cum gasifier can be operated between 650-700°C, limited by the $CaO/CaCO_3/CO_2$ equilibrium system for CO_2 capture. Since the gasification temperature is limited, this scheme is suitable for a biomass feedstock. On the basis of thermodynamic equilibrium modelling, CO_2 mol fraction in the product gas from the biomass gasification, with and without CaO, was predicted by Florin and Harris [2008]. At 650°C, the CO_2 concentration without the CaO was 13 vol-% and that with the CaO was 0.02 vol-%. Figure 2.3 shows the schematics of the process configuration. A carboniferous fuel is steam gasified in the BFB carbonator cum gasifier. The main components of the syngas produced by the steam gasification of a biomass are H_2 and CO. The latter is further oxidised with the available steam according to the reaction equation 2.2 and produces more H_2 and CO_2. Thus a H_2 rich syngas is generated. The H_2 concentration is further increased in the syngas by the in-situ CO_2 capture. The general form of the overall biomass steam reforming equation is given in reaction equation 2.3, Florin and Harris [2008].

$$\begin{aligned} &Water\ gas\ shift\ reaction: \\ &CO + H_2O \rightarrow CO_2 + H_2 \qquad \Delta H = -41.2\ kJ/mol \end{aligned} \tag{2.2}$$

$$\textit{General reaction of the biomass steam gasification}: \\ C_nH_mO_p + (2n-p)H_2O = nCO_2 + (m/2+2n-p)H_2 \qquad \Delta H < 0 \tag{2.3}$$

In case of coal feed, the temperature of the gasifier cum carbonator should be increased to ensure a substantial coal, especially char conversion. However at atmospheric pressure conditions, increasing the reactor temperature will also increase the CO_2 equilibrium partial pressure according to equation 2.1. That means, the CO_2 reduction beyond the equilibrium concentration becomes impossible and the capture efficiency will be reduced. There are two ways to solve this problem. One possible solution is to increase the total pressure of the reactor so that the partial pressure of the CO_2 becomes much higher than the equilibrium pressure which facilitates a more efficient capture. However the general complexity due to the pressurised systems cannot be avoided in this configuration. A LEGS process study for the brown coal at 2 MPa pressure and less than 800°C was presented by Weimer et al. [2008] and it is reported that its electrical efficiency coupled with the state of the art combined cycle is 42%. The second configuration works at atmospheric pressure conditions by having the gasification and the CO_2 capture in two separate reactors. Another advantage of this three reactor configuration is that the gasifier can be operated without any temperature limitations imposed by the $CaO/CaCO_3$ equilibrium system. The water gas shift reaction and the CO_2 capture will take place simultaneously in the carbonator. In this configuration, an inlet of sub stoichiometric oxygen is required to partially combust the coal and provide the heat necessary for the endothermic coal gasification. ASPEN plus thermodynamic cycle calculations of this process along with the post-combustion CO_2 capture process are given in section 2.2.

A general form of the reaction equations for a carbonator cum gasifier and the calciner with the coal feed are presented in equations 2.4 & 2.5, Scheffknecht et al. [2006]. It can be observed from the reaction equations that the sulfur in the coal is also removed by the sorbents, however it remained as $CaSO_4$ even after the regeneration in the calciner. This means that sulfur permanently disables the sorbent capture potential. A comprehensive experimental investigation of the SO_2 behaviour in the CaL post-combustion scheme will be discussed in chapter 5.

$$\textit{General reaction at the carbonator cum gasifier}: \\ coal + CaO + H_2O \rightarrow H_2 + CaCO_3 + C + CaS \tag{2.4}$$

$$\textit{General reaction at the calciner}: \\ (a-z)CaCO_3 + yC + zCaS + mO_2 \rightarrow (a-z)CaO + zCaSO_4 + (a-z+y)CO_2 \tag{2.5}$$

2.2 Thermodynamic cycle calculations of the CaL processes

General assumptions for the ASPEN Plus process simulations

Design conditions of various models established in the commercial software ASPEN Plus will determine the performance of a process and its final efficiency. For example, choosing a reactor model RGIBBS or RSTOIC would affect the final product composition since they are based on different operating principles. The RGIBBS model works on the Gibbs free enthalpy minimisation principle and the RSTOIC is depending on the input stoichiometry. Therefore it is important to define some general assumptions beforehand for the consequent process modeling.

The whole analysis is based on thermodynamic equilibrium model. Moreover the chemical and phase equilibriums are based on a Gibbs free energy minimisation model. The entire process scheme is modeled and simulated as a thermally integrated design. That means all the heat duties required for various processes are taken from the available hot streams. In addition, a steam cycle takes into account the excess heat from the process scheme. The only energy input is the fuel input to the gasifier/combustor and calciner.

There are two types of solid streams: homogeneous ones with a defined molecular weight called conventional, and the other is heterogeneous non-conventional ones with undefined molecular weight. As an example, the coal is defined in the second category. By defining the right stream classes one is able to incorporate both conventional and non-conventional types into a simulation model. Furthermore, the property method RK-SOAVE which uses the Redlich-Kwong-Soave equation to calculate thermodynamic phase equilibrium is selected for the simulations.

Coal definition

Coal is defined as a non-conventional component as it is a heterogeneous solid not participating in chemical equilibrium. The physical and thermodynamic properties required for the definition of non-conventional solids are enthalpy and density, which will be calculated respectively through HCOALGEN and DCOALIGT models available in ASPEN plus. The coal input data must be given in three categories, namely proximate analysis(PROXANAL), ultimate analysis(ULTANAL) and a sulfur analysis(SULFANAL) to calculate the enthalpy of coal. The type of coal used in all the simulations is Illinois#6. Its proximate & ultimate analysis are respectively given in table 2.1, Fan [2010]. The coal feed is maintained as 1000MW_{th} based on LHV to make the efficiency comparisons easier. The total coal flow is approximately 36 kg/s and its LHV is calculated as 27.5 MJ/kg.

Moreover, the wet coal is dried in a dryer to 5-%wt moisture by the hot N_2 stream from the ASU. The products stream emerging from the dryer goes through a separator which splits it into dried coal and a gaseous stream. The coal is now ready to enter a

Table 2.1: Proximate & Ultimate analysis of Illinois#6 coal

Constituents	Moisture	Fixed carbon	Volatiles	Ash
%-wt, As received	11.12	44.19	34.99	9.7
%-wt, Dry	-	49.72	39.37	10.91

Constituents	Moisture	Ash	C	H	N	Cl	S	O
%-wt, As received	11.12	9.7	63.75	4.5	1.25	0.29	2.51	6.88
%-wt, Dry	-	10.91	71.72	5.06	1.41	0.33	2.82	7.75

combustor/gasifier.

The following assumptions are also made:

- The ambient temperature is 25°C and the ambient pressure is 1 bar.
- Air consists of 21%-vol O_2 and 79%-vol N_2.
- CO_2 is compressed to 11 MPa for sequestration.
- The carbon conversion in the gasifier/combustor is more than 99%-mol.
- The pressure levels in the steam cycle are High Pressure(HP)=14 MPa, Intermediate Pressure(IP)=3 MPa & Low Pressure(LP)=0.1 MPa. The HP & IP steam are superheated to 540°C.
- All hot streams are cooled down to 150°C while exchanging heat with the steam cycle.
- There are no heat losses to the environment.

Definition of the performance indicators used in this simulations

The electrical efficiency and the hydrogen efficiency are defined in equations 2.6 & 2.7.

$$\eta_{El} = \frac{W_{net}}{\dot{m}_{coal}\, LHV_{coal}} \times 100 \tag{2.6}$$

$$\eta_{H_2} = \frac{\dot{m}_{H_2}\, LHV_{H_2}}{\dot{m}_{coal}\, LHV_{coal}} \times 100 \tag{2.7}$$

where η_{El} is the electrical efficiency in %; W_{net} is the net power, calculated by the steam turbines power output minus the parasitic power consumptions, such as by the air separation unit (ASU) in [MW]; $\dot{m}_{coal}$ is the coal mass flow in [kg/s]; LHV_{coal} is coal LHV in [MJ/kg]; η_{H_2} is the hydrogen production efficiency in %; LHV_{H_2} is LHV

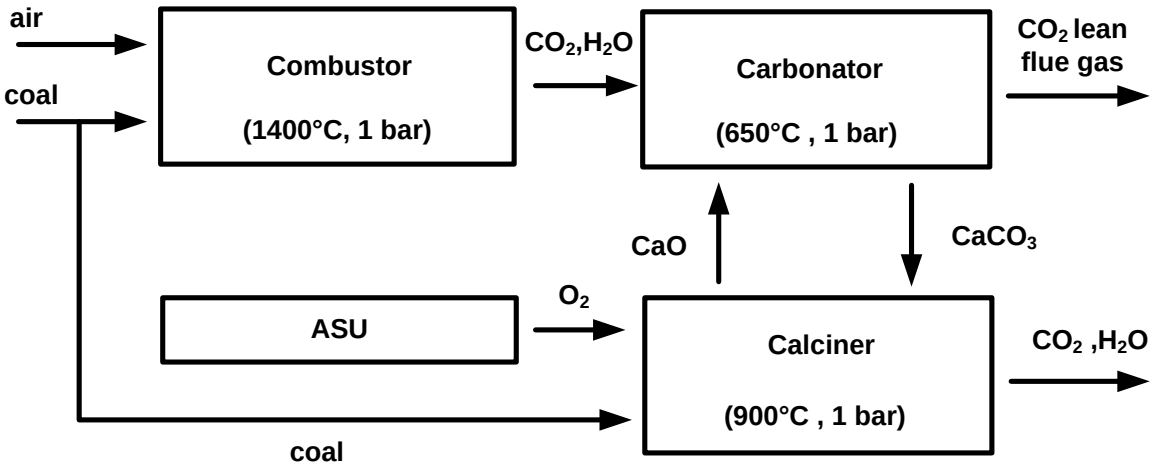

Figure 2.4: The CaL based post-combustion CO_2 capture block diagram modeled in ASPEN plus

of hydrogen in [MJ/kg] and $\dot{m}_{H_2}$ is the hydrogen production in [kg/s]. In case of a co-production of hydrogen and electricity, the total energy conversion efficiency is defined based on equivalent electrical efficiency for the sake of comparison with other CO_2 capture technologies. The equivalent electrical efficiency is defined by the equation 2.8.

$$\eta_{El,eq} = \eta_{El} + 0.6\,\eta_{H_2} \tag{2.8}$$

where, 0.6 denotes the average electrical efficiency of a combined cycle natural gas power plant.

The CO_2 capture efficiency of the CaL process can be measured by calculating the E_{CO_2}, a ratio between the CO_2 mols entering the carbonator and reacted with CaO, as defined in section 4.1.1.

2.2.1 Modeling of the CaL post-combustion CO_2 capture

Figure 2.4 shows the CaL process block diagram to be modeled in ASPEN Plus. The coal combustor is operated at ambient pressure and 1400°C and it is fed with the Illinois#6 coal equivalent to 1000MW_{th} based on LHV. The carbonator operates at 650°C and the calciner is at 900°C. An ASU supplies O_2 to the calciner.

Modeling of the air separation unit

The ASU is an important part of this process and expected to consume a substantial amount of parasitic power. ASU supplies oxygen to the calciner. The purity of oxygen is a key parameter as it influences the purity of CO_2 produced in the calciner. A high purity oxygen(>99%-vol) will drastically reduce CO_2 purification and compression power at the downsteam process.

Oxygen is separated from air through cryogenic distillation. At ambient pressure, the boiling points of oxygen and nitrogen are respectively -183°C and -198.5°C and it takes a lot of energy to reach this point. However, an increasing pressure, increases the boiling point and subsequently less energy is required to reach that point. Therefore the air separation at higher pressure conditions needs less cooling energy than at ambient conditions. Nevertheless compression of air also consumes a lot of power. As a trade off, the air separation process is performed at 6 bar. This pressure corresponds to a commercial air separation plant manufactured and supplied by the Universal Boschi of Italy. Air is first compressed and subsequently cooled down to -170°C. At this point, oxygen can be separated from nitrogen with a purity of more than 99%-vol. After being separated, the products stream exchanges heat with the incoming ambient air, and is reheated to 25°C. Then both streams, oxygen and nitrogen, will be sent to their next operating units within the process. The energy needed for cryogenic separation is taken from the electricity generated through the steam cycle. The chosen cooler operates with a coefficient of performance(COP) of two.

Modeling of the combustor

In reality a fluidised bed reactor will be used as combustor. Dried coal enters the combustor as a non-conventional component in ASPEN Plus model. It has to be decomposed into ash(also defined as non-conventional) and conventional components such as H_2O, O_2, N_2, NO_2, NO, S, SO_2, SO_3, H_2, Cl_2, HCl, CO and CO_2. This decomposition is modeled in an RYIELD reactor since the end products are known. The required heat is then taken from the combustor model. The combustor is modeled through a RGIBBS reactor, which is configured to identify possible equilibrium products from a predefined list of components. Figure 2.5 shows the scheme of the combustion block in ASPEN.

The air to fuel ratio is chosen in such a way that it is gradually increased until all the carbon in the fuel is converted to CO_2. Further downstream the CO_2 will be separated from the flue gas in the carbonator, releasing a CO_2 lean stream to the atmosphere.

Modeling of the carbonator

$$Carbonation : CaO + CO_2 \rightarrow CaCO_3 \qquad \Delta H = -178\ kJ \tag{2.9}$$

The CO_2 is removed from the flue gas stream by CaO according to the carbonation reaction in equation 2.9. The carbonator is defined as a RSTOIC reactor model in this simulations. The RSTOIC reactor model is chosen here because the equilibrium data and the kinetics are unimportant for this reaction. The optimum operating temperature for this reaction is assumed to be 650°C, Sivalingam et al. [2011b] Abanades et al. [2009]. Some key parameters which determine the performance of the capture process are the reactive fraction of the CaO particle (F_a), the ratio of the amount of reactive CaO in the bed(F_R) to the incoming CO_2(F_{CO_2}) and the rate of sorbent disposal(F_0, equals to

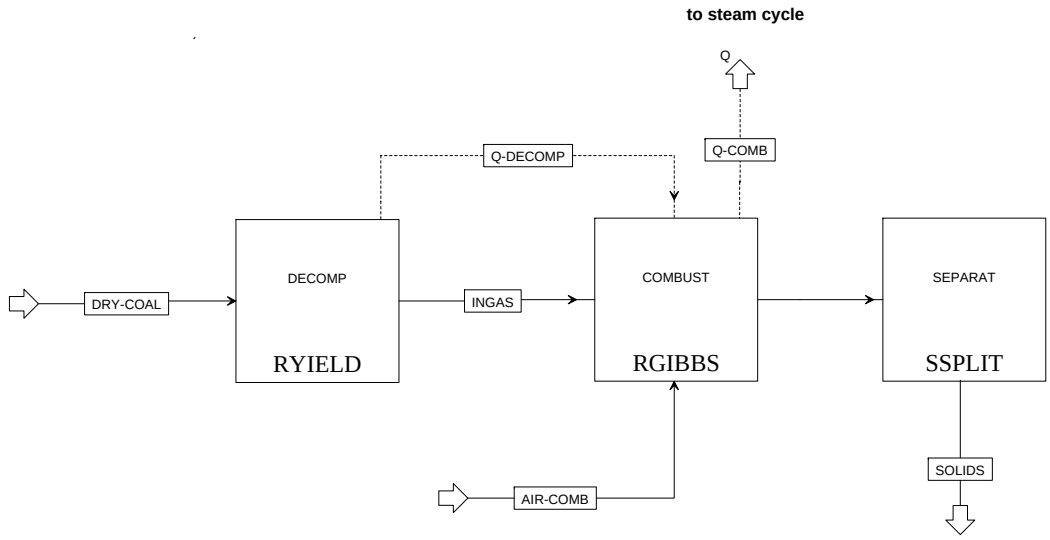

Figure 2.5: The combustor model in ASPEN plus

makeup flow). The interdependency of these parameters have been theoretically studied and reported by Abanades et al. [2005]. In order to reduce the complexity of the whole power plant simulations, it has been decided to choose appropriate values for the operating parameters based on reported data. The carbonator parameters and corresponding CO_2 capture efficiencies are extracted from the plot by Abanades et al. [2005] and tabulated in table 2.2. In a collaborative work with the Institute of Combustion and Power Plant Technology (IFK) in Stuttgart, these parameters were experimentally studied in a semi-pilot scale DFB reactor system and reported in chapter 4. E_{CO_2} in table 2.2 is the ratio of CO_2 mols reacted with CaO to the total incoming CO_2 mols, which indicates the CO_2 capture efficiency of the process. It can be observed in the table that, when decreasing the make-up flow(i.e. lowering the ratio of F_o/F_{CO_2}), more CaO is needed to achieve maximum CO_2 capture (i.e. F_R/F_{CO_2} is increasing). A set of values have been chosen from the spectrum of parameters in the table 2.2 in order to achieve maximum CO_2 capture (>95%) at relatively low solids circulation rate. These parameters are valid for less than 50 carbonation and calcination reaction (CCR) cycles. Therefore the standard case considered in the simulation consists in the following parameter values: F_R/F_{CO_2}=4 and the CaO disposal ratio (F_o/F_{CO_2}) of 0.1. Another important parameter F_a is assumed to be 0.15 based on the TGA experiments reported in chapter 4. The experiments revealed that the CaO conversion of the sorbents was well above 20 mol-% after more than 20 CCR cycles. Figure 2.6 shows the scheme of the carbonator model.

Modeling of the calciner

$$Calcination : CaCO_3 \rightarrow CaO + CO_2 \qquad \Delta H = +178\ kJ \tag{2.10}$$

In the calciner, additional coal is combusted with pure oxygen coming from the ASU

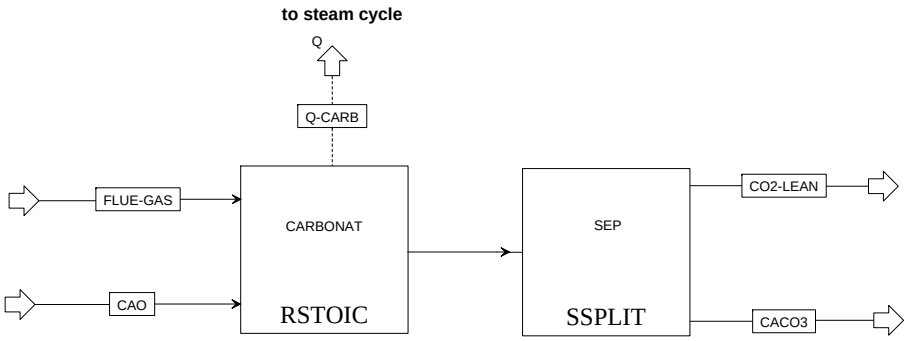

Figure 2.6: The carbonator model in ASPEN plus

Table 2.2: CO_2 capture efficiency at different sorbent flow rates, Abanades et al. [2005]

	E_{CO_2}				
F_o/F_{CO_2}	F_R/F_{CO_2}=1	F_R/F_{CO_2}=2	F_R/F_{CO_2}=3	F_R/F_{CO_2}=4	F_R/F_{CO_2}=5
0.05	0.28	0.46	0.63	0.81	0.99
0.1	0.36	0.57	0.76	0.95	0.99
0.2	0.46	0.72	0.95	0.99	0.99
0.3	0.52	0.84	0.98	0.99	0.99
0.4	0.58	0.95	0.99	0.99	0.99
0.5	0.61	0.97	0.99	0.99	0.99
0.6	0.64	0.99	0.99	0.99	0.99
0.7	0.67	0.99	0.99	0.99	0.99
0.8	0.7	0.99	0.99	0.99	0.99
0.9	0.75	0.99	0.99	0.99	0.99
1	0.8	0.99	0.99	0.99	0.99

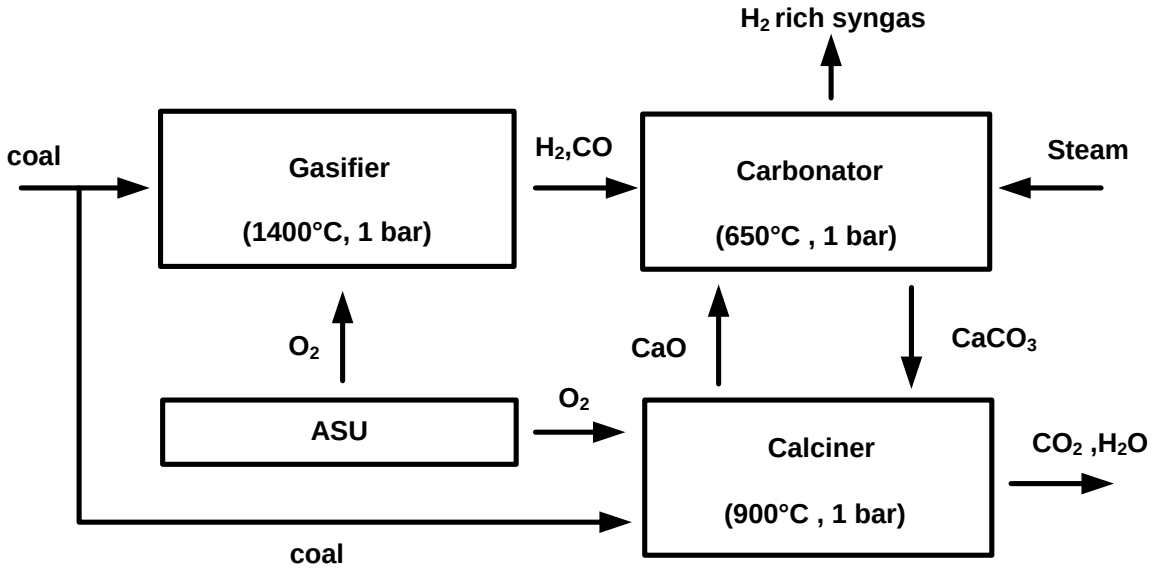

Figure 2.7: The CaL based pre-combustion CO_2 capture block diagram modeled in ASPEN plus

to provide the heat required to decompose the $CaCO_3$ into CO_2 and CaO. The optimum operating temperature for this reaction is assumed to be 900°C Alvarez et al. [2007] Borgwardt [1989] Borgwardt [1985]. The ASPEN model for the calciner is very similar to the combustor model as some additional fuel is combusted to generate the regeneration heat. Apart from combustion the main reaction taking place in this operating block is calcination according to the equation 2.10. After full conversion(>99%) to CaO, the pure solids stream of CaO is directed to carbonator. Equal molar rates of make-up ($CaCO_3$) and disposal(CaO) are taking place in the calciner. The simulation is performed with a disposal ratio of 0.1(i.e. 10% of incoming flue gas CO_2 mols).

2.2.2 Modeling of the CaL pre-combustion CO_2 capture

A three reactor concept for pre-combustion CO_2 capture suitable for high ranking coal is modeled here. Figure 2.7 shows the process block diagram to be modeled in ASPEN Plus. The coal is gasified with a substoichiometric O_2 stream coming from the ASU. The gasification products are then transferred to the carbonator where the CO is shifted with steam to produce more hydrogen while the resulting CO_2 is captured by the CaO. A hydrogen rich product gas is generated in the carbonator. Thereafter, the CO_2 laden sorbents are moved to the calciner where they are thermally decomposed to CaO and CO_2. By condensing the vapour, a pure CO_2 stream is obtained in the calciner. Part of the coal feed along with O_2 from the ASU is supplied to the calciner to provide the required energy for the thermal regeneration by oxy-combustion.

The process modeling is similar to the post-combustion capture discussed in the previous

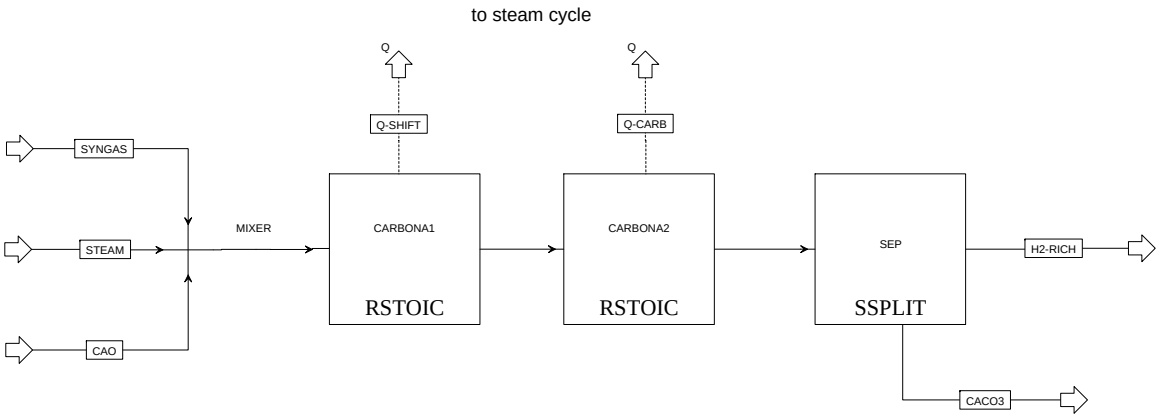

Figure 2.8: The carbonator model incorporating the shift reaction

section. A gasifier model has to be added for this pre-combustion scheme in addition to a carbonator incorporating the CO shift reaction.

Modeling of the gasifier and carbonator

Non-conventional coal is decomposed in a RYIELD reactor and the resulting components are introduced into an RGIBBS reactor in which all gasification reactions take place. The block is optimised to produce more CO that can be converted to hydrogen in the subsequent carbonator. The oxygen supply is varied to determine the operating point of the gasifier.

The carbonator design is different from the one in post-combustion capture, mainly because of hydrogen production in the reactor. However it is also operated at 650°C to achieve maximum CO_2 capture. Figure 2.8 shows the ASPEN model of the carbonator block. The reactor produces hydrogen while removing the carbon dioxide. The molar flow rate of steam has to be optimised to achieve full CO conversion. Any excess steam introduced in the carbonator will reduce the power generation potential at the downstream steam turbines. When less steam is introduced, CO conversion which affects the H_2 production, will be impaired. Therefore only stoichiometric amount of steam is introduced into the carbonator. As in the post-combustion case, 10% of the incoming CO_2 mols of CaO is renewed in the sorbent loop and four times active CaO than the incoming CO_2 (in mols) is maintained. Another important parameter F_a is also maintained as 0.15. This will result in a CO_2 capture efficiency of 95%.

Steam parameters

Table 2.3 shows the main steam parameters. The isentropic efficiency of the steam turbines are assumed to be 0.9.

Table 2.3: Steam parameters

High Pressure (HP)	Intermediate Pressure (IP)	Low Pressure (LP)	Exit Steam
14 MPa	3 MPa	0.1 MPa	3 kPa
575 °C	575 °C (reheated)	180 °C	27 °C

Table 2.4: Combustor, carbonator and calciner simulation parameters and the main simulation outputs for the CaL post-combustion CO_2 capture process

Combustor		**Carbonator**		**Calciner**	
Simulation parameters					
Temperature	1400°C	Temperature	650°C	Temperature	900°C
Ther.Power	700 MW_{th}	E_{CO2}	0.95	η_{comb}	99.9%
Coal	24 kg/s	F_R/F_{CO_2}	4		
η_{comb}	99.9%	F_0/F_{CO_2} & F_a	0.1 & 0.15		
Main simulation outputs					
Air	235 kg/s	Total CO_2 capture	96.5%	Coal	10.3 kg/s
Q-Comb.	497 MW_{th}	Q-Carb.	232 MW_{th}	Oxygen	24.5 kg/s
		Q-Carb. FlueGas	114 MW_{th}	Q-flue gas	115 MW_{th}
Total Power Produced			424 MW_{el}		
Parasitic Loss			38 MW_{el}		
Net Electrical Efficiency, η_{el}			38.6 %		

Outcome of the CaL process simulations

Figure 2.9 shows the simplified heat & mass balance and the heat integration diagram of the CaL based post-combustion CO_2 capture process modelled in ASPEN plus. The table 2.4 shows the main simulation parameters and the main simulation outputs of the combustor, carbonator and calciner together with an overall process output summary. The calculated net electrical efficiency is 38.6% at a CO_2 compression to 110 bar and an overall capture efficiency of 96.5%. It is more than the CO_2 capture efficiency of the carbonator itself(95%). This is due to the combined effect of a 100% CO_2 capture from the oxy-coal combustion in the calciner. The obtained net efficiency is slightly less than reported in the literature. Hawthorne et al. [2009] have reported 39.2% efficiency for a similar process configuration. The reason for this difference might be the lack of steam cycle optimisation which can be done by a software specifically tailored for steam cycle calculations similar to the one used in the reference literature. According to the calculations performed in this thesis the efficiency penalty for the CaL based post combustion CO_2 capture process is about 6-7%-points, when compared to an advanced coal power plant efficiency of 45% without the CO_2 capture. This value is within 6-8%-points reported in the literature, Abanades et al. [2007],Abanades et al. [2009],Hawthorne et al. [2009].

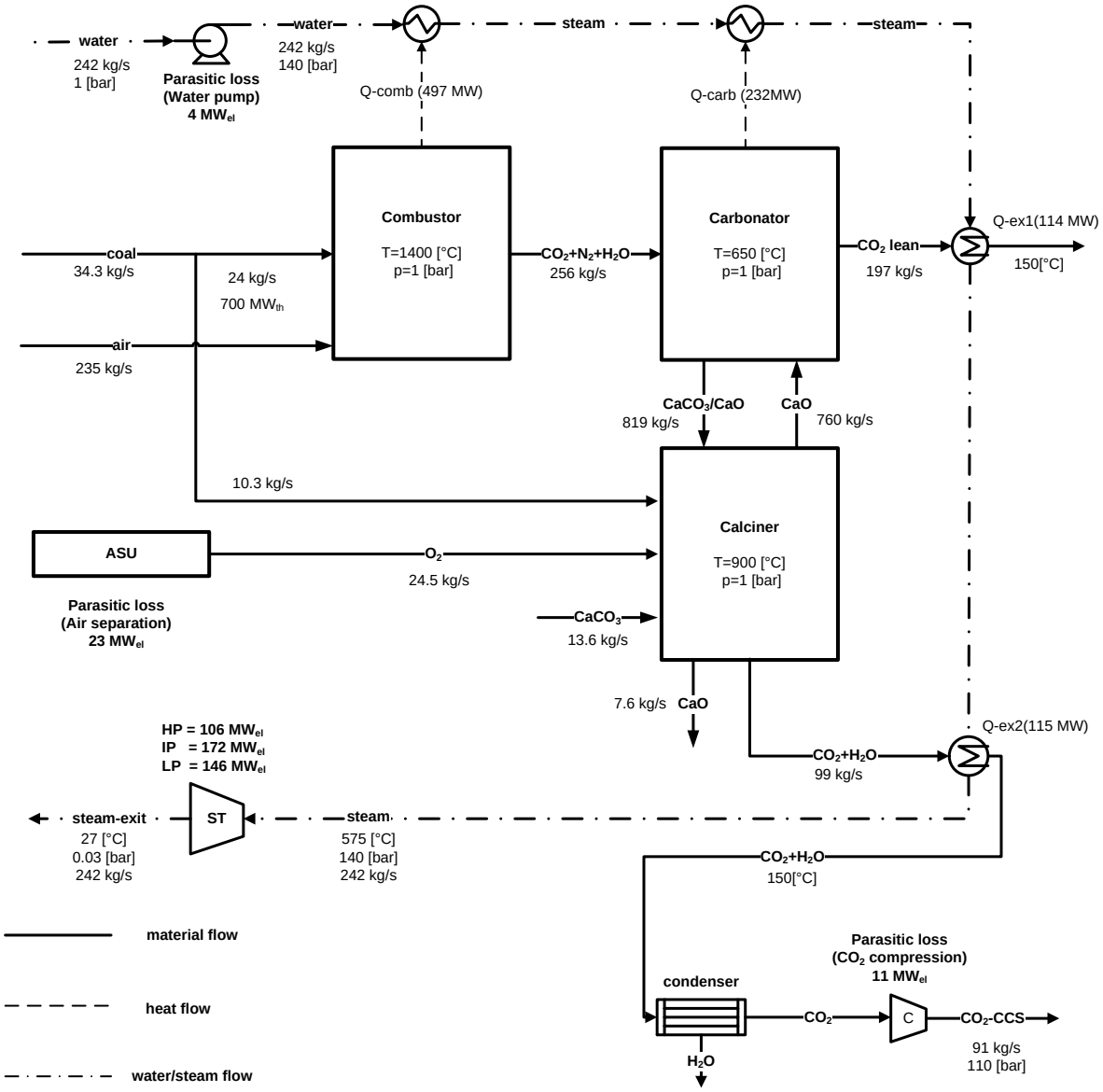

The net electrical efficiency with CO_2 compression (η_{El}) = 38.6 %

Figure 2.9: Simplified heat & mass balance and the heat integration diagram of the CaL based post-combustion CO_2 capture

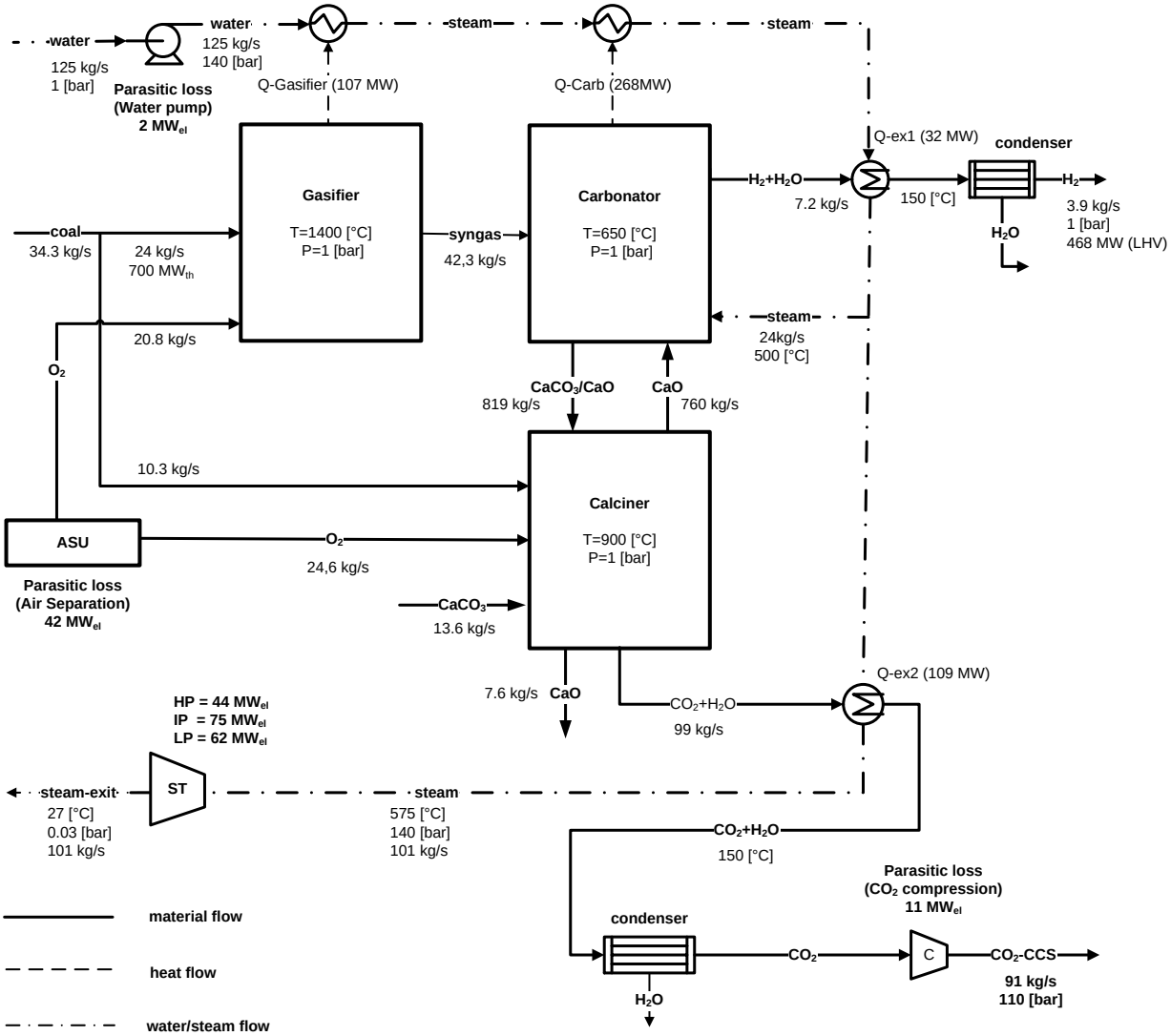

Figure 2.10: Simplified heat & mass balance and the heat integration diagram of CaL based pre-combustion CO_2 capture process

Table 2.5: Gasifier, carbonator and calciner simulation parameters and the main simulation outputs for the CaL pre-combustion CO_2 capture process

Gasifier		**Carbonator**		**Calciner**	
Simulation parameters					
Temperature	1400°C	Temperature	650°C	Temperature	900°C
Therm.Power	700 MW_{th}	E_{CO2}	0.95	η_{comb}	99.9%
Coal	24 kg/s	F_R/F_{CO_2}	4		
η_{comb}	99.9%	F_0/F_{CO_2} & F_a	0.1 & 0.15		
Main simulation outputs					
O_2	20.8 kg/s	Total CO_2 capture	96.5%	Coal	10.3 kg/s
Q-Gasi.	107 MW_{th}	Q-Carb.	268 MW_{th}	Oxygen	24.5 kg/s
		Q-Carb. FlueGas	32 MW_{th}	Q-flue gas	109 MW_{th}
Total Power Produced			181 MW_{el}		
Hydrogen Produced (3.9 kg/s, LHV based)			468 MW_{th}		
Parasitic Loss			55 MW_{el}		
Hydrogen Production Efficiency, LHV based, η_{H_2}			46.8 %		
Net Electrical Efficiency, η_{el}			40.7 %		

Figure 2.10 shows the simplified heat & mass balance and the heat integration diagram of the CaL based pre-combustion CO_2 capture process modelled in ASPEN Plus. The table 2.5 shows the main simulation parameters and the main simulation outputs of the gasifier, carbonator and calciner together with an overall process output summary. The calculated net electricity and hydrogen production efficiencies are 12.6 & 46.8% respectively. The latter is based on the LHV of the hydrogen. Moreover, the prior defined equivalent electrical efficiency was calculated as 40.7%. The overall CO_2 capture efficiency of the process is more than 96.5%. The CO_2 stream is compressed to 152 bar. It can be observed here as well that the overall CO_2 capture efficiency is more than the carbonator itself for the same reason explained in the post-combustion case. The purity of the hydrogen obtained in the carbonator is higher, above 94%-vol, than air blown AER processes since it is an oxygen blown gasification process. This process seems to be an interesting fuel conversion process applicable for coal. A comparison with the literature is not possible as up to the author's knowledge there is no process reported in the literature with the same configuration.

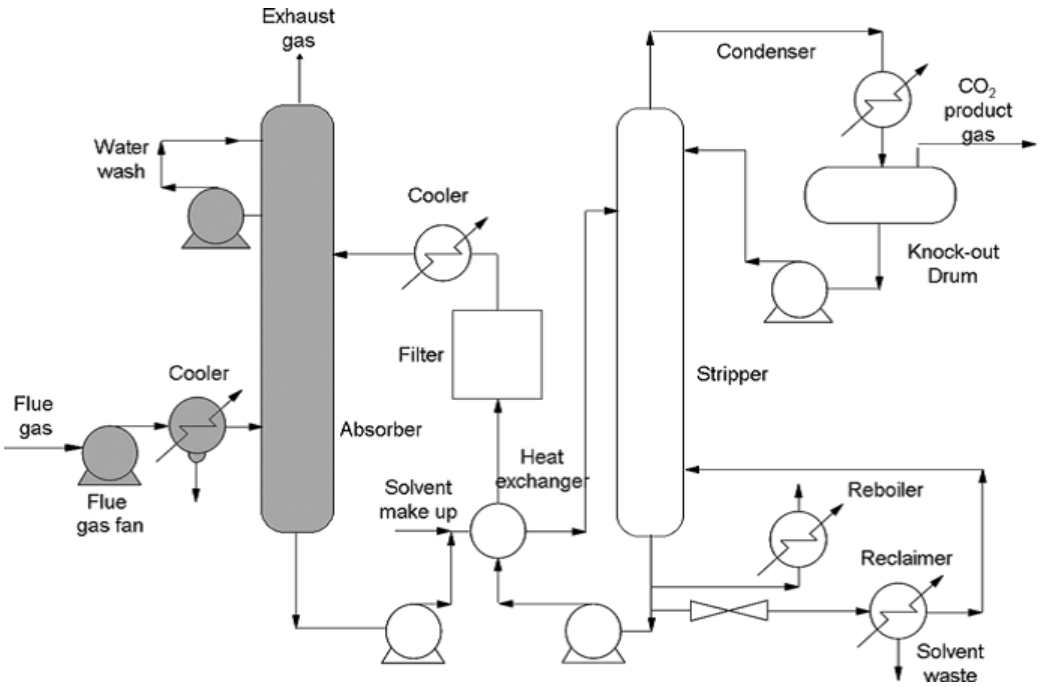

Figure 2.11: MEA process scheme for CO_2 separation, Spliethoff [2010]

2.3 Solvent based processes

2.3.1 MEA solvent

This absorption process technology is a well-established method of separating CO_2 and practiced for more than 65 years in petroleum industries. Moreover, the mechanisms and involved thermodynamics are well known. A most common and traditional solvent that can be used for CO_2 absorption is monoethanolamine(MEA). Figure 2.11 shows the process scheme with a CO_2 absorber and a stripper. The flue gas from a fossil fuel based power plant is passed through the absorption column in which MEA selectively absorbs CO_2. This CO_2 laden solution is then sent to the stripper column in which the CO_2 is released by thermal regeneration. As a general rule, high pressure and low temperature favor absorption, while low pressure and high temperature result in regeneration of the solvent. In general absorption systems the pressure can be manipulated to enhance absorption/desorption. However in MEA process, temperature manipulation to release the CO_2 and regenerate the MEA makes up 70–80% of the operating cost. The main areas of improvement for this process are finding a new solvent or refining the existing method to minimise regeneration conditions Aaron and Tsouris [2005].

However, there are concerns with the use of MEA for capturing CO_2 from combustion flue gas:

- Corrosion of equipments in the presence of O_2 and other impurities
- High solvent degradation rates due to reaction with oxygenated impurities

- Potential emissions of solvent to the environment

The efficiency penalty for CO_2 capture from a pulverised coal power plant is reported to be about 10-12%-points for the MEA-scrubbing, Florin and Fennell [2010].

2.3.2 Other solvents

There are number of solvents that can be easily regenerated. New solvents operating on the same principles as MEA are being developed. A promising absorption process is based on the KS-1^{TM}, KS-2^{TM} and KS-3^{TM} solvents developed by Mitsubishi Heavy Industries. This family of solvents shows higher CO_2 loading per unit solvent, lower regeneration conditions and almost no corrosion, degradation, or amine loss. Moreover, a novel packing material, KP-1^{TM}, was also developed to further improve this process. Refrigerated Methanol is also used as a solvent in most of the commercial acid gas removal processes. It is known as Rectisol^{TM} process and patented by Linde AG and Lurgi AG. Rectisol^{TM} can selectively remove CO_2 and H_2S from the syngas stream since the solubility of these components varies significantly.

Alternative mixtures derived from amines such as methyldiethanolanmine(MDEA) requires only one third of the steam necessary for regeneration compared to MEA, but on the other hand with a slower rate of CO_2 capture. Another promising sorbent which attracted a lot of attention is ammonia. Alstom is developing a chilled ammonia process, which uses only 15% of the amount of steam consumed using MEA for regeneration and also demonstrates higher CO_2 removal capacity per gram of solvent. The chilled ammonia process is likely to be even more efficient in places where cold cooling water is available, which will minimise the amount of energy needed for refrigeration, Rhudy and Black [2007]. Amine grafted on high surface area solid supports are considered to be the future generation sorbents. The advantage with these solid sorbents are that they avoid the thermal penalty associated with the use of aqueous-based amine systems. However it is suitable to mention here that the ultimate capture capacity of CO_2 currently demonstrated with supported-amines is low in comparison to alternative solid sorbents, such as CaO.

2.4 Oxy-fuel process

Oxy-fuel process involves burning a carboniferous fuel(e.g.,coal) in pure oxygen. However in reality, the combustion is carried out in a mixture of oxygen and a CO_2-rich recycled flue gas to moderate the flame temperature. Moreover, burning coal in a pure oxygen atmosphere results in an adiabatic combustion temperature of over 3500°C at which currently available materials cannot withstand, Notz et al. [2011]. Figure 2.12 shows a power plant layout based on an oxy-fuel process. The steam cycle is indicated by dotted lines. The oxygen is supplied from an air separation unit. Since the oxy-fuel method avoids

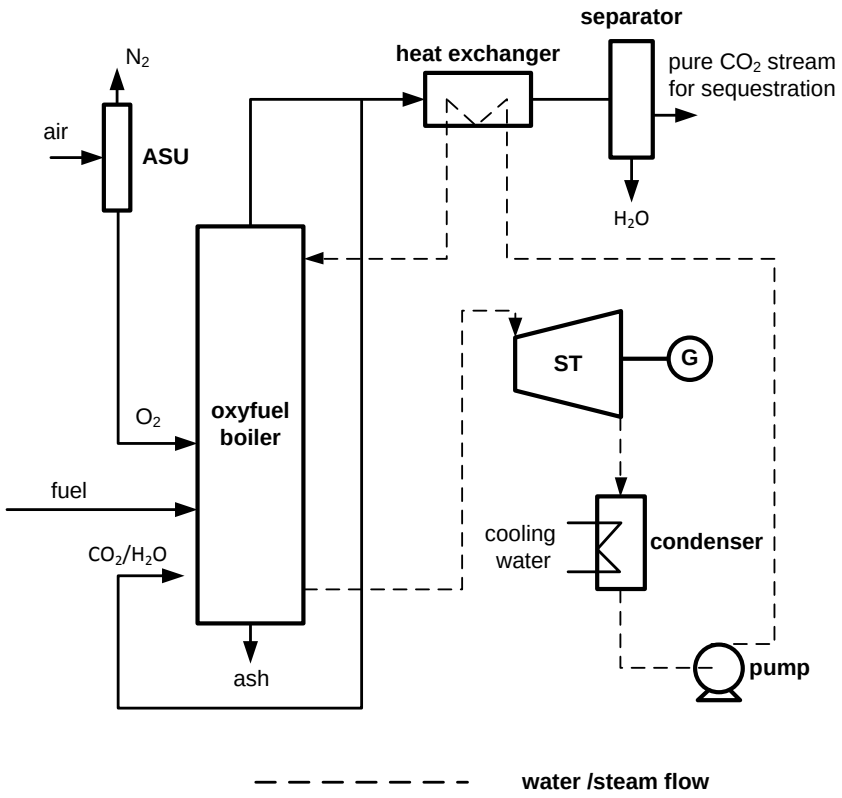

Figure 2.12: Schematic of an oxy-fuel power plant

nitrogen from the comburent, a flue gas mixture is obtained essentially with CO_2 and water vapour. As a consequence, the concentrated CO_2 can be relatively easily separated by condensing the water vapour, eliminating the use of solvents and the associated environmental impacts. At the end a stream with 70-95% CO_2 can be obtained depending on the oxygen purity, the type of fuel and particular oxy-fuel combustion process. The concentrated CO_2 stream can then be compressed and further purified before permanent storage, Spliethoff [2011], Buhre et al. [2005], Ponzio et al. [2008], Ponzio et al. [2009]. The major issue with the oxy-fuel technology is the requirement of an ASU. The present conventional cryogenic air separation is very energy intensive and expensive, Davidson and Santos [2010], Nsakala et al. [2007].

2.4.1 Air separation

The current methods of oxygen production by air separation are cryogenic distillation, adsorption using multi-bed pressure swing units and polymeric membranes. For all larger applications including power station boilers, the most economic solution among them is cryogenic air separation. This method causes a significant efficiency loss over the entire process because of its considerable energy demand. The higher the purity of the oxygen, the higher the energy per mass of oxygen and the costs. In order to switch a power plant with the net efficiency of 45% to an oxy-fuel combustion (excess oxygen 10%), about 0.6

kg of O_2 per produced kWh_{el} is required. The energy required to produce 1 kg of 99.5% purity oxygen is 0.29 kWh. This results in an energy requirement of 0.174 kWh per kWh of electrical power produced and it alone reduces the overall power plant efficiency by almost 8 percentage points. Current oxy-fuel designs assume an oxygen purity of 95% with an energy requirement of 0.23-0.25 kWh/kg O_2 (corresponding to a 6.2 - 6.8%-points efficiency loss). A further 3.5 percentage points efficiency is lost for the compression of the CO_2 to 110 bar suitable for transportation. The total loss in efficiency is then about 11-12%-points, with a slight potential reduction in the future, Spliethoff [2010].

The research and development of the oxy-fuel technology are at the stage of pilot plant demonstration. It could offer a cost effective method for CO_2 sequestration while keeps the reliability of steam power plants. However costs of an oxy-fuel process are dependent on the CO_2 purity requirements. Worldwide several demonstration projects are ongoing, or planned for the near future. Both pulverised coal and fluidised bed firing technologies are investigated, Spliethoff [2011], Wall [2007].

2.5 IGCC with carbon capture

Integrated gasification combined cycle (IGCC) process can be deployed for fuel conversion with and without the CO_2 capture. Only the latter is considered in this section to enable comparison between different CO_2 capture technologies. The concept of the IGCC process is that the fuel is converted into a syngas from which the carbon is removed before the combustion in a gas turbine followed by steam turbine. A heat recovery steam generator(HRSG) generates steam for the bottoming steam cycle. In a nut shell, after carbon is removed the syngas is fed to a combined cycle, Gray et al. [2004].

The IGCC scheme offers favourable conditions for CO_2 separation, not only because its CO_2concentration is higher but also the stream is at high pressure. Capturing CO_2 at these conditions involves less energy loss than downstream removal from atmospheric flue gas. Two additional components are required to capture the CO_2 in an IGCC power plant. The first one is the shift reactor where the CO in the syngas is shifted to CO_2 while generating H_2. The second component is the CO_2 capture loop consisting of a chemical or physical sorbent. A hydrogen rich product gas emerges after the carbon removal, Penea and Coca [2009]. Figure 2.13 shows the IGCC process block diagram with carbon capture.

2.5.1 Impact of CO_2 capture

IGCC with CO_2 capture inherently suffers from efficiency loss as of other competing process schemes. The biggest penalty is due to the water gas shift reaction itself (refer the reaction equation 2.2), as the heat of combustion of hydrogen (242 kJ/mol) is less than that of CO(283 kJ/mol). However, penalties incurred due to CO_2 removal are limited since the stream is at high partial pressure. At these conditions, an amine based

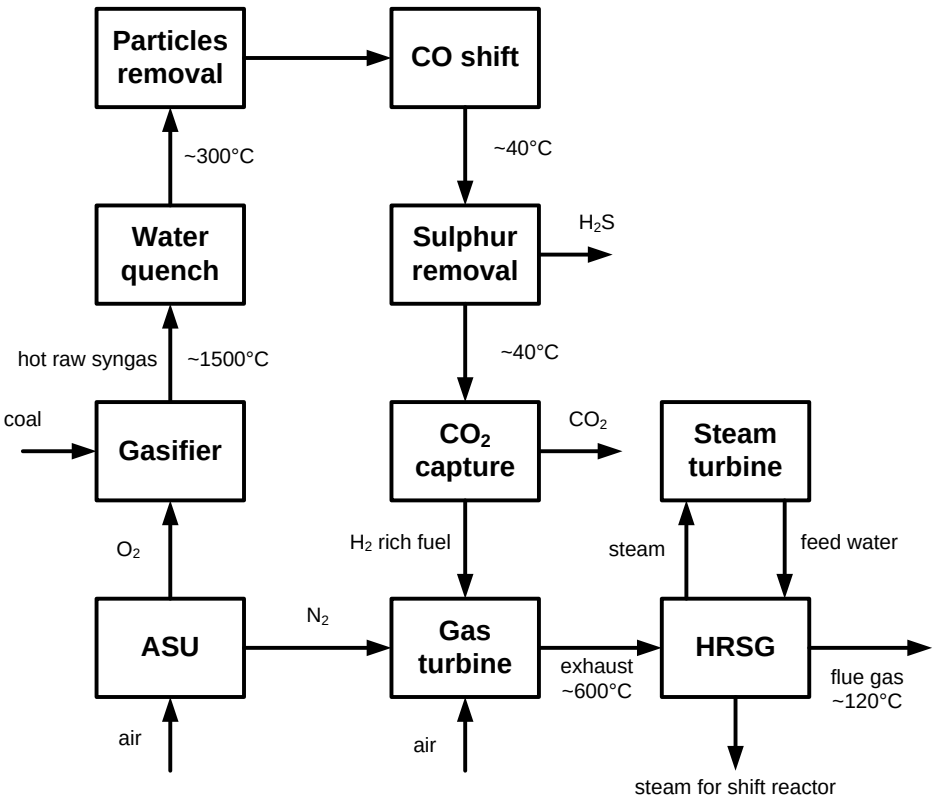

Figure 2.13: IGCC process block diagram with CO_2 capture, Spliethoff [2010]

separation requires relatively less steam and power, Prins et al. [2009]. Nowadays a two-stage Selexol^{TM} and Rectisol^{TM} processes are preferred for selective removal of sulphur and CO_2, Martelli et al. [2009]. There are number of conceptual studies focused on novel IGCC plant configurations. Kunze et al. [2011] have proposed a scheme integrating oxygen separation from air by ceramic membrane and post-combustion CO_2 capture by calcium looping. The simulation of this new IGCC concept reached a net efficiency of 43.2% based on LHV for hard coal while capturing almost 98% CO_2.

IGCC power plants can separate CO_2 with two additional components and can be regarded as the most advanced power plant technology for CO_2 separation, because the necessary additional components (CO shift and CO_2 scrubbing units) are already employed elsewhere for the production of hydrogen. Expectations are that the IGCC efficiency with CO_2 capture will drop by about 8-10%-points to settle somewhere around 42%. In a long term perspective further developments are necessary to overcome the disadvantages of low availability and high costs, Spliethoff [2010] Prins et al. [2009].

2.6 Conclusion

Fundamental aspects of the CaL based pre- and post-combustion CO_2 separation processes were discussed. ASPEN plus simulations of these two processes were performed. The CaL based pre-combustion capture process showed an equivalent electrical efficiency ($\eta_{El,eq}$) of 40.7% and the post-combustion capture process electrical efficiency(η_{El}) is 38.6%. According to the calculations the efficiency penalty for the CaL based post-combustion CO_2 capture process is about 6-7%-points, when compared to an advanced coal power plant efficiency of 45% without the CO_2 capture. Other competing technologies briefly discussed in this chapter are solvent based capture(post-combustion), oxy-fuel and the IGCC(pre-combustion). In order to provide a comparison between these competing CO_2 capture technologies, the efficiency penalties are presented from the literature. The efficiency penalties reported for MEA based process is 10-12%-points, oxy-fuel process is 11-12%-points and the IGCC process is 8-10%-points. It is important that one must be cautious when comparing process efficiency estimates because, a significant uncertainty is introduced when comparing technologies at different stages of development. Amine based post-combustion capture & the IGCC are more mature than oxy-fuel and CaL processes. Therefore it is suggested here that the large-scale demonstrations of CaL based pre- and post-combustion capture processes are required to compete with the mature technologies. A well proven but sub-optimal CO_2 capture technology is more likely to get commercialised than an optimum technology in development. It is worth to mention here that another CO_2 capture technology based on solid oxygen carriers, the chemical looping for solid fuel combustion, is way too far from commercialisation since it is still in lab-scale development stage.

Chapter 3

Analysis and comparison of sorbents

Sorbent reactivity plays a vital role in achieving high efficiencies in any CaL based CO_2 capture system. A number of parameters influence the rate of sorbent deactivation, hence the reactivity. The effects on sorbent reactivity due to the following three parameters, geographical origin of the sorbent, calcination temperature and the number of capture & release cycles are experimentally determined in various test apparatus. There are mainly two forms of calcium sorbents, limestone(mainly $CaCO_3$) and dolomite ($CaCO_3.MgCO_3$)exist in nature. Three limestone and one dolomite samples from various geological origins are used in the experiments. Samples are analysed in differential thermal analyser(DTA), thermogravimetric analyser(TGA), Scanning electron microscope(SEM)and specific surface area analyser to determine respectively the CaO content, reactivity with CO_2, texture & pore structure and specific surface area. It is revealed that high temperature calcination accelerated the decay in sorption capacity of each sample. Calculated decay coefficients also varied with calcination temperatures. Apparent calcination and carbonation rate constants are determined and compared. At low calcination temperatures (750 °C),
Dolomite 1 emerged as potential sorbent because it showed not only the highest amount of CO_2 separated per kg of parent sample but also fairly high calcination and carbonation rates. A calciner design concept is proposed to sustain the reactivity of sorbents in a CaL process.

3.1 Experimental equipments and procedure

There were three limestones, Limestone 1 - 3 and a dolomite, Dolomite 1 samples used in all experiments. The particle size of the samples are 125-180 μm and originate from diverse geographical locations.

3.1.1 Differential thermal analysis

The Differential Thermal Analyser(DTA) records the weight of the sample as a function of time and any temperature difference between the sample under study and an inert reference. Weight change of the sample and the differential temperature are plotted against increasing temperature. Exothermic/endothermic changes occurring in the sample can

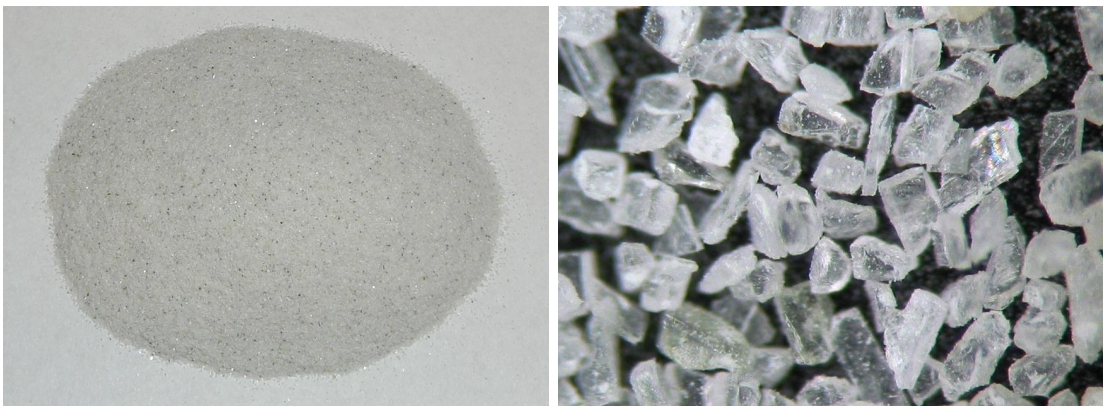

(a) Sample's bare eye view (b) Microscopic view 100X

Figure 3.1: Dolomite 1 sample

be detected by the change in differential temperature measurement. All the four samples were decomposed in DTA Model SDT Q600 version 8.3. The analyser was operated without any sample to clean up the test section. Nearly 15 mg sample, which was grounded into fine particles to avoid popping out of the sample holder during heat up, was loaded in a Platinum holder and placed on one of the two cantilevers of the analyser. The other cantilever was left with an empty sample holder. A heating rate of 20°C per minute with a purge gas flow of 100 ml/min of 100% N_2 was set. The analyser was run until it reached 1000°C to make sure 100% calcination.

3.1.2 Thermogravimetric analysis

The pressurised thermogravimetric analyser(PTGA) records the weight change of a sample against temperature. A PTGA was used to measure the sample's reactivity along with a number of calcination and carbonation reaction(CCR) cycles. The maximum operating temperature and pressure of this PTGA are 950°C and 30 bar respectively. However all the experiments were carried out at atmospheric pressure conditions as of the CaL process. A schematic diagram of the apparatus is shown in figure 3.2. The cylindrical reactor section is 24.5 cm high and electrically heated. The reactor was constructed of Incoloy 800, and lined with quartz glass to minimise the risk of corrosion. The inner diameter of the quartz glass tube is 19 mm. The sample holder is kept 17 cm from the bottom of the heated section during the experiments. The desired gas mixture of 2 litres/min was supplied by a set of gas bottles via mass flow controllers. This gas stream was preheated in the lower sections of the reactor chamber and entered into the reactor from the bottom. A purge gas flow of (inert Helium gas) 0.4 litres/min was supplied from the top of the reactor to protect the balance from corrosive gases. Both gases exit as one stream from the reactor.

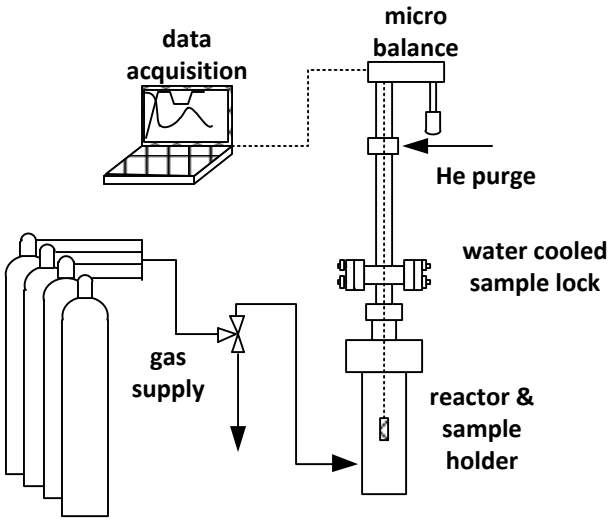

Figure 3.2: Schematic of the pressurised thermogravimetric analyser

The sample holder

The cylindrical sample holder consists of a fine mesh of Incoloy 800 and is hanged on a platinum chain connected to a winch system to move the sample holder up and down into the reactor chamber. The outer diameter of the sample holder is 10 mm, and the length is 20mm. The sample was placed in the shell between an inner core and the outer net. The thickness of the sample layer was about 1 mm. The figure 3.3 shows the assembly of the sample holder. Before the beginning of each run, the sample holder was placed in a water cooled sample lock chamber above the reactor section. Once the desired conditions are(temperature and gas composition) established in the reactor, the sample holder was lowered into the reaction chamber. The gas flow rate in the reactor has an influence on the weight signals of the thermo balance. In order to determine the buoyancy and the drag forces, a zero run with inert sample(Quartz) was made. For all different types of experimental conditions, the weight of the sample and the temperature of the reaction chamber were logged at certain interval between 1-1000 s.

3.1.3 Scanning electron microscopy analysis

The Scanning Electron Microscope (SEM) can be used to analyze the texture and the composition of samples. The pore structures of the calcined as well as carbonated samples were analysed in an SEM. There were two different methods used to prepare the samples for this analysis. In order to see the cross-section of the sample, epoxy resin was used to clamp the particles as seen in figure 3.4a. Then it was polished with number 1000 sand paper and ethanol, cleaned in vacuum and carbon coated with a carbon thread to get its surface conductive before being loaded into the SEM. In this way the particles' cross-sections could be analysed.

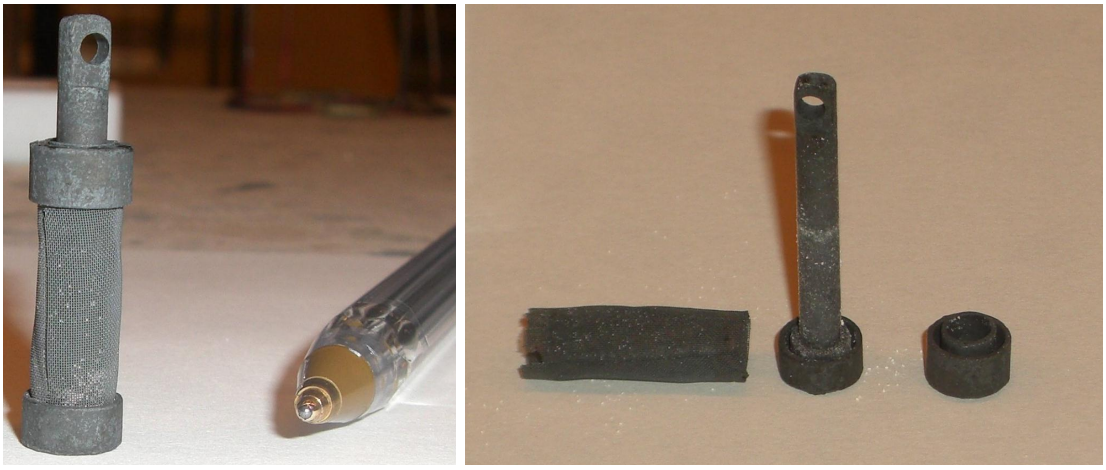

(a) Sample holder (b) Sample holder assembly

Figure 3.3: TGA sample holder

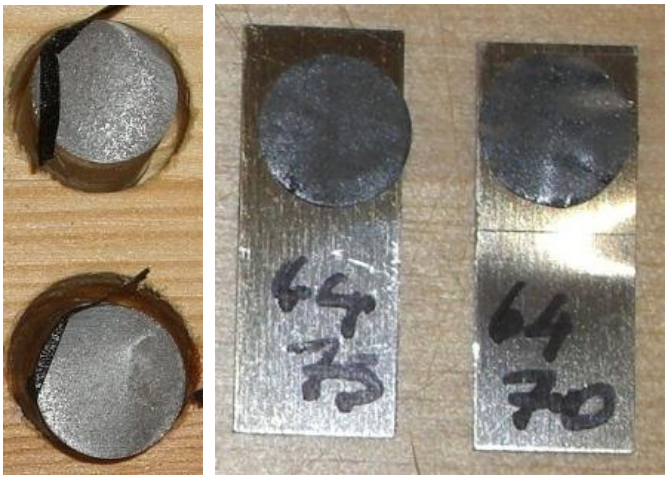

(a) (b)

Figure 3.4: Samples mounted for SEM analysis (a) on epoxy resin (b) on carbon tape

The second sample preparation method was used for the particles' surface analysis. The particles were placed on a sticky carbon tape which was then placed on thin narrow Aluminium plate as seen in figure 3.4b. The samples were cleaned in vacuum while carbon was coated to increase the conductivity to be able to analyse in the SEM. In some cases, limestone samples were crushed between two plates before being placed on to the sticky carbon tape, in order to reveal fresh inside pore structures.

3.1.4 Specific surface area analysis

The Brunauer Emmett Teller(BET) specific surface areas of the samples were measured using Carlo Erba Sorptomatic 1900 apparatus. The samples were analysed before and after calcinations for two different temperatures. This measurement was based on the isothermal adsorption of nitrogen and the surface area was calculated by a multi point method. A separate furnace was used to produce samples for this BET measurements as the minimum amount required for this analysis is about one g which is far higher than what was obtained from the PTGA.

3.2 Experiments, Results and Analysis

3.2.1 Carbonate content calculation by DTA&TGA

By DTA measurements

DTA experiments were carried out to measure the carbonate content and existence of impurities in the sample. The result for Limestone 1 calcination obtained from the DTA (Model SDT Q600 version 8.3) is shown in figure 3.5. The temperature difference curve shows only one downward peak, referring to the endothermic phase change of $CaCO_3$ to CaO. The carbonate content of the sample can be calculated from the weight loss during the same phase change. The following formula was used to calculate the carbonate content of the samples.

$$Carbonate\ content\ [\%-wt.\,] = \frac{\frac{wt.\,loss}{M_{CO_2}} \times M_{CaCO_3}}{initial\ wt.\ of\ the\ sample} \times 100 \tag{3.1}$$

By TGA measurements

The carbonate contents of the samples were also calculated using the TGA data and the equation 3.1. The averaged value from several TGA measurements were compared with the value obtained from DTA for each of the sample and tabulated in table 3.1. Both values tally very closely. However the DTA figures are slightly higher than TGA, perhaps the 1000°C heating, instead of 930°C in the TGA, ensured 100% calcination in DTA.

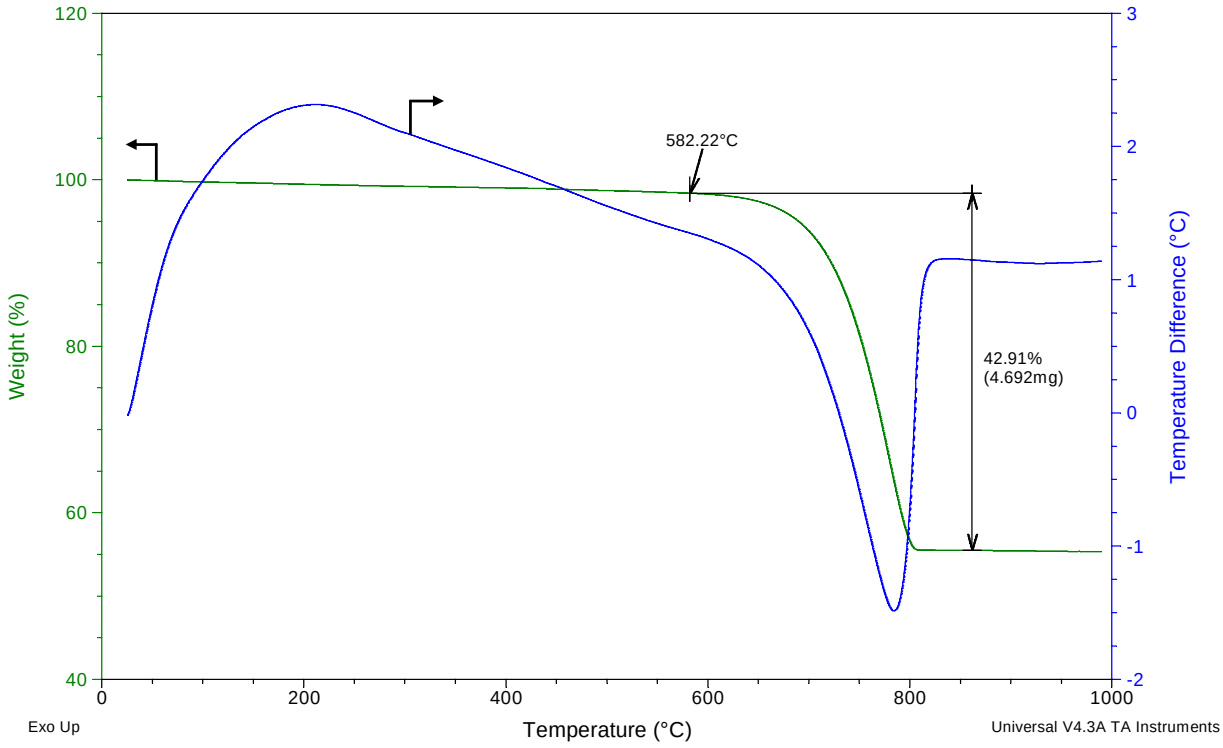

Figure 3.5: DTA analysis of Limestone 1

There had been a slight weight loss continuouly registered by the DTA util it reached 1000°C. The dolomite 1 contains 61.63%-wt of $CaCO_3$ as calculated by TGA data. It was unable to separate the weight loss due to $CaCO_3$ and $MgCO_3$ decomposition from the Dolomite 1's DTA curve. So that in case of Dolomite 1, a varification with the DTA was not possible.

3.2.2 Reactivity calculation and comparison

The reactivity and the CO_2 capture capacity of the samples were calculated respectively based on the rate and the degree of CaO mol-% to $CaCO_3$ conversion during carbonation.

Table 3.1: Carbonate content(%-wt) of the samples calculated by DTA&TGA measurements

	Carbonate content of the samples	
	by DTA measurement	**by TGA measurement**
Limestone 1	97.52	94.64
Limestone 2	84.25	80.42
Limestone 3	98.97	93.28
Dolomite 1	-	61.63

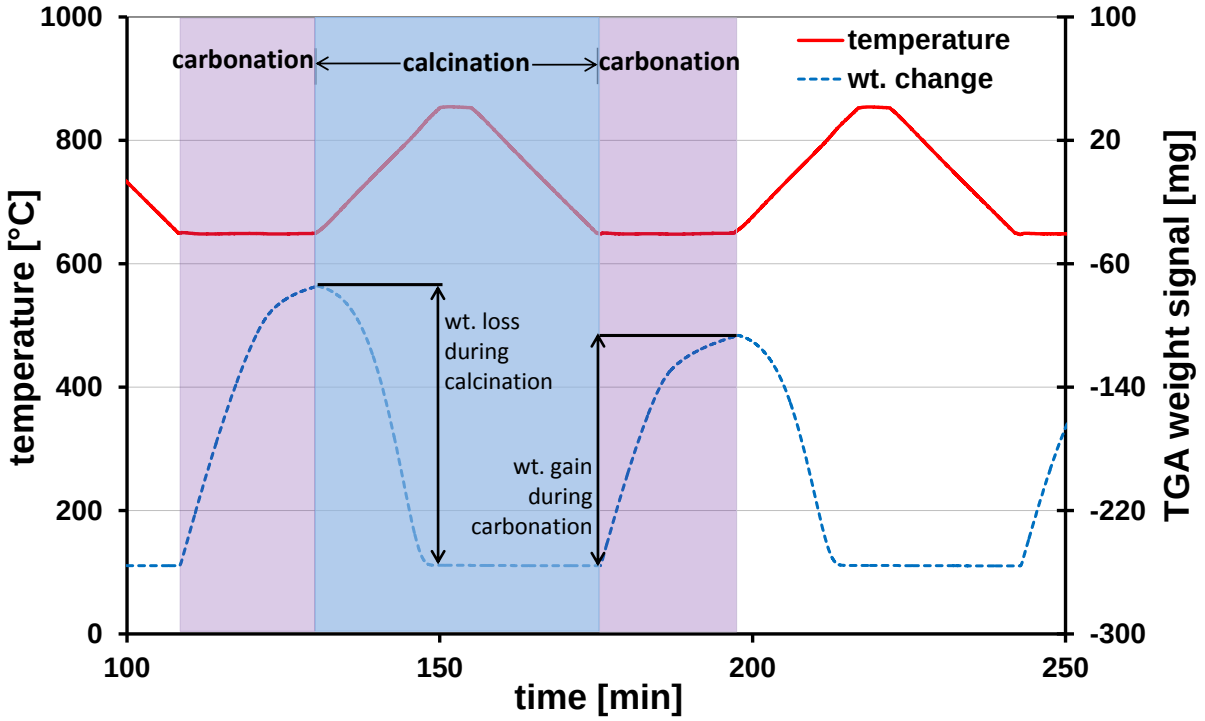

Figure 3.6: Typical TGA curve showing calcination&carbonation cycles

TGA experiments were used to obtain the data for all conversion calculations. In all the TGA test runs the carbonation conditions were kept unchanged at 650°C isothermal, atmospheric pressure, the duration at 400 seconds and the flue gas composition at 20%-vol CO_2 and 80%-vol N_2. The temperature of the carbonation had been chosen according to the $CaCO_3$-CaO phase equilibrium data and the flue gas compositon represents a typical maximum CO_2 concentration of a coal power plant. The flue gas was continuously flowing through the reactor. However the calcination conditions were varied, in particular the calcination temperatures were set as 750°C, 800°C, 875°C and 930°C. In all cases the calcination occurred in 100%-vol N_2 environment. In each test, the carbonation/calcination cycle was repeated for four times.

Figure 3.6 is a typical TGA curve showing several CCR cycles. Both temperature and weight change of the sample were plotted together. In this particular case the carbonation temperature is 650°C and the calcination temperature is 850°C. The inlet CO_2 concentration was kept at 15-%-vol during the carbonation phase and pure N_2 for the calcination phase.

The conversion of CaO mol-% to $CaCO_3$ for each of the tests was calculated by assuming that the weight gain of the sample was due to the CO_2 reacting with CaO-carbonation. The following equation was used to calculate the CaO mol-% conversion during the carbonation:

$$CaO\ to\ CaCO_3\ conversion, \lambda\ [mol-\%] = \frac{wt.\ gain\ during\ carbonation}{total\ wt.\ loss\ during\ first\ calcination} \times 100 \tag{3.2}$$

$$CaCO_3\ to\ CaO\ conversion\ [mol-\%] = \frac{wt.\ loss\ during\ calcination}{total\ wt.\ loss\ during\ first\ calcination} \times 100 \tag{3.3}$$

Comparison of CaO conversions against the type&origin of sample

The rate and the degree of CaO mol-% conversions were calculated and compared for type and origin of samples. The samples were calcined at 875°C in pure N_2 and carbonated at 650°C&20%-vol CO_2 for 400 seconds. Figure 3.7 shows the conversion of CaO mol-% for the 1^{st} carbonation as a function of the residence time in a TGA for all four samples. The Dolomite 1 showed the highest conversion of all limestone samples though it has the lowest CaO content. Among the limestone samples, Limestone 3 showed the highest conversion and the Limestone 2 was the lowest. One can observe a significant difference in conversion of Dolomite 1 (83 mol-%) and Limestone 2, which showed the lowest conversion(56 mol-%). It can be stated based on the various degrees of conversion shown by the samples that the geographical origin and the type of sample play a vital role in the initial conversion of CaO, i.e. the CO_2 capture capacities of natural sorbents.

The reaction rate variation of each individual sample is also visible in figure 3.7. There are clearly two distinct reaction phases existing in each of the carbonation. The first and faster phase which lasted for ∼60 s, followed by a much slower phase. The initial fast reaction occurs when the fresh CaO surfaces are exposed to the reaction gas CO_2, which spontaneously react and form a $CaCO_3$ product layer over the exposed surfaces. The highest rate is shown by the Dolomite 1 and the lowest is Limestone 2 during this phase. A rapid change of reaction rate can be seen during the second phase. The shift in reactivity is attributed to the diffusion resistance offered by the $CaCO_3$ product layer formed during the first reaction phase. The reaction gases need to penetrate the readily formed $CaCO_3$ coating to reach unreacted CaO remain underneath. Moreover the observed shift in reaction rate implied the existence of a critical product layer thickness beyond which the reaction would go into the second slow phase. This critical product layer thickness was measured as 49 nm by Alvarez and Abanades [2005b].

Comparison of CaO conversions against the calcination temperatures

The rate and degree of CaO mol-% to $CaCO_3$ conversions were compared with changing calcination temperature. The Limestone 1's calcination temperatures were varied as 750°C, 800°C, 875°C and 930°C and the corresponding CaO mol-% conversions for the 1^{st} CCR cycle were ploted against the temperatures in figure 3.8. The carbonation conditions were kept at 650°C isothermal and 20%-vol CO_2 and lasted for 400 seconds.

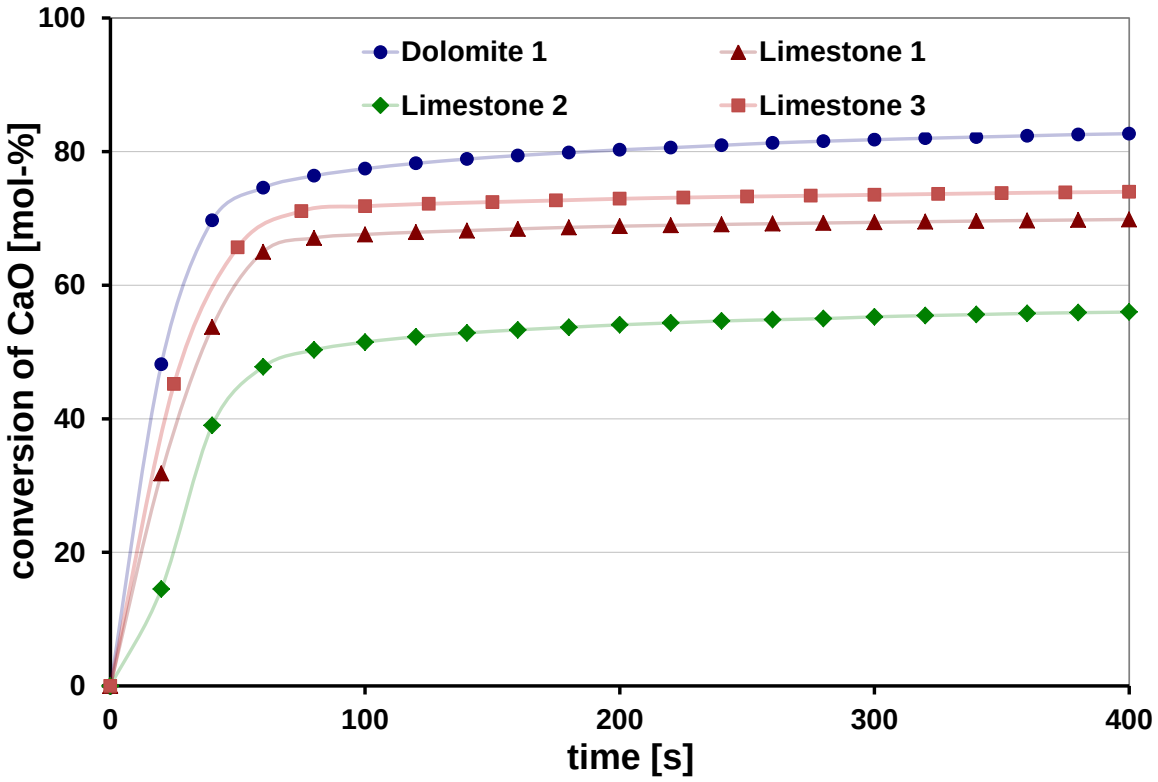

Figure 3.7: Comparison of CaO mol-% conversion against types of samples

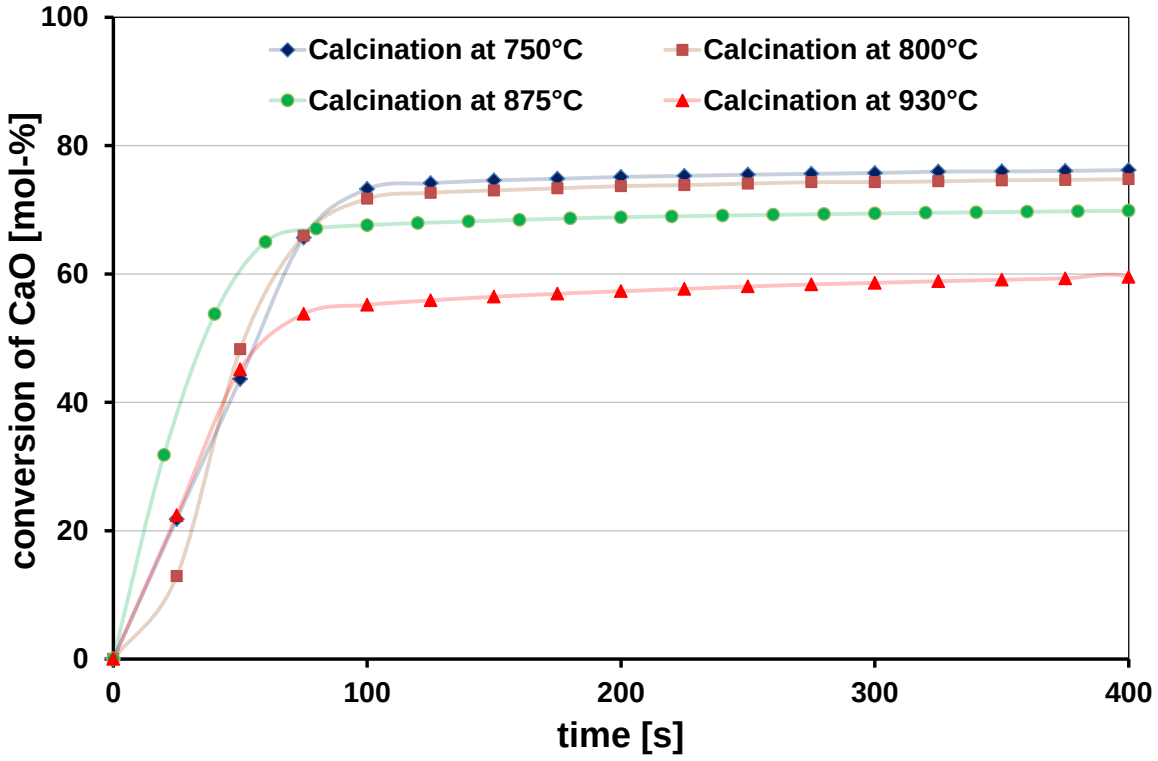

Figure 3.8: Comparison of CaO mol-% conversion against calcination temp. for LS 1

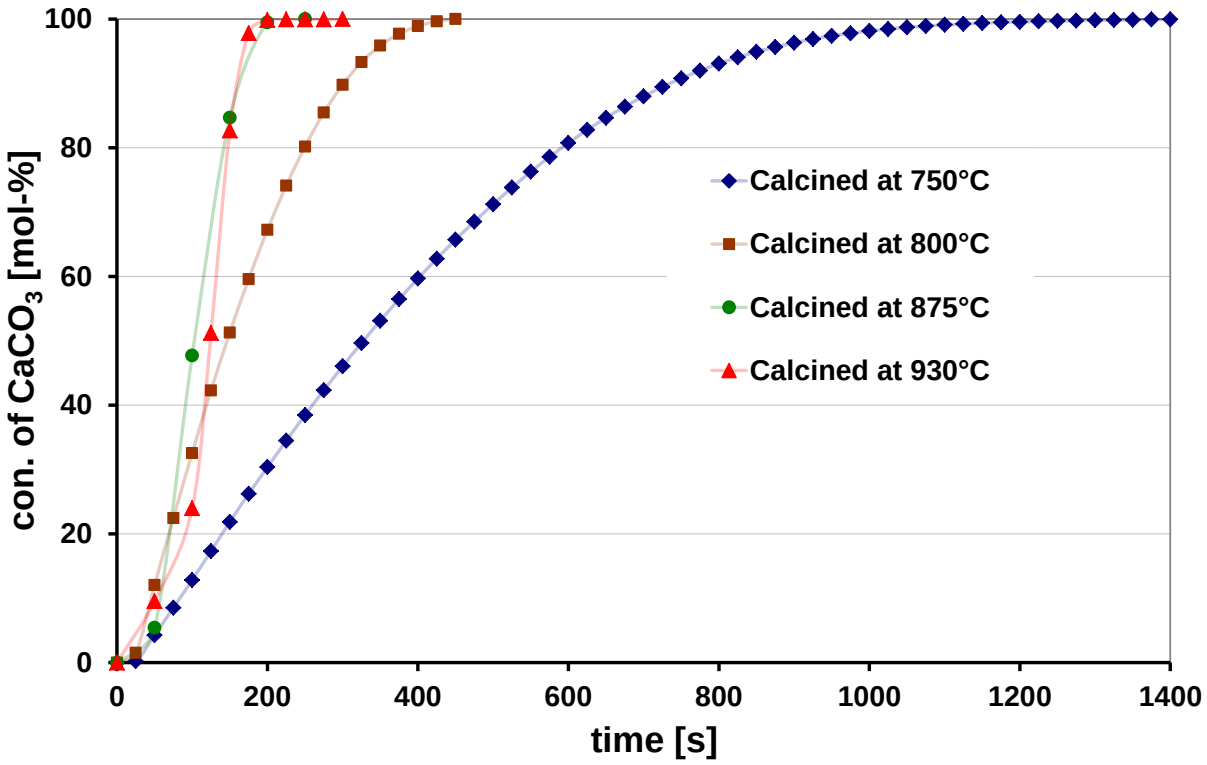

Figure 3.9: Comparison of $CaCO_3$ to CaO mol-% conversion against calcination temperatures

It is seen in figure 3.8 that the higher the calcination temperature the lower the conversion of CaO mol-% to $CaCO_3$. At relatively low calcination temperatures of 750°C and 800°C, there is not much difference in total conversions. But the difference is significant between 800°C and 875°C and also between 875°C and 930°C. The reason for this decreased conversion at high calcination temperatures may be referred to the sintering of particles. Sintering is a process that bonds the adjacent surfaces of particles by heating. The higher temperatures enhance this process thus reducing the specific surface area of the sorbents. The lower the specific surface area the lower is the carbonation conversion. A qualitative and quantitative analysis of the specific surface areas of the sorbents will be presented in sections 3.2.5 & 3.2.5.

It is also interesting to look at the plot in figure 3.9, which shows the 1^{st} calcination of Limestone 1($CaCO_3$ to CaO mol-%) as a function of the residence time in the TGA at various temperatures. There is no significant calcination rate differences observed between 930°C and 875°C, however it differs between 750°C, 800°C and 875°C. It can be concluded that the calcination rate increased with increasing temperature and a rapid calcination(within 400 s) was ensured beyond 875°C. Higher calcination temperature on the other hand, reduces the specific surface area of the calcined particle.

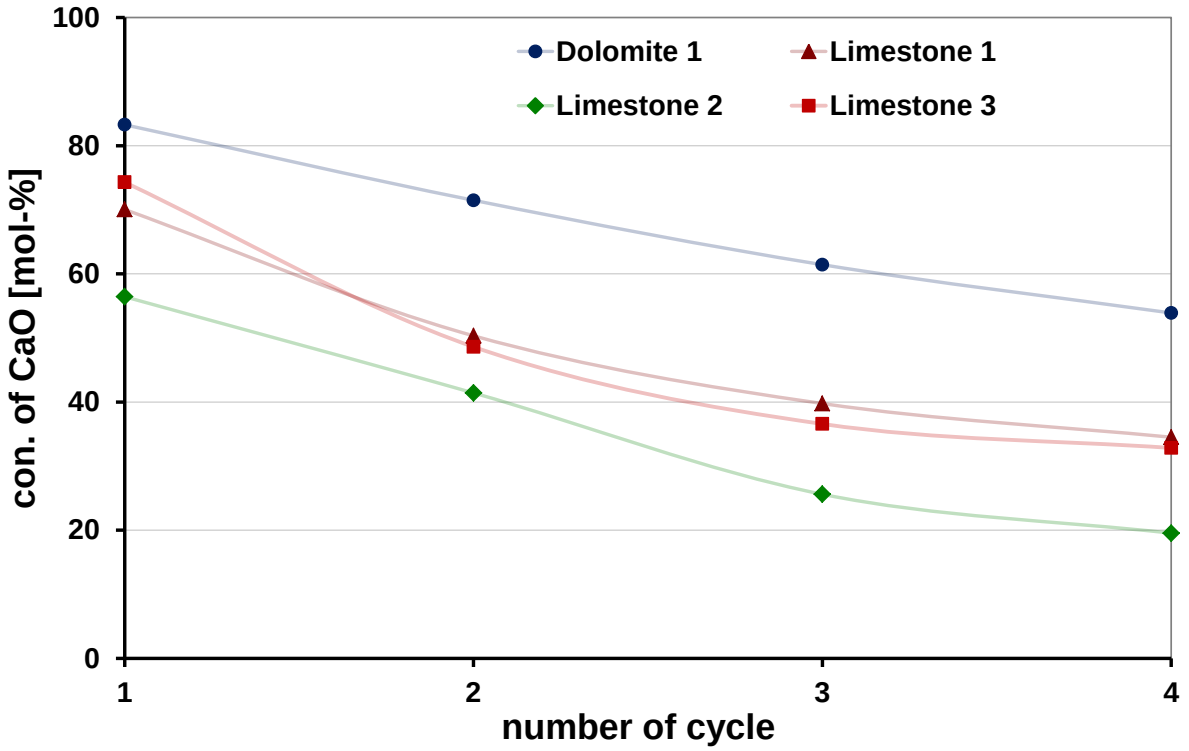

Figure 3.10: Comparison of CaO mol-% conversion against the number of CCR cycles, calcination at 875°C

Comparison of CaO conversions against the number of CCR cycles

Figure 3.10 shows the samples' CaO mol-% to $CaCO_3$ conversion for four CCR cycles. A significant decrease in conversion with increasing CCR cycles is clearly observable. Further on, the rate of decay in conversion seems to follow a certain trend. As stated in Chapter 1, decrease in reactivity with increasing number of cycles poses a challenge to the CaL process. Measures to enhance/sustain the reactivity will be discussed in sections 3.3 and 4.2.5. In an actual CaL process, the sorbents will undergo hundreds of CCR cycles before being replaced by makeup flows. The data of the four CCR cycles from this experiments were used in a model equation from the literature to predict the conversions for many number of cycles in section 3.2.3.

3.2.3 Analysis of CaO conversion decay with increasing number of CCR cycles

Several semi empirical formulas are suggested in the literature for predicting the sorbent decay with increasing number of CCR cycles. Most of them are meant for a large number of cycles where the sorbents decayed to a residual conversion of 8-10 CaO mol-% in about 100 CCR cycles. Beyond that the conversion remained constant for as many as 500 cycles, Grasa and Abanades [2006]. But for a certain limited number of cycles, it is proposed by

Table 3.2: Coefficient of decay, k values of the samples

	Limestone 1	**Limestone 2**	**Limestone 3**	**Dolomite 1**
750°C calcination	0.22	0.24	0.24	0.1
875°C calcination	0.3	0.43	0.26	0.19
930°C calcination	0.44	0.52	0.59	0.28

Wang and Anthony [2005], that the decay of sorbent conversion depends on its own initial conversion; i.e., the decay is low for high initial conversion and vice versa. The following equation was used to predict the decay rates of the samples:

$$\lambda_n = \lambda_{n-1}\left(1 - k\lambda_{n-1}\right) \tag{3.4}$$

where, λ is the conversion of CaO mol-% to $CaCO_3$, n is the number of CCR cycle and k is the coefficient of decay. The k values for 750°C, 875°C and 930°C calcinations were calculated by a curve fitting exercise and tabulated in table 3.2. It can be seen that the Limestones' k values for the 750°C calcination are similar and much smaller than those of the high temperature calcinations (875°C & 930°C). However, at higher calcination temperatures, the decaying rates differ significantly among the samples. Remarkably the Dolomite 1 has the lowest decaying rate in all calcination temperatures and its decay coefficient at the highest calcination temperature is nearly the same as that of the limestones at low temperature.

Calculated and measured conversions (CaO mol-% $CaCO_3$) are plotted against each other in figure 3.11. The deviations are seemed to confine within ±10%. Overall the predictions are in good agreement with the measured values while the best fits are observed at higher conversions i.e., at low calcination temperatures, except the LS 2 which conversion was over predicted at the 1^{st} cycle. At 930°C calcinations, DM 1 conversions were over predicted for the 2^{nd} and 4^{th} cycle.

The decay coefficients from the table 3.2 were used to calculate the conversions of samples in 25 CCR cycles. It has been decided to calculate only for 25 CCR cycles because the formula has been validated with the TGA measurements for 21 CCR cycles with the data obtained form the section 4.2.1 in chapter 4. Figure 3.12 shows the measured and the calculated CaO to $CaCO_3$[mol-%] conversions against the number of CCR cycles of a limestone sample. It can be seen that the predicted values are closely tally with the measured TGA values. The decay coefficient(k) of the limestone sample was 0.275.

Therefore, based on the decay coefficients the CO_2 capture potential of a kilogram parent sample in 25 CCR cycles was summed up and plotted against the calcination temperatures of 750°C, 875°C and 930°C in figure 3.13. At each of the three calcination temperatures, various individual samples show highest capture potentials. At the lowest calcination temperature (750°C), DM 1 shows the highest capture potential. Among other

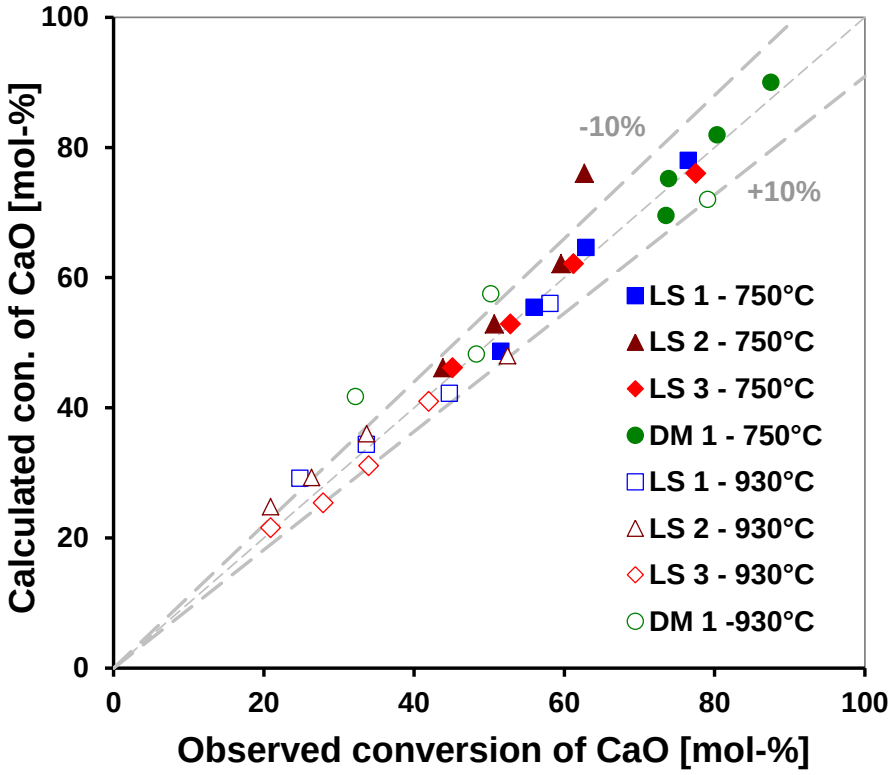

Figure 3.11: Comparison of CaO mol-% conversion for all four CCR cycles at 750°C & 930°C - measured vs calculated

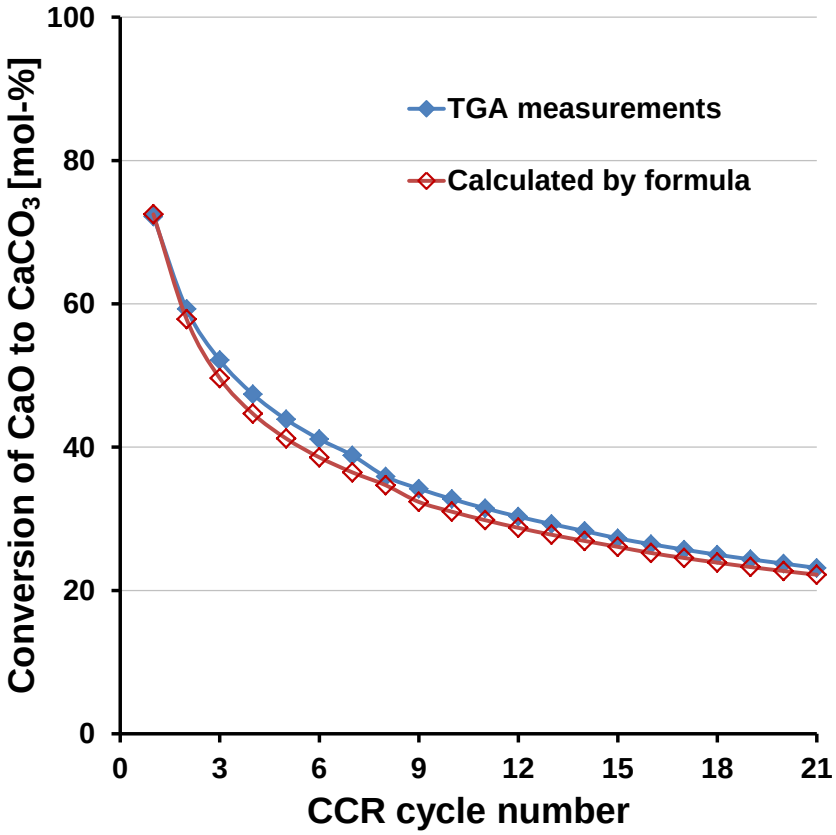

Figure 3.12: Measured and calculated CaO to $CaCO_3$[mol-%] conversions against the number of CCR cycles of a limestone sample

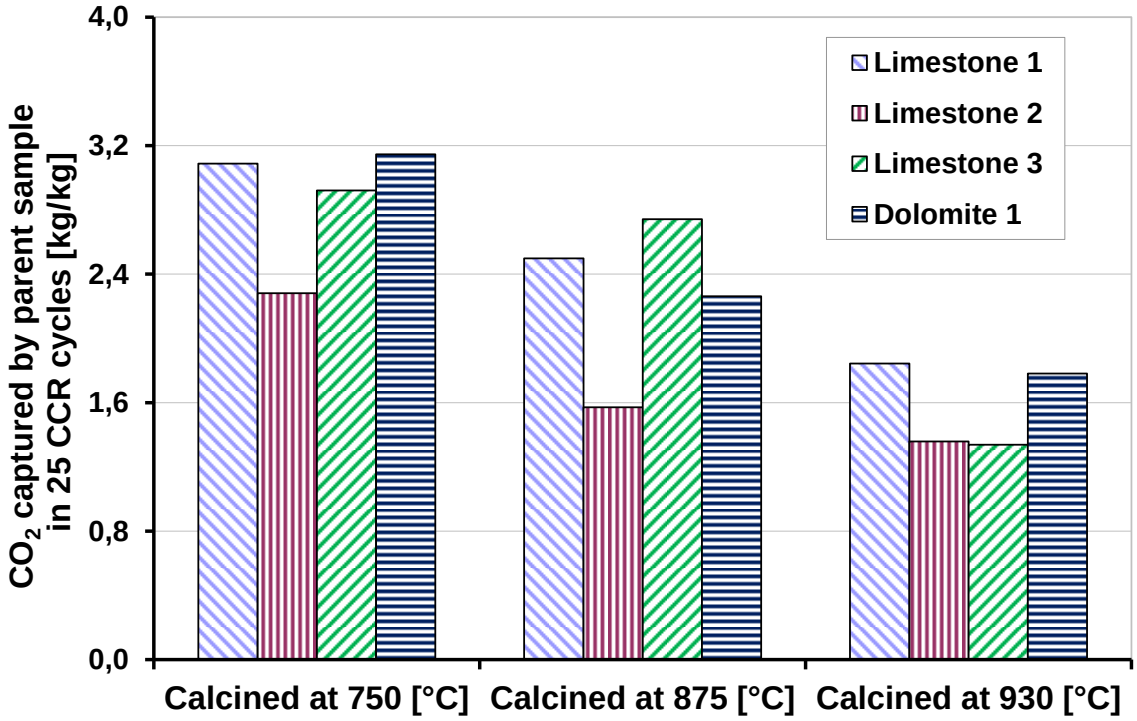

Figure 3.13: Calculated CO_2 capture potentials of one kg of parent samples in 25 CCR cycles

samples at 930°C calcination, LS 1 has the highest capacity and similarly at 875°C, LS 3 has the highest. In all three calcination temperatures, DM 1 showed either the highest or was close to the highest capture potential. This phenomenon clearly suggests the potential benefit to deploy dolomite rather than limestones in CaL processes, especially at low temperature calciner operations. Moreover, in a CaL scheme, the choice of an effective sorbent seems to depend also on calciner operating temperature.

3.2.4 Analysis of carbonation and calcination rates

The general form of Jander's equation, frequently used for solid-gas reactions, can be adapted for the carbonation reaction, Aihara et al. [2001]. It is expressed in the following equation.

$$Kt = \left[1 - (1 - \alpha)^{1/3}\right]^r \tag{3.5}$$

where, t is time (s), α is the fraction of reaction completed in time t (-), K is the reaction rate constant (s^{-1}) and r is reaction order (-). When r=1, the rate determining step is chemically controlled and if the rate determining step is diffusion, r=2. Carbonation is also divided into two reaction phases. A fast reaction phase which occurs on the surface of the reacting particles is followed by a second phase of diffusion controlled slow reaction. The fast carbonation reaction can be analysed by substituting r=1 in equation 3.5 and

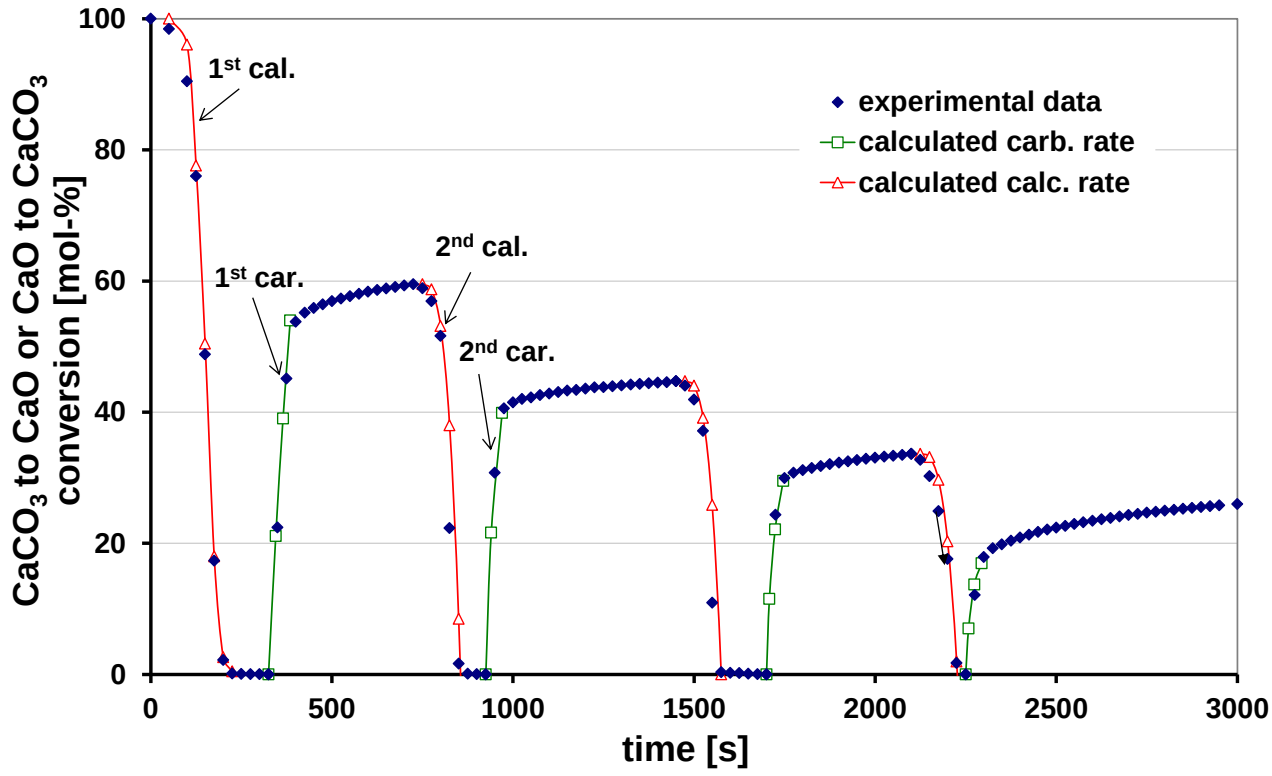

Figure 3.14: LS 1's calcination and carbonation rates calculated by equation 3.5 & compared to the measured rate

for the second diffusion controlled phase r=2. However, only the fast reaction phase was analysed in this study since it happens in a real CaL process. In case of calcination, the reaction ratio α was replaced with (1-α), as it is a reverse of carbonation reaction. Again, r=1 was substituted, assuming that the rate determining step during calcination was the surface interface reaction. Figure 3.14 shows the experimental and the predicted conversions ($CaCO_3$%-mol to CaO and CaO mol-% to $CaCO_3$) of four CCR cycles of the Limestone 1. The sample was calcined at 930°C and carbonated at 650°C in 20% CO_2 & the rest N_2. It can be observed that the predicted values closely tallied with those of the experimental points.

The K_{calc} values for four CCR cycles of all the samples were tabulated in table 3.3. Higher and scattered K_{calc} values were observed at 930°C compared to 750°C for all the types of samples. At 750°C, K_{calc}s were around 0.002 s^{-1}. These values did not change significantly either with the increasing number of CCR cycles or in between the samples. That means, at low temperatures, calcination occurred at a slow and equal rate regardless of sample variations and number of CCR cycles. At 930°C, K_{calc} varied significantly between the samples but not considerably with the number of CCR cycles. Limestone 1 and Dolomite 1 calcined faster than Limestone 2 and Limestone 3. However, these rate variations would not make a significant change in total calcination time as it was as short as 200 seconds at this temperature (930°C).

Table 3.3: Apparent calcination rate constant, K_{calc} of the samples - calcined at 750°C and 930°C

	$\mathbf{K_{cacl}x\ 10^3\ s^{-1}}$							
	Limestone 1		**Limestone 2**		**Limestone 3**		**Dolomite 1**	
	750°C	**930°C**	**750°C**	**930°C**	**750°C**	**930°C**	**750°C**	**930°C**
CCR cycle 1	2	8.5	2.5	4	2.5	4	2	8
CCR cycle 2	1.6	9.5	2	4	2	4	2.2	5.5
CCR cycle 3	1.9	10	2.5	4	2	4	2.2	8
CCR cycle 4	1.9	9.8	2.5	4.5	2	5	2.5	8

Table 3.4: Apparent carbonation rate constant, K_{carb} of the samples - calcined at 750°C and 930°C

	$\mathbf{K_{carb}x\ 10^3\ s^{-1}}$							
	Limestone 1		**Limestone 2**		**Limestone 3**		**Dolomite 1**	
	750°C	**930°C**	**750°C**	**930°C**	**750°C**	**930°C**	**750°C**	**930°C**
CCR cycle 1	4.7	3.8	3.1	4.7	4.2	4.7	5.1	3.8
CCR cycle 2	4.7	5.2	4.9	1.6	3.5	4.7	5	5.2
CCR cycle 3	4.7	5	4.3	1.2	4.7	4.7	5.1	5
CCR cycle 4	4.7	3	3.5	1.8	4.2	3	5.1	3

Table 3.5: BET surface area of the LM 1 and DM 1

	Raw sample (m^2/g)	**Calcined at 750°C (m^2/g)**	**Calcined at 875°C (m^2/g)**
Limestone 1	0.027	6.032	4.980
Dolomite 1	0.030	26.925	22.753

Similarly, the apparent carbonation rate constants (K_{carb}) were tabulated in table 3.4 with the number of CCR cycles for the samples calcined at 750°C and 930°C. K_{carb} values of all samples except Limestone 2 were between 0.003 to 0.005 s^{-1} despite different calcination temperatures. That means that carbonation rates of the samples did not seem to be affected by variations in the calcination temperatures. It has to be noted that only the fast carbonation phase was considered in this analysis and it occurs on the surface of a particle as explained previously. As an exception, Limestone 2 showed varying carbonation rates with calcination temperature. K_{carb} of Limestone 2 was lower at higher calcination temperature and vice versa. Since it is the fast carbonation phase, the differences in the carbonation rate would have less effect on the total carbonation time. However, the K_{calc} and K_{carb} analysis provided a useful means to compare the different samples used in this study.

3.2.5 Analysis of the samples' surface areas and texture

BET surface area analysis

It was shown in section 3.2.2 that the low calcination temperatures led to high CaO to $CaCO_3$ conversions for all tested samples. Since the carbonation time was limited to 400 seconds in this study, only the first&fast phase reaction could take place over the surface of the particle. The BET surface areas were measured to quantify the differences caused by varying calcination temperature. Samples from Limestone 1 and Dolomite 1, fresh and calcined at 750°C and 875°C, were used for the BET specific surface area measurement. The results are shown in table 3.5.

The BET specific surface areas of the calcined Limestone 1 and Dolomite 1 are 200 and 750 times higher than the respective raw samples. Moreover, the higher the calcination temperature the lower the BET surface area. It can be explained that a slow release of CO_2 at low calcination temperature (corresponds to small calcination rate constant, K_{calc} in table 3.3) produced a higher BET surface area. However at higher temperatures, sintering of particles could have resulted in low BET surface areas. When comparing the BETs with the types of samples, calcined Dolomite 1 showed nearly 5 times higher BET than that of the Limestone 1 for the same calcination conditions. Dolomite 1's highest surface area may have been the reason behind its exhibited highest conversion (CaO mol-% to $CaCO_3$) in all the experiments. These BET measurements provided a quantitative

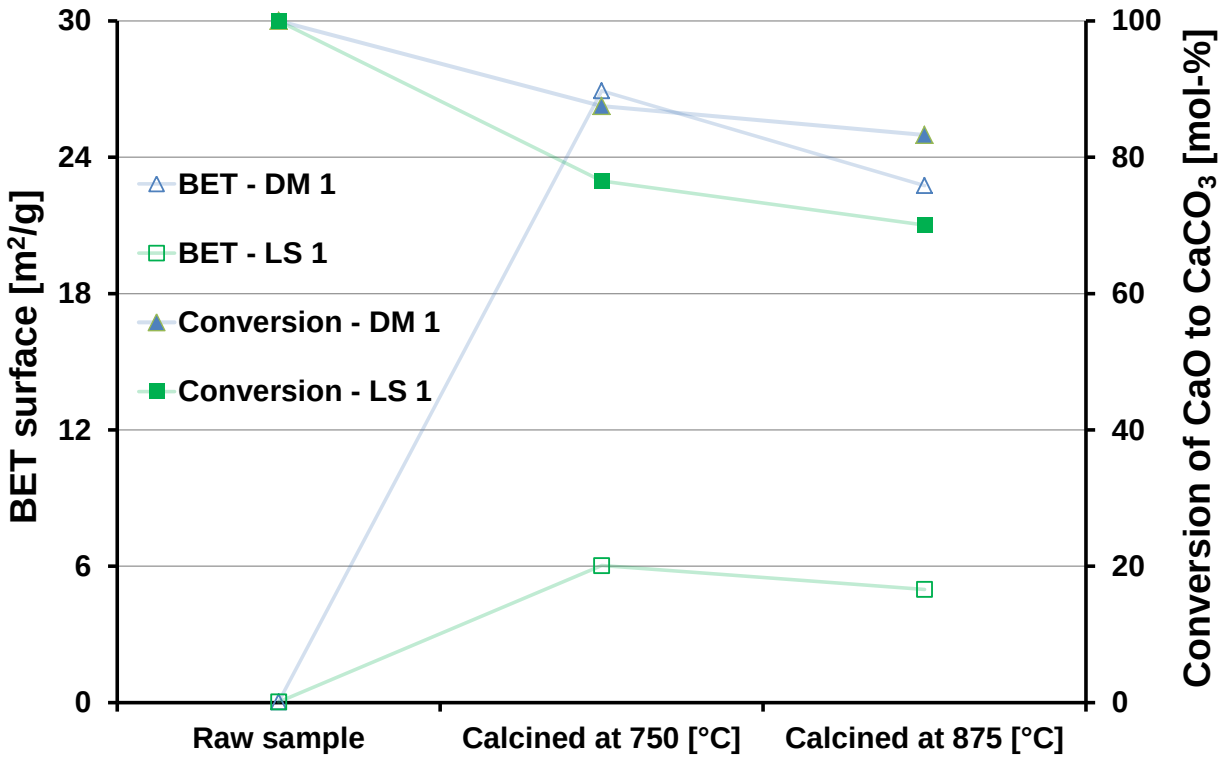

Figure 3.15: BET surface areas and respective conversions of LS 1 and DM 1 at 750°C & 875°C

evidence for the effect of calcination temperatures over the carbonation conversion.

The BET surface areas of raw and calcined samples of Limestone 1 and Dolomite 1, along with their respective CaO mol-% to $CaCO_3$ conversions were plotted in figure 3.15. The conversion of raw sample was considered as 100%. The conversion decreased with decreasing BET surface area between 750°C and 875°C calcinations. It is visible in the same figure that the reduction in specific surface area of Dolomite 1 from 750°C to 875°C calcination is higher than that of the Limestone 1. However its value is still several times higher than the LS 1 at 875°C.

SEM analysis

The SEM images of Dolomite 1 and Limestone 1 samples calcined at 750°C and 875°C in 100% N_2 are shown in figures 3.17 & 3.16. The impact of calcination temperature on the surface texture of the particles can be observed by the distinct nature of the images. In both Dolomite 1 samples, the one calcined at 750°C resulted in plenty of sharp edges over the surfaces than the other calcined at 875°C. This means that the enhancing specific surface area would lead to a higher conversion of CaO to $CaCO_3$ as evidenced in section 3.2.2. At 875°C, the calcination produced rather smooth edged surfaces which account to less surface area and lead to low conversion. These images provided qualitative evidence to the enhanced CaO to $CaCO_3$ conversions at low calcination temperatures.

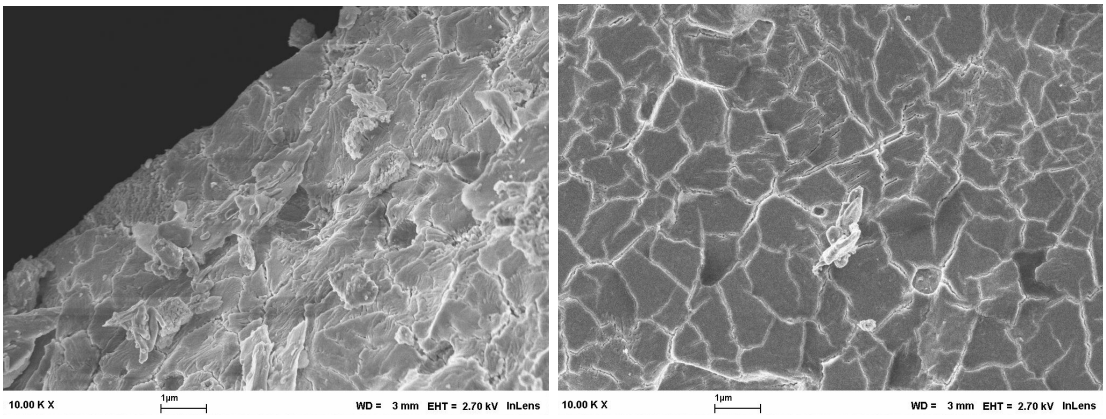

(a) Surface, calcined at 750°C (b) Surface, calcined at 875°C

Figure 3.16: SEM images of calcined DM 1X10k & indicated scale bar is 1μm

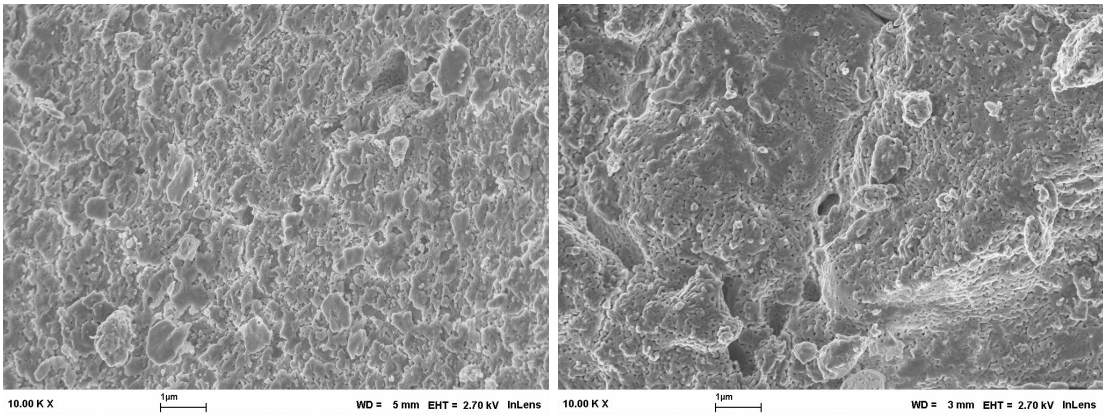

(a) Surface, calcined at 750°C (b) Surface, calcined at 875°C

Figure 3.17: SEM images of calcined LS 1X10k & indicated scale bar is 1μm

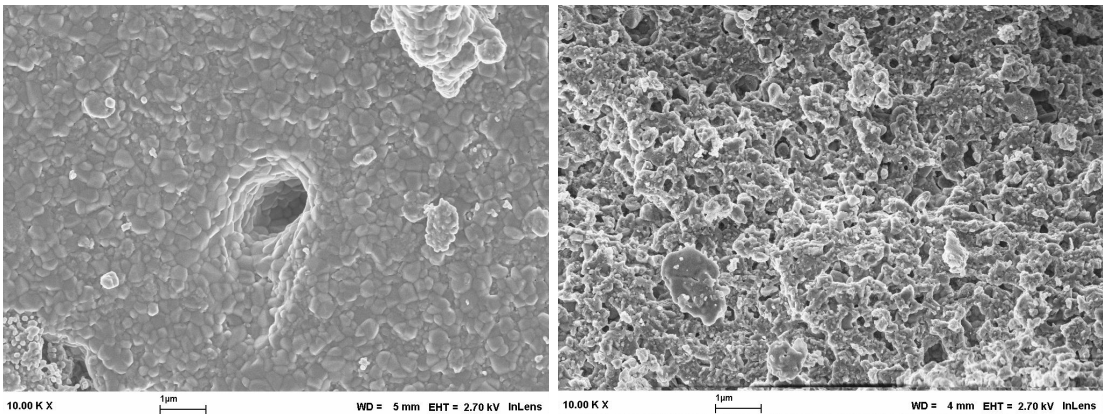

(a) Surface, carbonated at 650°C (b) Cross-section, carbonated at 650°C

Figure 3.18: SEM images of carbonated LS 1X10k & indicated scale bar is 1μm

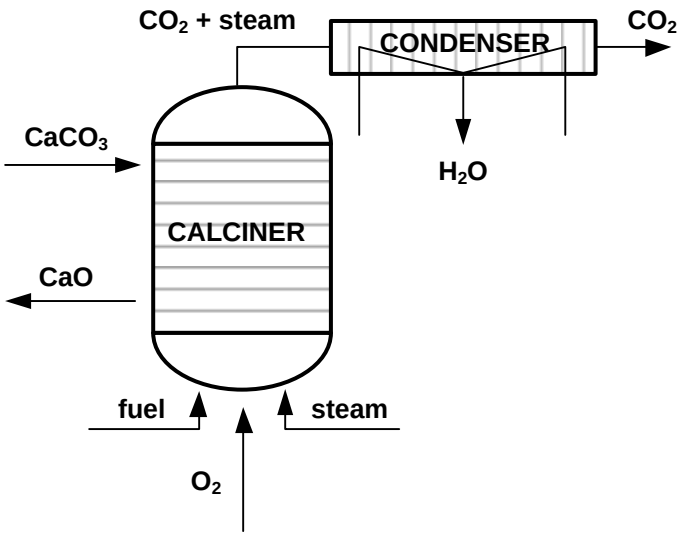

Figure 3.19: Sketch of a low temperature calciner

The SEM images in figure 3.18a & b are respectively from a carbonated Limestone 1 surface and cross-section. The surface seemed to be covered with the $CaCO_3$ product layer as it looks smooth. Figure 3.18b shows the cross-section that reveals the pore structures of Limestone 1. Some of the cross-sectional surfaces resembled unreacted CaO, similar to the ones observed in figures 3.16 & 3.17. It is possible that some unreacted CaO could still remain underneath after the fast carbonation phase.

3.3 Outcome of the experiments

It can be deduced from the experimental data that the total CaO conversion of a given limestone/dolomite sample is a function of calcination temperature and the number of CCR cycles. The higher the calcination temperature, the lower the conversion and the higher the number of CCR cycles, the higher is the sorbent decay. In order to sustain the reactivity of the sorbent, both the calcination temperature and the number of CCR cycles must be reduced. Reducing the number of CCR cycles of the sorbent population in a CaL process would require excessive make-up flows, which would increase the cost and reduce the overall efficiency despite the sorbent being abundant and relatively cheap. However, it is possible to reduce the calcination temperature to a certain extent by adjusting the CO_2 partial pressure. It means that in a CaL process scheme, the calciner should be operated at the lowest possible temperature while ensuring a reasonably high calcination rate.

According to the thermodynamic data in chapter 2, the CO_2 partial pressure in the calciner determines the equilibrium temperature of the $CaCO_3$/CaO system. A slightly higher equilibrium temperature would favour the calcination reaction. The calciners can either be heated by direct firing with oxygen and fuel, to avoid the air nitrogen mixing

with CO_2 stream or indirectly through heat exchangers. In both cases, the CO_2 partial pressure must be brought down to lower the calcination temperature (an atmospheric direct fired calciner would have a P_{CO2} of >0.9 bar). Steam can be the most suitable gas stream available in a power plant to be supplied into the calciner to lower the CO_2 partial pressure. The supplied steam can then be separated from the CO_2 in a condenser at the calciner exit. A calciner sketch with an steam supply is illustrated in figure 3.19, Sivalingam et al. [2009].

3.4 Conclusion

The influence of widely varying calcination temperatures on sorbent reactivity was studied in a thermogravimetric analyzer using naturally occurring limestone and dolomite samples. High temperature calcination accelerated the decay in sorption capacity. Calculated decay coefficients of samples varied with calcination temperatures. The higher the calcination temperatures the higher the decay coefficients. At 750°C calcination, dolomite decay coefficient was the lowest (k=0.1) and its calculated CO_2 capture capacity per kg of parent sample for 25 CCR cycles (3.15 kg of CO_2) was higher than for all tested limestones, despite its low $CaCO_3$ content (∼60%-wt.). Apparent calcination and carbonation rate constants were determined and compared. Calcination rate constants of samples were nearly equal ($K_{calc} \approx 0.002\ s^{-1}$) at low temperature calcination (750°C) and widely varied with increasing calcination temperature. At 750°C, Dolomite 1 is favored as potential sorbent than all tested limestones, because, it not only separates the highest amount of CO_2 per kg of parent sample but also achieved fairly high calcination (K_{calc}=0.0022 s^{-1}) and carbonation (K_{carb}=0.0051 s^{-1}) rates. The performance of a CaL process scheme to separate CO_2 from gas mixtures can be further enhanced by operating the calciner at a low temperature.

Chapter 4

Scaled calcium looping reactor model experiments

Sorbent samples are collected from a 10 kW_{th} dual fluidised bed(DFB) calcium looping(CaL) test facility, installed at the Institut für Feuerungs- und Kraftwerkstechnik(IFK) in Stuttgart, at steady state operating conditions and tested in a Thermogravimetric analyser(TGA) at the Lehrstuhl für Energiesysteme(LES). The aim of the TGA experiments is to determine the active space time, τ_{active} which in combination with process data, can be used to characterise the CO_2 capture capacity of the carbonator of a CaL system. The second part of this chapter presents a comparison of reactivities of spent sorbent samples from the same test facility with that of fresh ones. The CaO conversion of the spent samples is very low and shows no significant change with increasing number of CCR cycles. Hydration of spent samples restores the reactivity to almost the equivalent of a fresh sample. A carbonator concept is proposed to sustain sorbent reactivity in a CaL process.

4.1 Analysis of DFB CaL process operating parameters

4.1.1 Theoretical analysis of the CaL process parameters

Figure 4.1 shows the CaL process scheme with a simple CO_2 mol balance. A detailed description of the process scheme can be found in sections 1.2.1 & 2.1. Flue gas containing F_{CO_2} mols of CO_2 enter the carbonator and react with the active fraction of the CaO bed. The CO_2 separation efficiency of the process, E_{CO_2} is defined as the ratio of CO_2 mols reacted with CaO and the CO_2 mols entering the carbonator, F_{CO_2}. Hence the CO_2 lean flue gas leaving the carbonator contains F_{CO_2}.(1- E_{CO_2}) mols of CO_2 and the mols of CO_2 captured is $F_{CO_2}.E_{CO_2}$. In order to keep the same amount of active CaO, F_0 mols of CaO is purged from the calciner and replaced by the same mols of fresh $CaCO_3$.

The rate of CaO carbonation was firstly reported by Bhatia and Perlmutter [1983]. Since then the formula for CaO conversion is being modified. Hawthorne et al. recently took into account the limit of maximum carbonation of CaO and modified the formula as

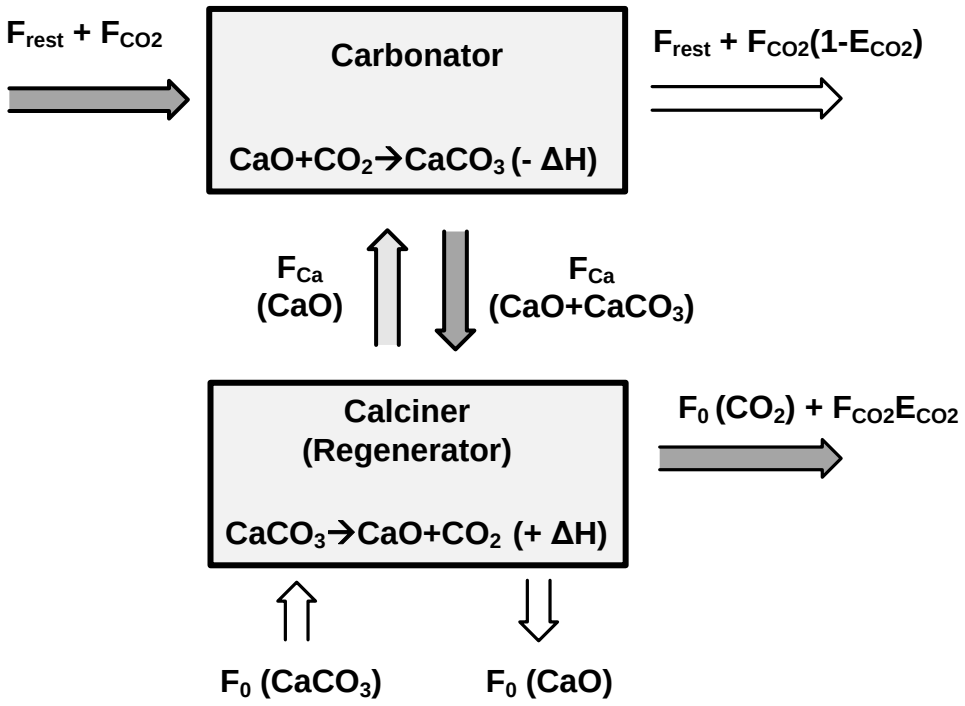

Figure 4.1: CaL process scheme with CO_2 mol balance

in equation 4.1, Hawthorne et al. [2008].

$$\frac{d\lambda_{carb}}{dt} = \frac{K_s S_0}{1 - e_0}(\lambda_{max} - \lambda_{carb})^{2/3}(Y_{CO_2} - Y_{CO_2,eq}) \tag{4.1}$$

where, K_s is the reaction rate constant for surface carbonation, S_0 is the initial CaO specific surface area and e_0 is the particle porosity. These three terms are constant for a given limestone type. Y_{CO_2} is the local CO_2 concentration. In case of a carbonator it is the incoming flue gas CO_2 concentration which depends on the type of fuel and the air fuel ratio of the combustor. Moreover, the $Y_{CO_2,eq}$ is the equilibrium CO_2 concentration at a given temperature as defined by the equation 2.1 in chapter 2. The λ_{carb} is the actual conversion of CaO mol-% to $CaCO_3$ in the carbonator. This parameter can also be calculated by dividing the total CO_2 mols captured in the carbonator ($F_{CO_2}.E_{CO_2}$) by the total CaO mols in the loop F_{Ca}, which transports the captured CO_2 to the calciner. The λ_{max} is the maximum possible CaO conversion achievable within the fast carbonation phase and with the given carbonator process conditions.

$$\lambda_{carb} = \frac{E_{CO_2} F_{CO_2}}{F_{Ca}} \tag{4.2}$$

Abanades et al. defined a parameter F_a, which is the active fraction of a CaO particle in the carbonator, Abanades et al. [2004] as in equation 4.3. The authors used the F_a to explain and model the behavior of a batch BFB carbonator. F_a represents Limestone particle's remaining CO_2 capture capacity in a carbonator at a given temperature and

CO_2 concentration, according to the equation 4.1.

$$F_a = \lambda_{max} - \lambda_{carb} \tag{4.3}$$

The CO_2 capture efficiency of a carbonator is dependent on the space time τ, which is defined as the ratio of mols of calcium (Ca) present in the carbonator (N_{Ca}) and the mols of CO_2 entering into the carbonator per hour from the flue gas, Charitos et al. [2010a]. The carbonator space time is given according to equation 4.4.

$$\tau = \frac{N_{Ca}}{F_{CO_2}} \tag{4.4}$$

The carbonator bed inventory or the total calcium present (N_{Ca}) can be divided into three portions. The first portion is the active CaO which is able to react with the incoming CO_2 at particular carbonator conditions ($F_a.N_{Ca}$), the second portion which has already been carbonated ($\lambda_{carb}.N_{Ca}$) and the third portion is the inactive CaO, due to either loss of surface area & sintering or fall beyond the fast carbonation reaction regime, (1-λ_{max}).N_{Ca}. The ratio of these three portions mainly depends on the carbonator operating conditions for a given limestone. Charitos et al. [2010a] has defined another parameter called active space time τ_{active}, to analyse the capture efficiency as in equation 4.5.

$$\tau_{active} = \frac{F_a.N_{Ca}}{F_{CO_2}} \tag{4.5}$$

4.1.2 Description of the IFK DFB CaL test facility & sample collection

Figure 4.2 shows the schematic diagram of the IFK's 10 kW_{th} DFB CaL test facility and the location of the sampling port. The 114 mm diameter BFB (1) is used as the carbonator and the 71 mm diameter and 12.4 m high riser (2) is used as the calciner. A significant design feature, that differs from other similar test rigs is the cone valve which regulates the sorbent flow F_{Ca}, between the carbonator and the calciner. A double exit loop seal(3) right after the calciner cyclone separator(9) is used to moderate the CaO flow to the BFB carbonator by adjusting the cone valve opening. Partially carbonated CaO over flows from the BFB carbonator and proceeds through lower loop seal (8) to the calciner where it is regenerated and conveyed back to the carbonator, thus completing the loop. A detailed description of the test facility and the experimental procedure can be found elsewhere, Charitos et al. [2010a].

Sorbent samples were collected at steady state operation of the test facility. Partially carbonated sorbents were taken from the carbonator over flow via a sampling vent located at the lower loop seal (15). The vent was turned on and the sorbents that were stagnant in the vent were collected separately for reuse. The samples for further analysis were

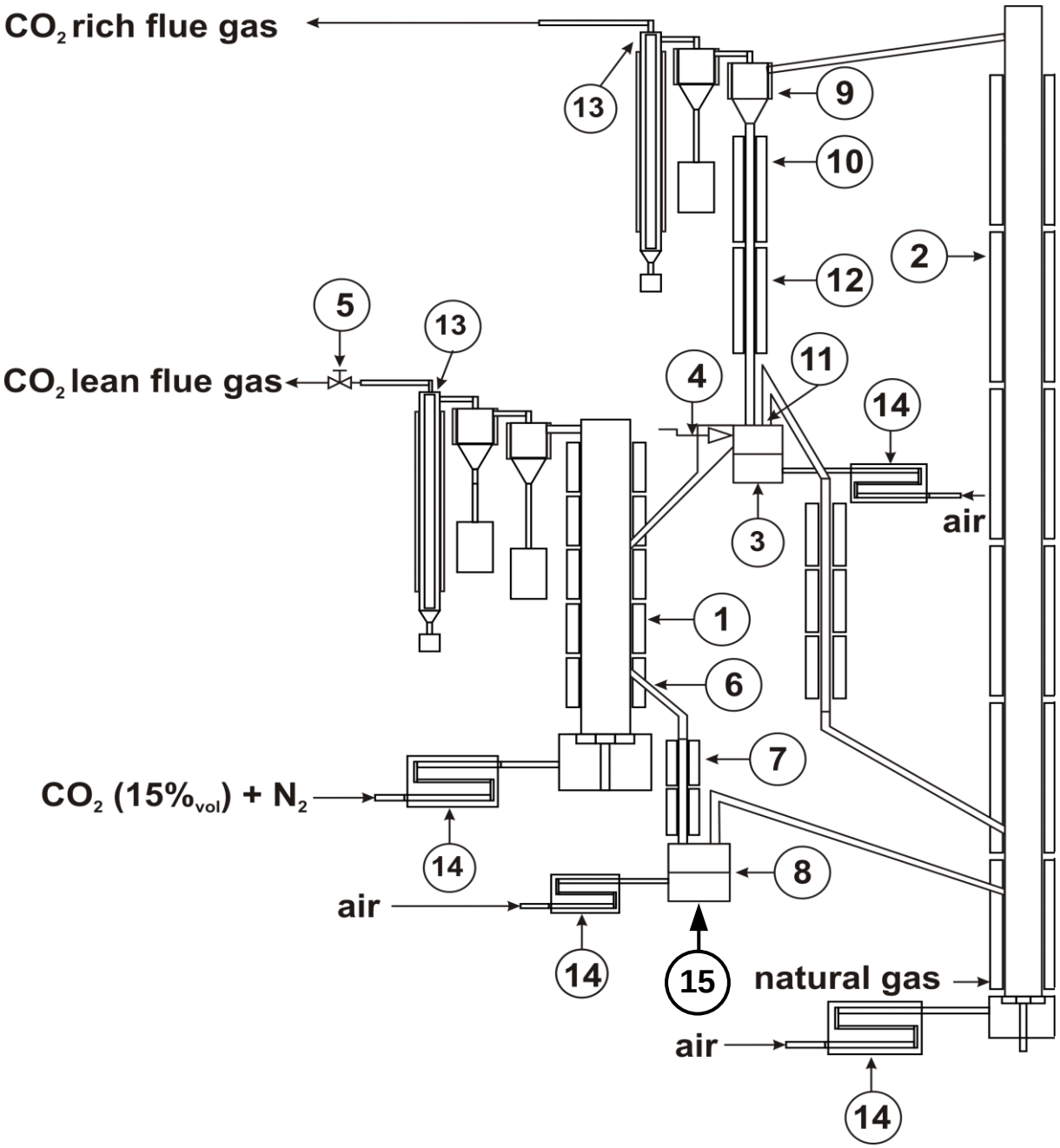

(1) BFB carbonator, (2) riser regenerator, (3) double exit loop seal, (4) cone valve, (5) pressure control valve, (6) BFB overflow, (7) lower standpipe, (8) lower loop seal, (9) cyclone, (10) upper standpipe, (11) loop seal weir, (12) quartz standpipe segments, (13) candle filters, (14) electrical gas pre-heaters, and (15) carbonator sampling position.

Figure 4.2: Schematic diagram of IFK DFB CaL test facility

Charitos et al. [2010a]

tapped once the sorbents began to flow directly from the lower loop seal. The collected sample at each time was well mixed and nearly a 25 grams of representative sample was sealed in a container for further TGA analysis. The sample container was tightly closed and labeled with the DFB operating conditions and collection time.

4.1.3 Description of the TGA at LES & the design of sample holder

Selected samples from the collected ones at the IFK's DFB CaL experiments were analysed in a TGA at LES for determining the λ_{carb} and λ_{max}. The samples were studied in a TGA(LINSEIS^{TM} STA PT1600) supplied by Linseis Messgeraete GmbH. The experimental conditions for the TGA study were kept as similar to the IFK's DFB operating conditions at which that particular sample was collected.

A sample holder was designed at LES to maximise the solid gas contact. The design had to overcome the two constraints that it should weigh less than 10 grams and that it must fit in the available TGA reactor space. Moreover, it should also be able to withstand high temperatures and potential corrosive environments. Figure 4.3 shows the design and measurements of the sample holder to be manufactured at LES workshop. Part A and part B were divided into two cylindrical parts and manufactured from a 1.4841 steel work piece in a lathe machine. After that the parts were joint by welding. The weight of the sample holder was about 5 grams. The wire mesh used to hold the samples was made of Incoloy 800. Figure 4.4 shows the TGA with the sample holder used for the study.

4.1.4 Determining the important CaL process parameters

The parameters λ_{carb} and λ_{max} are to be determined by following TGA experiments.

TGA test procedure

Samples from the IFK's DFB test facility (500-600 mg) were placed between the cylindrical wire mesh and the stem of the sample holder in order to form a layer of 2 mm. The test procedure is similar to the one explained in section 3.1.2 in chapter 4. Here the timing for switching gases and temperatures was controlled by a software program and it can be set in the program prior to the start up. A heating & cooling rate of 10°C/min was maintained for all the experiments. The reaction gas was set at 150 ml/min and consisted of CO_2 and N_2. A purge gas flow of 50 ml/min N_2 was used to protect the weighing mechanism from corrosive gases. Calcinations were performed in pure N_2 environment while the carbonations were at varying CO_2 concentrations and temperatures depicting the DFB conditions. Temperature, weight and gas flow data were recorded every second.

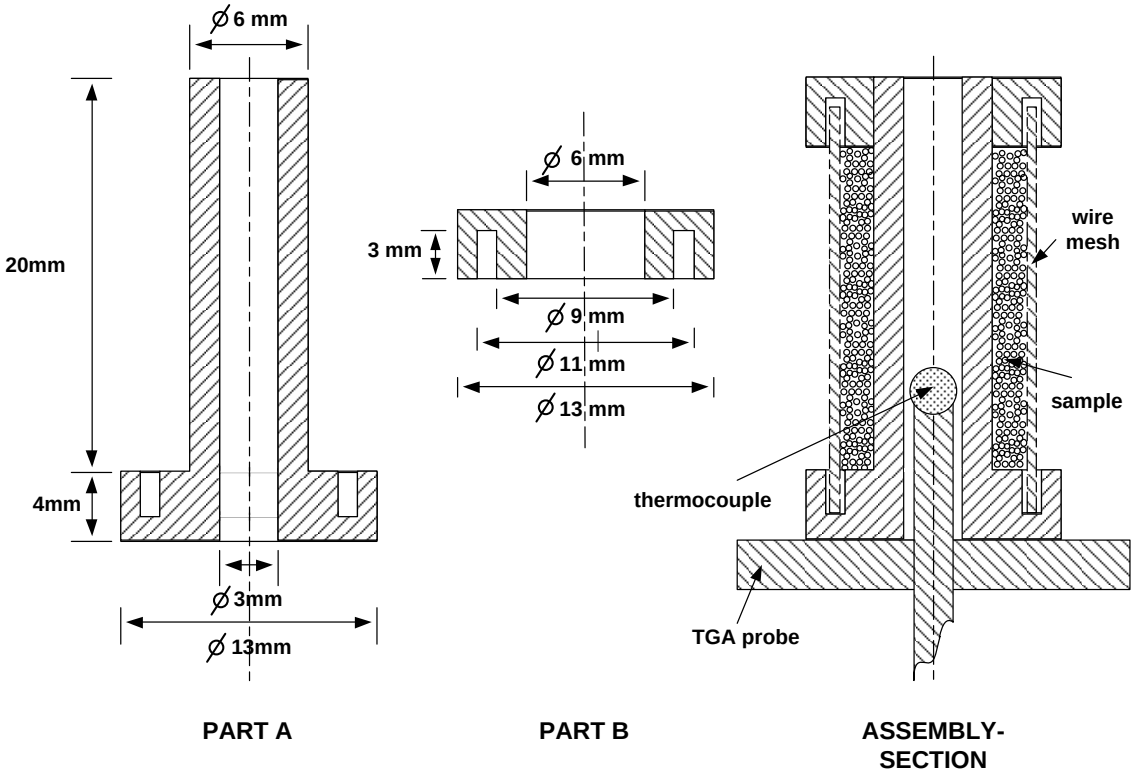

Figure 4.3: Sample holder design for the TGA at LES

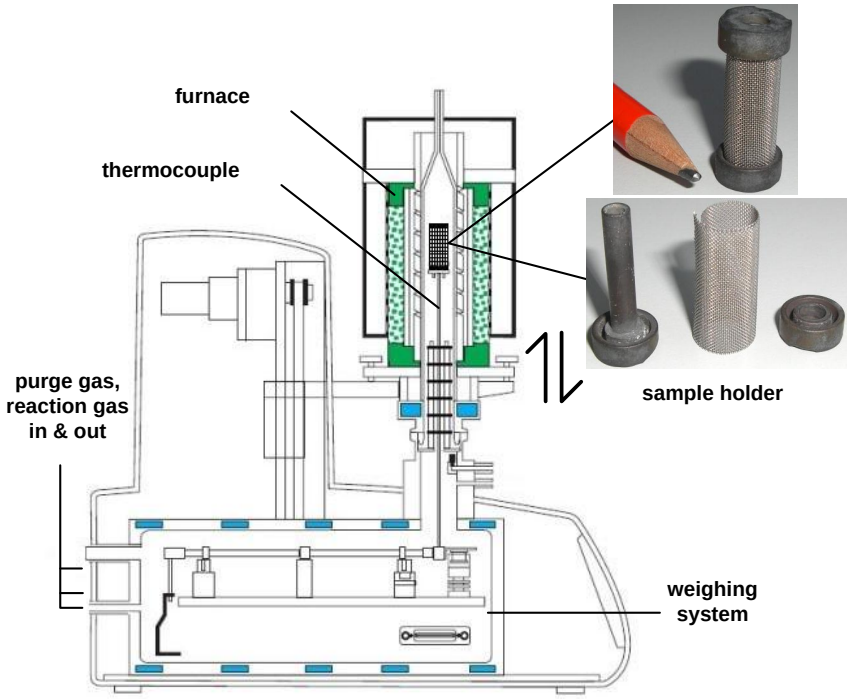

Figure 4.4: LINSEIS^{TM} TGA and custom made sample holder

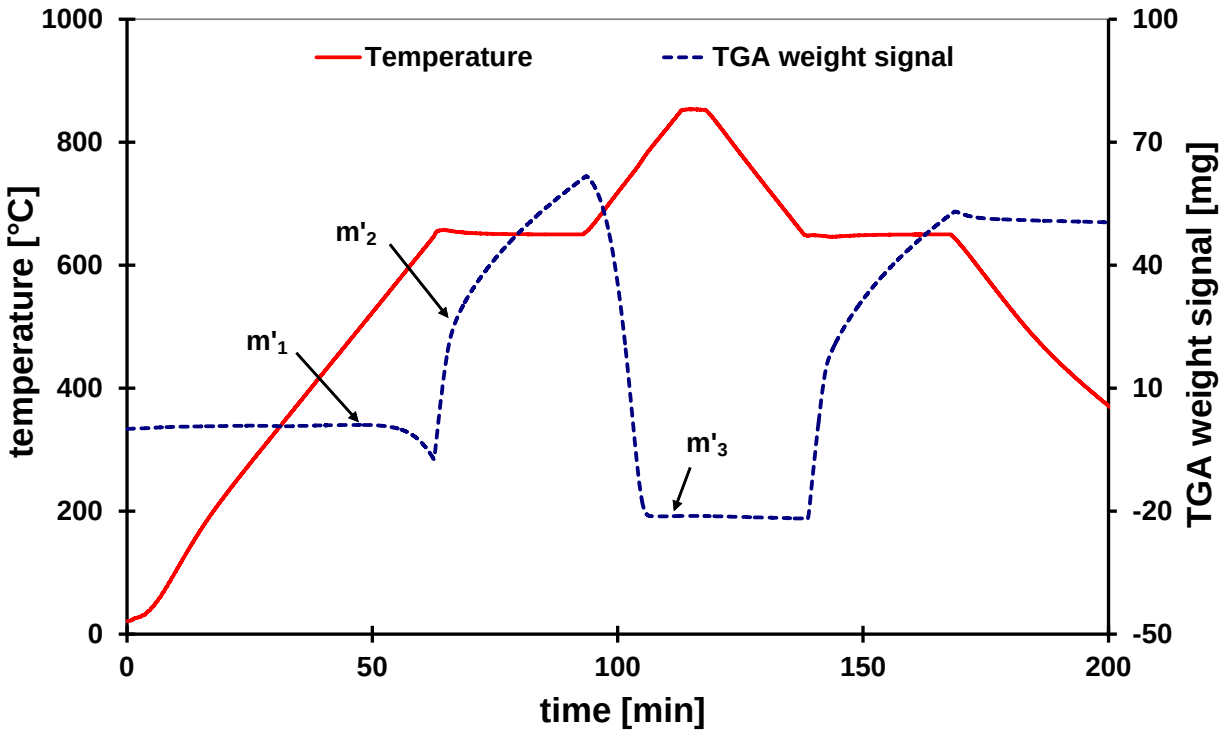

Figure 4.5: TGA curve of a DFB sample

Calculation of the parameters

Samples collected from the DFB test facility had already been through a number (n) of CCR cycles. In the TGA, to determine the λ_{carb} and λ_{max} of that sample, one could first perform carbonation or calcination. If the calcination was performed first, the CCR cycle number will become $(n+1)$ and the determined parameters will belong to the $(n+1)^{th}$ CCR cycle. In order to determine the parameters for the n^{th} CCR cycle, it was decided to carry out carbonation in the TGA before calcination. Figure 4.5 shows the weight and temperature change curve versus time for a DFB sample. In this particular case carbonation was performed at 660°C in 15%-vol CO_2 and calcination was at 850°C in pure N_2. The TGA weight signals necessary for the calculation are $m_1^{'}$, $m_2^{'}$ & $m_3^{'}$ as marked in figure 4.5. $m_1^{'}$ is the initial steady state TGA weight signal, $m_2^{'}$ is the TGA weight signal during the end of fast carbonation reaction phase and $m_3^{'}$ is the TGA reading after the calcination.

All except $m_2^{'}$ can directly be obtained from the plot in figure 4.5. The λ_{carb}, the carbonation achieved in DFB, can be calculated using the equation 4.6a, provided that the carbonate content is negligible after the calcination. However, the $m_2^{'}$ should be determined to calculate the λ_{max} using the equation 4.6b. A graphical method was developed to find out the $m_2^{'}$, the weight change of the sample at the end of fast carbonation phase. First and second derivatives of the weight change measurements for an estimated time span of the reaction phase change were calculated and plotted with time. Figure 4.6 shows

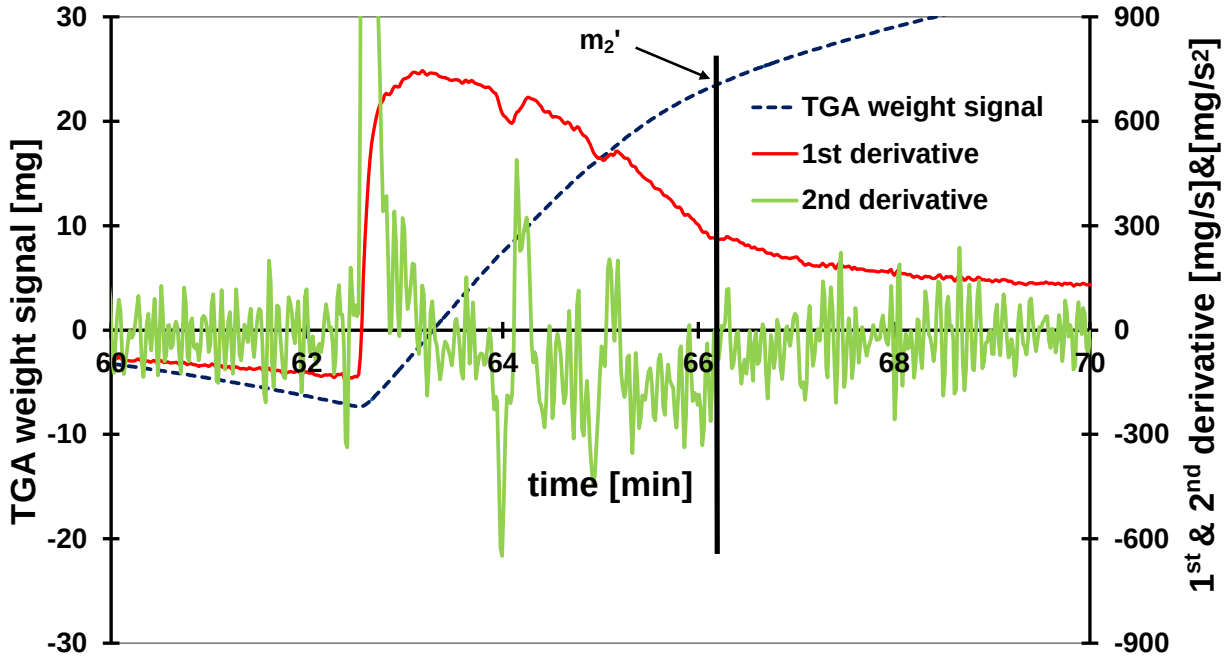

Figure 4.6: Graphical method for $m_2^{'}$ determination

such a plot of a DFB sample. The first derivative clearly shows an overview of the rate change, however, it is hard to pinpoint the time in which the fast reaction phase ends. The combination of first and second derivative provides a much clearer way to find the time. As can be seen in figure 4.6, the second derivative oscillates across X axis while the first derivative keeps falling from the peak during the carbonation. At some point when the first derivative begins to reach a stable value at around 66^{th} minute, the second derivative also get stabilised over the X axis. The point at which the second derivative stabilises was taken as the time of reaction phase change, thus the corresponding weight change is the m_2. The λ_{max} can now be calculated by the equation 4.6b.

$$\lambda_{carb} = \frac{(m_1^{'} - m_3^{'})/M_{CO_2} \times 1000}{mols\ of\ CaO\ in\ the\ sample} \tag{4.6a}$$

$$\lambda_{max} = \frac{(m_2^{'} - m_3^{'})/M_{CO_2} \times 1000}{mols\ of\ CaO\ in\ the\ sample} \tag{4.6b}$$

Once the λ_{carb} and λ_{max} are determined, the F_a can be calculated from equation 4.3. As the number of Ca mols in the carbonator, N_{Ca} is known from the total inventory, the active space time, τ_{active} can then be determined by the equation 4.5. A number of samples obtained at various steady state conditions from the IFK's DFB CaL test facility have been analysed in the TGA at LES and the corresponding λ_{carb} and λ_{max} values were determined and the active space times were calculated. The active space time, at a given inlet gas CO_2 concentration and carbonator temperature is useful in characterising CO_2 capture efficiency of the BFB carbonator, E_{CO_2} of a CaL system. However the space

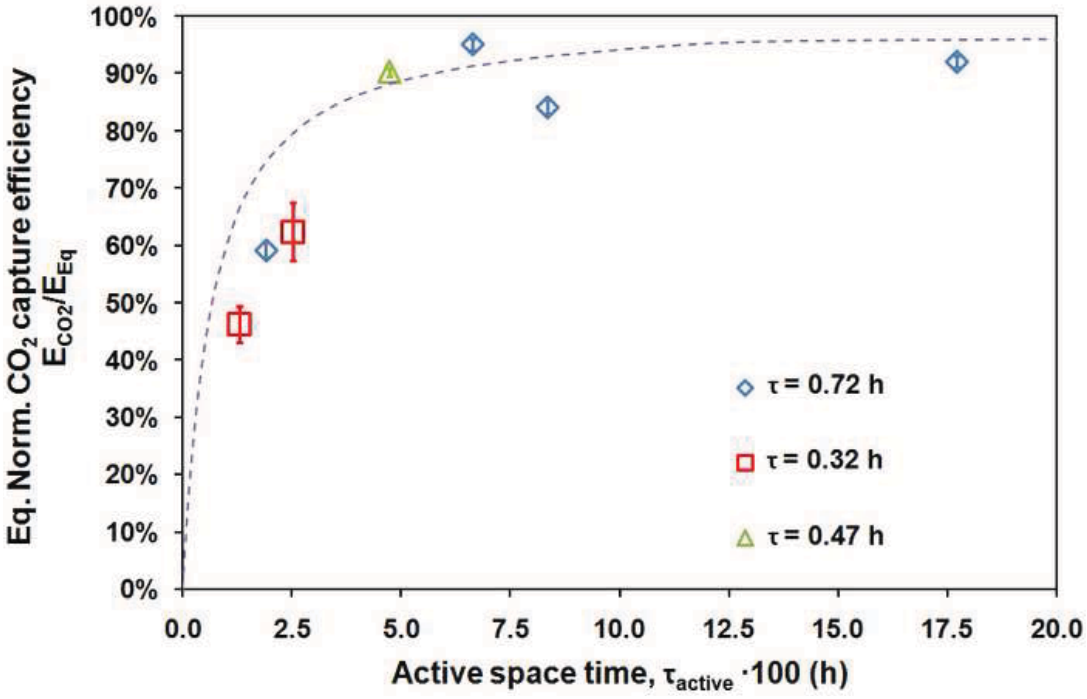

Figure 4.7: The effect of active space time on capture efficiency Charitos et al. [2010a]

time, τ based on the bulk Ca content of the bed, cannot be used to assess the carbonator performance.

Discussion of the process parameter, active space time, τ_{active}

Figure 4.7 plots the equilibrium normalised CO_2 capture efficiency ($E_{CO_2}/\ E_{eq}$) against the active space time, τ_{active}, Charitos et al. [2010a] for various steady state carbonator conditions at 660°C and 15%-vol CO_2. It can be observed that the $E_{CO_2}/\ E_{eq}$ increases, while the space time, τ remains constant. The capture efficiency with active space time, τ_{active} increases already at relatively low values of τ_{active}. After a certain active space time, its effect on the CO_2 capture efficiency becomes insignificant. That means, for the DFB carbonator used in this study, the critical active space time seems to be in the range of 0.05h. Above this critical τ_{active} value,the equilibrium-normalised CO_2 capture efficiency determined by the experiments and predicted by fitted curve is above 90% except for one outlier point.

4.2 Spent sorbents analysis, comparison and reactivation

Multi-cycled samples from the lab scale 10kW$_{th}$ DFB reactor were collected at steady state operation and analysed in the TGA. The influence of the following three parameters on reactivity were analysed: the CCR cycle number, CO_2 concentration and the carbonation temperature. The results were compared with that of the fresh limestone. The sample collection procedure, description of the TGA and the DFB test facility can be found in section 4.1. The limestone used in the DFB originated from the region of Swabian Alb in Germany and it contains more than 94-%wt $CaCO_3$.

4.2.1 Influence of the number of CCR cycle

The sorbents undergo at least dozens of CCR cycles in a real CaL DFB reactor system to capture the CO_2 from flue gases. The reactivity of the sorbents is reduced with increasing number of CCR cycles and it is discussed in chapter 3, section 3.2.3. It is reported that the sorbent reactivity reaches a residual value after hundreds of CCR cycles, and the conversion value was measured as 7-8 CaO mol-% to $CaCO_3$, Grasa and Abanades [2006]. If the sorbents are utilised in such a way that they remain in the loop for several hundred cycles, the scale of the reactor would become large to maintain a certain CO_2 capture rate due to its low residual reactivity. Moreover the construction cost of the capture plant would also be higher. However this type of operation requires a low purge as the sorbents stay in the loop for a prolonged time. Another type of operation is that the sorbents are allowed to undergo only a limited number of CCR cycles so that the same level of reactivity as in the previous case can be maintained with low amount of sorbents in the reactor bed. This will reduce the required reactor size and the construction cost. On the other hand it needs a high amount of purge flow which will increase the operating costs. In any type of operation it is important to monitor the level of sorbent reactivity in a DFB carbonator throughout the process.

Figure 4.8 plots CaO mol-% to $CaCO_3$ conversion as a function of the residence time in the TGA for both the fresh limestone material and the sample taken from the DFB carbonator after multiple CCR cycles. It can be visually seen that the capture capacity of the fresh limestone sample decreases with increasing CCR (1-20) cycles in the TGA. However, the sample taken from the DFB, while having a substantially lower carbonation capacity, does not degrade with the CCR cycle number(N=4). This indicates that the DFB sorbent particles are at or near their residual conversion value.

Estimating the cycle number of DFB samples

The number of CCR cycles undergone by a sorbent sample in a CaL system can be estimated by comparing its CaO conversion in a TGA with that of the fresh limestone

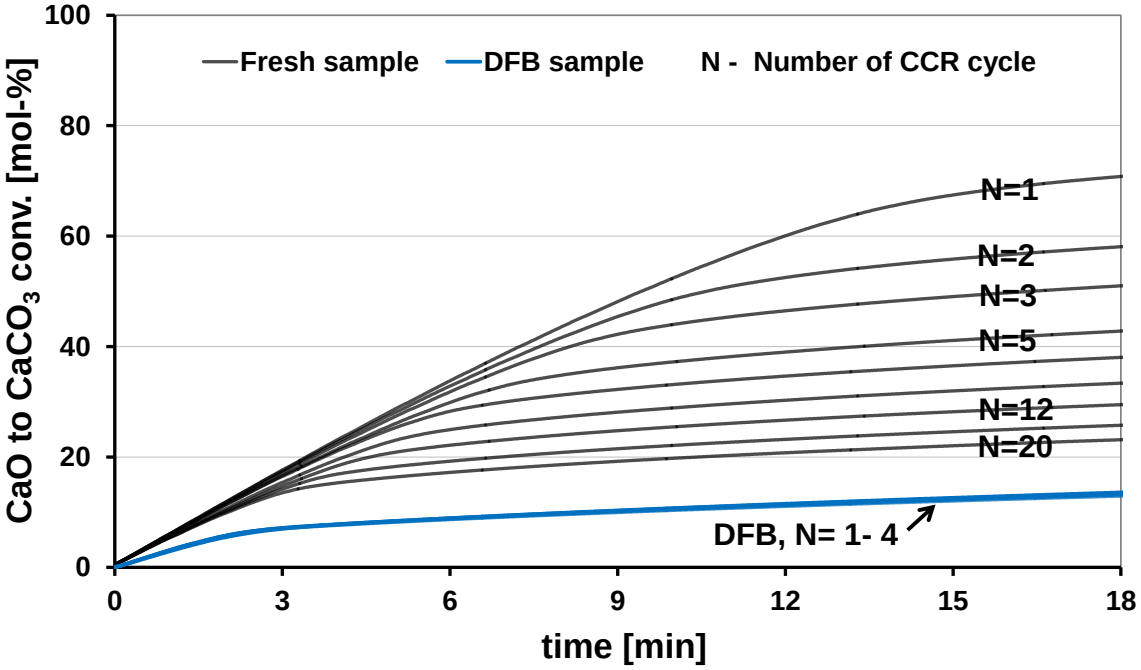

Figure 4.8: Comparison of the CaO mol-% conversion of the DFB sample and fresh limestone

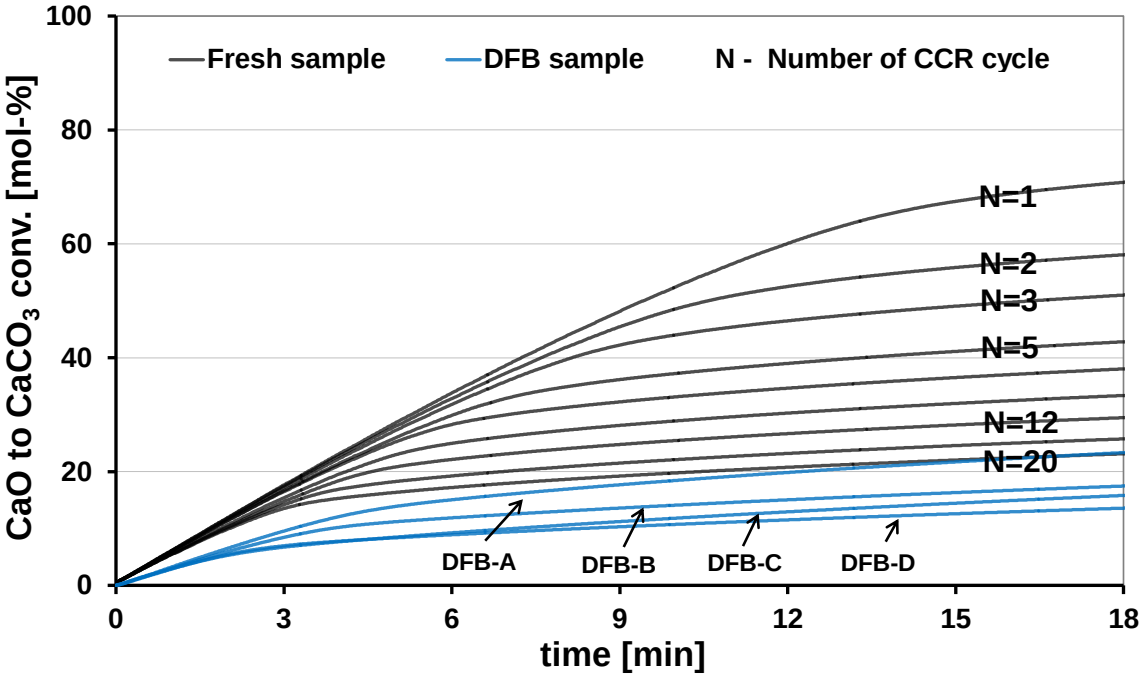

Figure 4.9: Estimation of CCR cycle number by comparing the CaO mol-% conversion

profile representing several CCR cycles. The estimated CCR cycle number of a DFB carbonator sample will indicate how far the sorbents were utilised and help to maintain the overall bed reactivity by accordingly adjusting the process parameters, e.g. the purge flow. Figure 4.9 shows the fresh limestone conversion profile for 20 CCR cycles and n^{th} CCR conversion of four different DFB carbonator samples taken at various times. It can be deduced that all four DFB samples have been through more than 20 CCR cycles in the CaL system since the CaO mol-% conversion of their initial fast reaction phase fall well below that of the 20^{th} CCR cycle of the fresh limestone. It can also be suggested that the DFB-D is near its residual conversion as it shows only a little more than 10 mol-% conversion. The apparent second carbonation rate of sample DFB-A is grater than that of the 20^{th} cycle of the fresh limestone thus reaching to the same carbonation conversion at the end of the experiment. One possible explanation could be that the DFB-A sample might have contained some amount of fresh sorbents from the make up which could have increased the second phase conversion. In general, one would require a profile of at least 100 fresh limestone CCR cycles to precisely determine the cycle number of DFB samples. The TGA used in this study is not an ideal one to perform this many number of CCR cycles in a stretch. Long series of CCR experiments can easily be performed with a dual furnace TGA as described elsewhere in published literature, Grasa and Abanades [2006], Alvarez and Abanades [2005b].

4.2.2 Influence of CO_2 concentration

Figure 4.10 plots CaO mol-% to $CaCO_3$ conversion,λ as a function of residence time in the TGA for a fresh and a DFB samples at 650°C for concentrations of 5, 10 and 15%-vol CO_2. These are in the range of typical values prevailing in a carbonator. The calcination happened at 850°C in pure N_2 and carbonation at 650°C. One can observe that the carbonation conversion for both fresh and DFB samples increase with increasing concentration of CO_2 in the gas phase. This is because the reaction rate is directly proportional to the difference between local and equilibrium CO_2 concentrations. It is clear that when the local CO_2 concentration increases while the equilibrium concentration remains same for the constant temperature of 650°C, the difference increases. This phenomenon eventually leads to a higher total conversion for both types of samples at 10%-vol & 15%-vol CO_2 concentrations.

However, eventually after 600 seconds, 10%-vol fresh sample achieved higher conversion, at a comparatively lower reaction rate within its fast reaction phase, than 15%-vol fresh sample. Perhaps the slower rate of carbonation permits the CO_2 to reach the particles' interior and get contact with more fresh active surfaces which leads to more conversion. The initial reaction at 15%-vol could possibly be too fast, thereby forming a thick layer covering the particle and thus preventing further direct exposure of more active surfaces. A notable difference in conversion can be seen between DFB and fresh samples. The DFB samples have significantly lost their reactivity (specific surface area) due to the differences

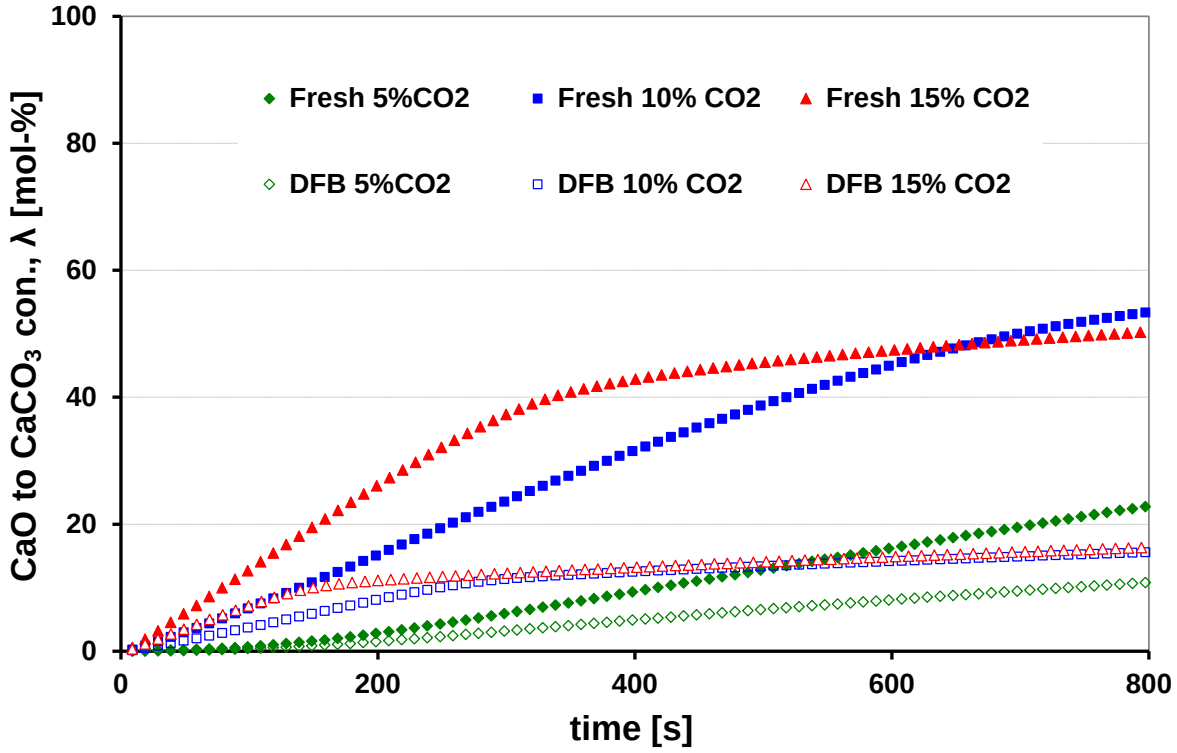

Figure 4.10: Comparison of the CaO mol-% conversion of the DFB sample and fresh limestone with varying CO_2 concentration

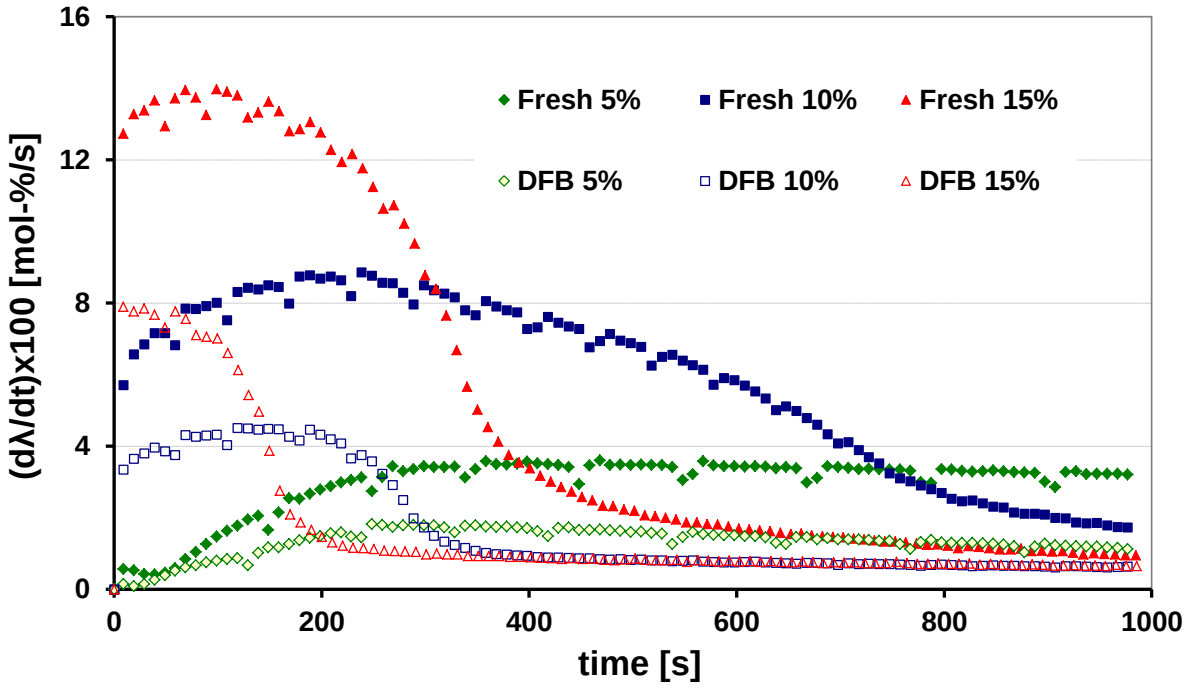

Figure 4.11: Comparison of the rate of λ change for the DFB sample and fresh limestone

between a DFB and a TGA environment.

Figure 4.11 plots the rate of carbonation versus time for the same set of experiments as in figure 4.10. Only the fast reaction phase is of significance for DFB-based systems. The higher the carbonation rate in the fast reaction phase, the higher is the capture efficiency of the DFB. It is visible in this plot that there are significant rate variations between the samples in the fast reaction phase with respect to the varying CO_2 concentrations. The rate of carbonation of the fresh sample at 15%-vol CO_2 is almost twice as high as that at 10%-vol CO_2, although the length of the fast reaction regime is much longer for the latter concentration. One important difference between the two CO_2 concentrations is the rate of change between the fast reaction and the diffusion-controlled reaction regimes: a CO_2 concentration of 15%-vol results in an abrupt transition, whilst the 10%-vol is much more gradual. This could explain why the final carbonation conversion is higher at 10%-vol CO_2 than for 15%-vol CO_2. On the other hand, the DFB samples at 15% and 10% CO_2 both exhibit a sharp transition between the fast and diffusion-controlled reaction regimes. Similar to the raw samples, the rate of reaction at 15%-vol CO_2 is the double of the rate at 10%-vol CO_2. In summary, the DFB samples get carbonated at roughly half the rate of their fresh limestone counterparts(in the first cycle).

4.2.3 Influence of carbonation temperature

Figure 4.12 plots the CaO conversions as a function of residence time in the TGA at 600, 650 and 700°C for the fresh and DFB samples. The calcination happened at 850°C in pure

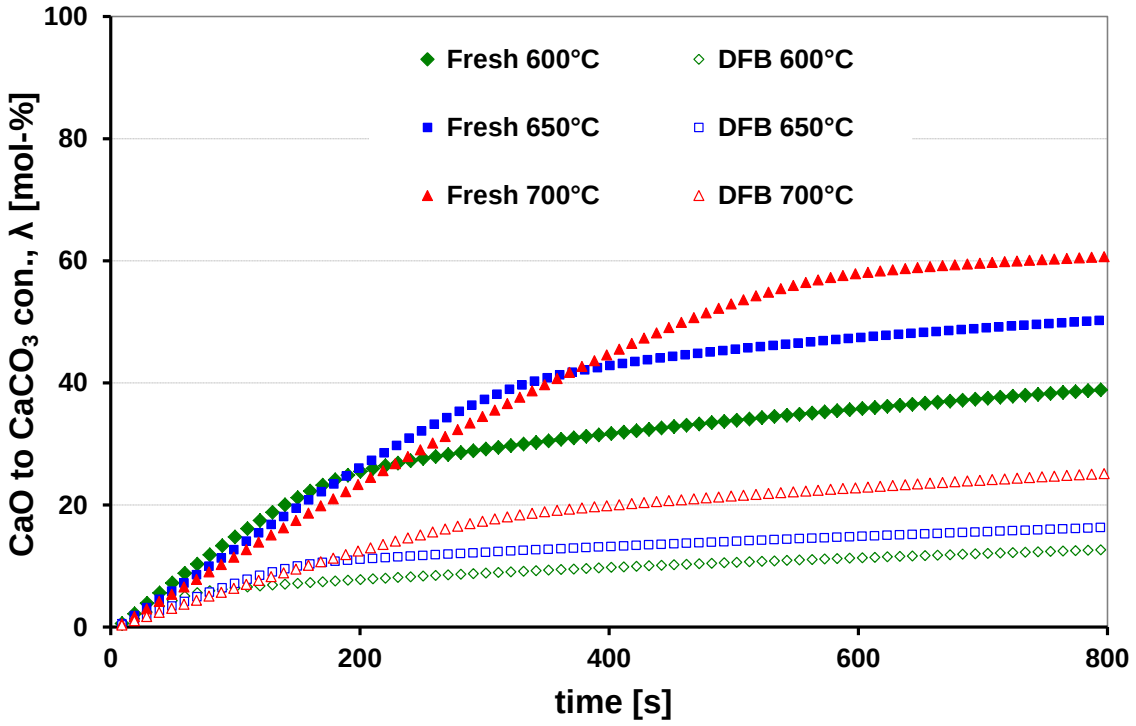

Figure 4.12: Comparison of CaO mol-% conversion of the DFB sample and fresh limestone with varying carbonation temperature

N_2 and carbonation was in 15%-vol CO_2. There is a clear difference in total conversion between the two types of samples. Moreover conversions vary significantly for each of the two samples due to temperature influence. The carbonation can be analysed with a fast and a slow reaction regime. The reaction rate at the fast reaction regime follows the following descending order for both the samples with regard to the carbonation temperature; 600°C > 650°C > 700°C. This can be explained by the CO_2 concentration difference between the gas phase and the equilibrium, a parameter which is directly proportional to reaction rate that varies with the temperature. Equilibrium CO_2 concentration increases with increasing temperature, thus the difference decreases as the gas phase CO_2 concentration is kept constant. However, in this fast reaction phase the rate variations among samples are not significant.

Moreover the duration of the fast regime follows the reverse order as 600°C < 650°C < 700°C. This leads to the higher conversion of CaO at 700°C and the lower at 600°C. This could be due to the rate of carbonation within the fast reaction regime which influences the loss of active CaO, as similarly observed in section 4.2.2 with regard to the CO_2 concentrations. Decreasing the temperature decreases the equilibrium CO_2 concentration, thus increasing the driving force of the reaction, as the gas phase CO_2 concentration is kept constant. It is the same effect as increasing the CO_2 concentration at constant carbonation temperature. It seems that the high reaction rate has a slight negative effect on the total conversion at the end.

Table 4.1: CaO to $CaCO_3$ mol-% conversion for four CCR cycles

Sample Name	λ mol-%			
	N=1	N=2	N=3	N=4
DFB	33.6	33.4	32.9	32.1
Hydrated DFB	63.7	58.0	54.2	51.4
Fresh limestone	76.6	65.6	58.8	54.1

Another possible contributing factor for this behavior lies in the diffusion phenomena. The higher the temperature, the higher the diffusion rate. Once the fresh CaO particle is exposed to the CO_2, it reacts spontaneously and forms a $CaCO_3$ layer over the particle. The CO_2 in the gas phase has to diffuse through this product layer to further react with unconverted CaO hidden under this layer. Increasing carbonation temperature facilitates this process to a certain extent thus achieving higher carbonation conversions. This temperature increase is limited by the equilibrium CO_2 concentration. A trade-off regarding reaction rates and duration of the fast reaction regime suggest that a carbonation temperature in the range of 650-700 °C is advantageous for optimum CaO conversion, thus the CO_2 capture.

4.2.4 Reactivation of the DFB samples through hydration

It is clearly evidenced that the rate of reaction is noticeably slower for the DFB sample compared to fresh sample. The total conversions of the DFB samples remained almost unchanged for four TGA cycles. One can argue that it may be near or at the residual conversion, after which its conversion remain constant for hundreds of cycles, Grasa and Abanades [2006]. However, it is vital to sustain the reactivity of the sorbents with increasing number of cycles to maintain the capture efficiency without deploying huge and expensive pure and make up flows. In an attempt to renew the capture capacity of the DFB sample, it was hydrated to 30-40%-wt with distilled water and left for 2 hours in open atmosphere. The produced sample, referred as hydrated DFB was tested in the TGA. It was first calcined at 850°C and then carbonated at 700°C in 15%-vol CO_2. This process was repeated for 4 TGA cycles.

Figure 4.13 plots the λ versus time in the primary axis and $d\lambda/dt$ versus time in the secondary axis for fresh, DFB and hydrated DFB samples' first carbonation. It can be seen that the reaction rate of the hydrated DFB sample is shifted to match that of the raw sample in the fast reaction regime. In addition, the conversion of CaO to $CaCO_3$ also almost doubled for the hydrated DFB in the first cycle when compared to the DFB sample. Table 4.1 indicates the λ values of all three samples for four TGA cycles.

As shown in table 4.1 the λ values of the hydrated DFB sample, after a carbonation period of 30 min., slightly decrease with increasing number of cycles in a very similar way to the fresh samples. On the other hand the λ value of the DFB sample remains almost

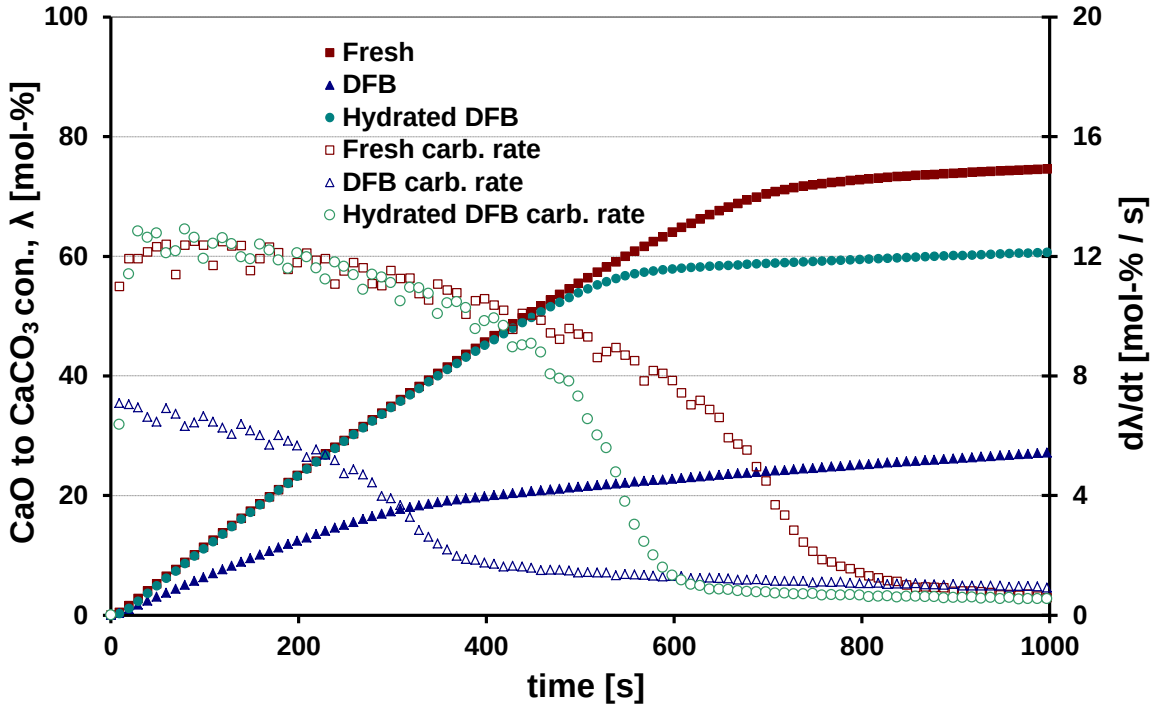

Figure 4.13: Comparison of CaO mol-% and rate of conversion for DFB, fresh and hydrated DFB samples

unchanged. One might need to observe more cycles to make any concrete conclusion. However the trend observed indicates that the hydration significantly renewed the capture capacity of DFB sample. Sun et al. recently reported that the water and steam hydration of calcined and sintered particles regenerated their capture capacity, Sun et al. [2008]. However they concluded that the water hydration for partially carbonated particles did not result in sorbent regeneration, contrary to the results presented here. DFB samples tested in this study were partially carbonated (12 mol-%) and sintered, as it was taken from the bubbling fluidised bed carbonator under stable operating conditions at IFK's DFB test facility.

Comparison of the fast phase maximum CaO conversion

The amount of active mass (CaO) based on the fast reaction regime is an important parameter for an effective CO_2 capture in the carbonator. Under realistic process conditions, the CaO particle only spends an average residence time of minutes in the carbonator and therefore, the capacity of the fast reaction regime is of major interest. The maximum conversion of CaO to $CaCO_3$ in the fast reaction regime, λ_{max} is determined based on the first and second derivatives of the conversion plots described in section 4.1. Figure 4.14 plots λ_{max} versus number of cycles for fresh, DFB and hydrated DFB samples.

The λ_{max} is noticeably low for the DFB sample compared to the fresh sample and the hydrated DFB sample. It can be seen in the plot that the hydrated DFB sample almost

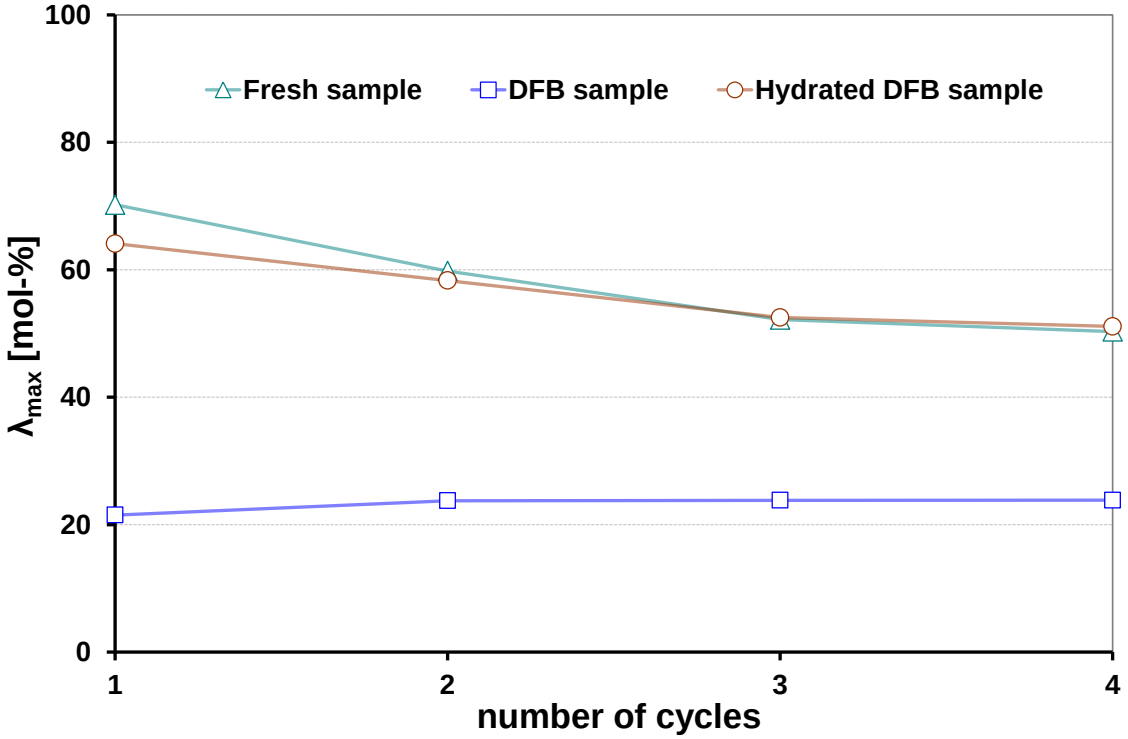

Figure 4.14: Comparison of λ_{max} for DFB, fresh and hydrated DFB samples

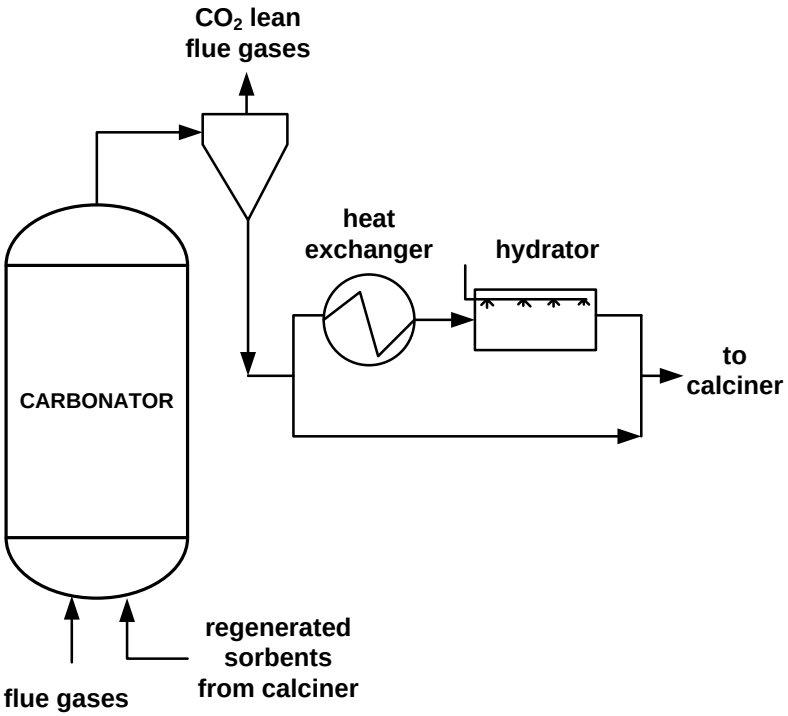

Figure 4.15: Schematic diagram of a water spraying system for CaL process for CO_2 capture

overlaps with the fresh sample and even shows slightly bigger λ_{max} in the 4^{th} cycle. However with this data it is hard to predict the behavior of both the samples for more cycles. It is certain that the hydration renewed most of the CO_2 capture capacity of the partially carbonated DFB sample. It is also important to mention that hydration might alter the particle size distribution of the sorbents, especially since some of the hydrated particles turned to powder. Further investigations are required to see if the DFB sample retains its maximum conversion after many cycles.

4.2.5 Outcome of the experiments

Hydration can be an effective tool to regenerate the sorbents' lost capacity with increasing number of calcination and carbonation cycles in a CaL process. Water sprayers can be used in the process to hydrate the sorbents. A significant issue is to define which part of the process is to be more effective to perform hydration. Based on the TGA experiments, it is proposed that it may be suitable to mount a water spray after the carbonator cyclone separator since the tested hydrated DFB samples were partially carbonated and taken after the carbonator of the IFK's DFB test facility. A part of the flow (5-10%-wt) from the carbonator to the calciner may be hydrated to substitute for fresh make-up flow and to avoid excessive energy needs in the calciner for heating up the solids to regeneration temperature. The proposed hydration system for the CaL process is illustrated in figure 4.15.

4.3 Conclusion

The carbonator active space time τ_{active}, is an important process parameter to characterise the CO_2 capture efficiency of a carbonator. The τ_{active} of the IFK's DFB carbonator at steady state 660°C and 15%-vol CO_2 inflow was determined by analysing the sorbent samples in a TGA at LES. The critical τ_{active} was in the vicinity of 0.05 h, beyond which the equilibrium normalised CO_2 capture efficiency $E_{CO_2}/\ E_{eq}$, was more than 90%. Spent samples from the IFK's DFB CaL test facility and corresponding fresh ones were compared with respect to the number of CCR cycles, carbonation temperature, and CO_2 concentration. DFB samples showed very low CaO conversions which were not affected with increasing number of CCR cycles. Hydration of DFB samples proved successful in restoring the lost capture capacity. However more investigation is required to see the effect of hydration on the CaO particle morphology. A process modification concept to sustain the CO_2 capture efficiency of the carbonator via partial particle hydration was outlined.

Chapter 5

SO_2 and CO_2 co-capture

Limestone samples are analysed in a TGA at calciner and carbonator operating conditions for CO_2 capture in the presence of SO_2 in a CaL process. Simultaneous carbonation and sulfation tests are performed, depicting the carbonator operating conditions, to optimise the CO_2 capture in presence of SO_2. Carbonation to sulfation ratio against various residence times between 5 and 50 minutes at 650°C and 700°C are determined and compared for optimum carbonator operation. Finally sulfation-only rates of limestone derivatives are measured at both reactor temperatures

5.1 Introduction

TGA studies in chapter 3 & 4 were carried out in CO_2/N_2 environment that simulates the combustion flue gases from a power plant. However in reality, the flue gases especially from a coal power plant would also contain small amounts of SO_2 which can react with calcium sorbents in CaL reactor conditions. In the past, the lime (CaO) sulfation was extensively studied to contain SO_2 emissions from fluidised bed combustion process. In these studies the carbonation of lime was not considered since the actual CO_2 concentration is less than the equilibrium concentration where the lime is injected. The limestone is injected at about 800°C and the corresponding equilibrium CO_2 partial pressure with the CaO is above 0.2 bar which is above the flue gas CO_2 concentration. Therefore CaO will not react with the CO_2 at these conditions. On the other hand, in the case of CaL, SO_2 can react with both the calciner and carbonator operating conditions. There are studies in literature concerning a sequential SO_2 and CO_2 capture, Grasa et al. [2008] Li et al. [2005]. Moreover, two other studies were also found in the literature on simultaneous SO_2 and CO_2 capture. One of them was based on high reactivity precipitated CaO, Iyer et al. [2004] at 700°C and the other one with natural limestones and dolomite at 850°C, Sun et al. [2007]. However, simultaneous carbonation and sulfation of limestone particles at typical carbonator conditions require further investigations. This chapter presents the sulfation of naturally occurring limestones in both the calciner and carbonator conditions of a CaL based CO_2 separation process. Simultaneous sulfation and carbonation experiments representing the carbonator reactions at two different temperatures are an important part of this study.

5.2 Experimental procedure, calculation methods and results

5.2.1 Experimental procedure

TGA experiments were carried out in a simulated environment that prevail in a carbonator and calciner. Two limestone samples originate from Germany and Greece (limestone 1 and limestone 2) and a spent sample (DFB sample) from IFK's DFB test facility were studied. A detailed description of the TGA and the sample holder construction are given in section 4.1.3 of chapter 4. Samples of 500-600 mg in the size range of 200-300 μm were used in all the analyses. Initial and final weights of the samples were measured in an external micro balance for comparison. A 100 ml/min reaction gas mixture was continuously supplied to the reaction chamber at desired gas concentrations in adiabatic conditions. Another flow of 50 ml/min N_2 purge was supplied to the housing of the measuring system to protect from corrosive gases (SO_2, CO_2 etc.). The experimental parameters such as the temperature and the gas concentrations were chosen according to the prevailing conditions in a carbonator and a calciner.

5.2.2 Sulfation reactions

Apart from CO_2, the flue gas from a typical coal fired power plant also contains H_2O and SO_2 that react with both the CaO and the $CaCO_3$ at certain concentrations and temperatures.

$$Hydration: \; CaO + H_2O \longrightarrow Ca(OH)_2 \quad \Delta H = -81 \; kJ \tag{5.1}$$

$$Sulfation\ 1: \; CaO + SO_2 + 1/2\, O_2 \longrightarrow CaSO_4 \quad \Delta H = -501 \; kJ \tag{5.2}$$

$$Sulfation\ 2: \; CaCO_3 + SO_2 + 1/2\, O_2 \longrightarrow CaSO_4 + CO_2 \quad \Delta H = -323 \; kJ \tag{5.3}$$

All three chemical reactions in 5.1, 5.2 and 5.3 can occur at certain conditions. However, in a carbonator and calciner (both operate above 600°C and atmospheric pressure) the hydration reaction will never take place according to the thermodynamic equilibrium analysis shown in figures 5.2 & 5.1, Iyer et al. [2004]. The sulfation 1 and 2 reactions can occur in carbonators while in the calciners mostly sulfation 1 since a rapid calcination would leave no $CaCO_3$ for the sulfation 2 reaction. Hence experimental investigations are required to understand the sulfation reactions and to optimise the carbonation reaction in the presence of SO_2. This study concerning the influence of sulfation on the CaL process was divided into two parts: the first part is the sulfation at calciner conditions and the second part is the sulfation at carbonator conditions-a simultaneous carbonation and sulfation.

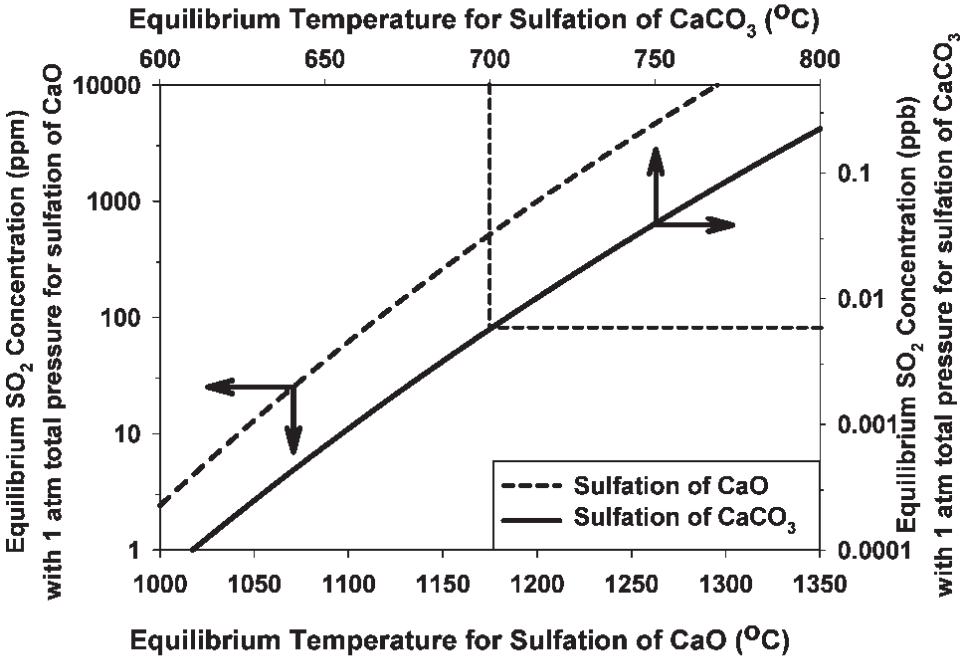

Figure 5.1: Thermodynamic data for predicting temperature zones for the sulfation of CaO and $CaCO_3$ (sulfation was considered at 1 atm, 4% O_2 and 10% CO_2) Iyer et al. [2004]

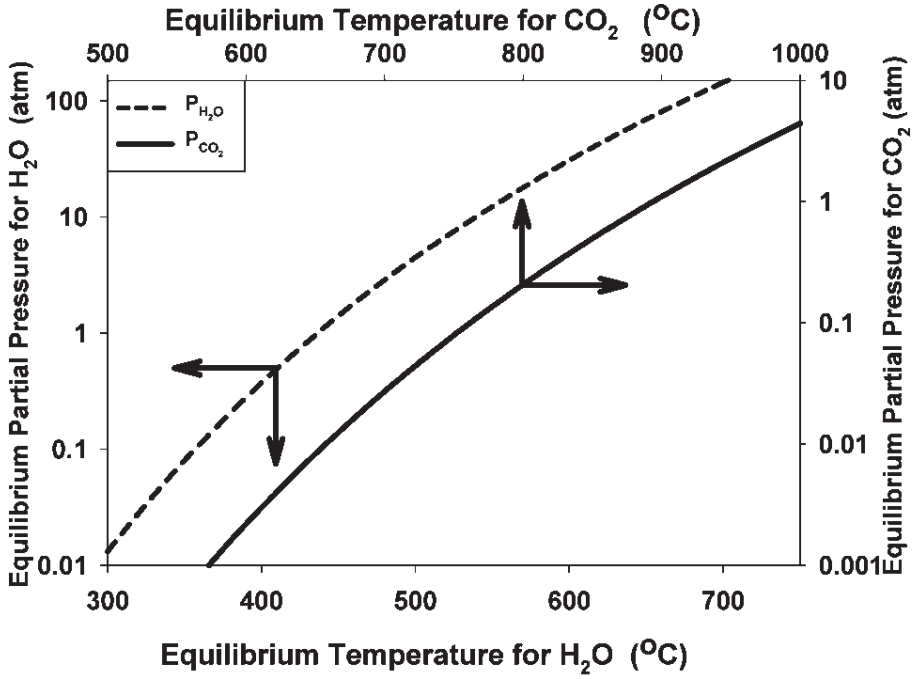

Figure 5.2: Thermodynamic data for predicting temperature zones for the hydration and carbonation of CaO Iyer et al. [2004]

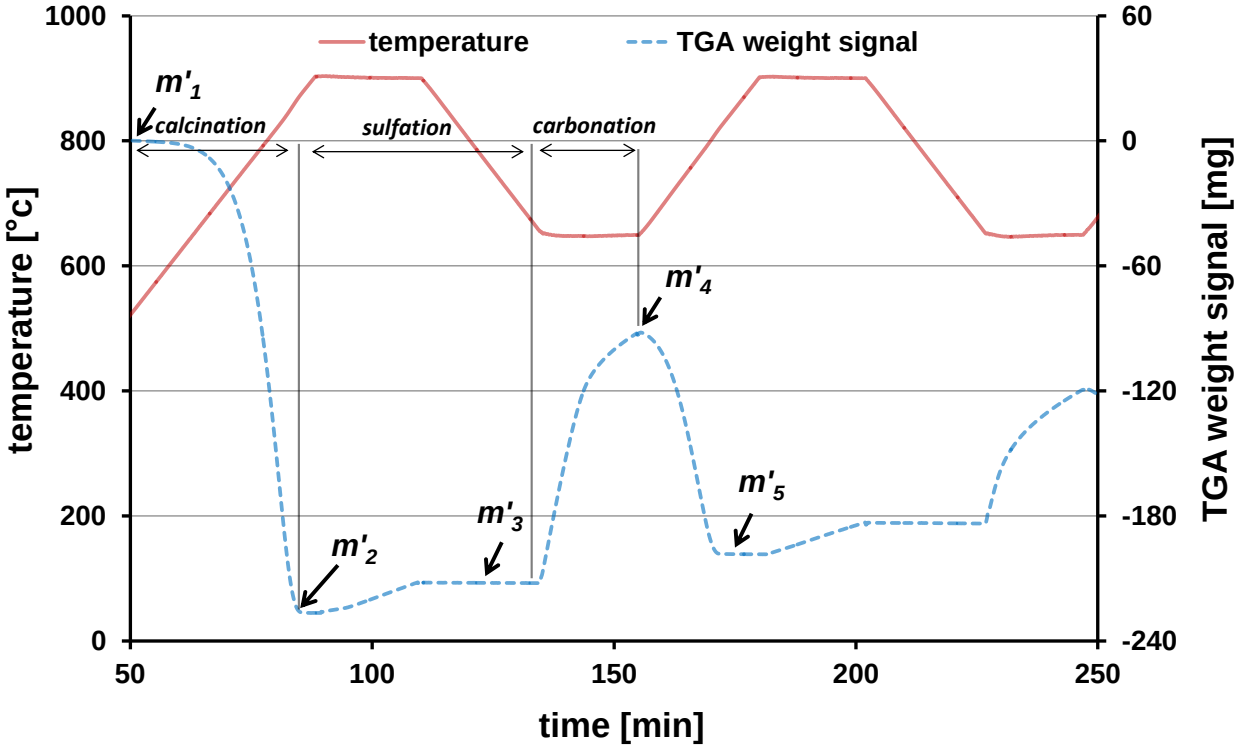

Figure 5.3: TGA curve showing calcination, sulfation and carbonation

5.2.3 Calculation procedure

Figure 5.3 is a typical TGA curve showing two calcination-sulfation-simultaneous carbonation & sulfation cycles at both the calciner and carbonator conditions. The TGA weight signal and the temperature are plotted together. In this particular case the calcination occurred at 900°C in 100% N_2 ($m_1^{'}$ - $m_2^{'}$ of the TGA curve) followed by sulfation in 3000ppm SO_2, 5%-vol O_2 and N_2 ($m_2^{'}$ - $m_3^{'}$ of the TGA curve) depicting the calciner conditions. At carbonator conditions, simultaneous carbonation and sulfation take place in 10%-vol CO_2, 2700ppm SO_2, 4.5%-vol O_2 and N_2 ($m_3^{'}$ - $m_4^{'}$ of the TGA curve)at 650°C. Then again the calcination of the following cycle happens from $m_4^{'}$ to $m_5^{'}$. From $m_1^{'}$ to $m_4^{'}$ of the TGA curve represents one complete cycle.

The degree of sulfation achieved at the calciner CaO mol-% to $CaSO_4$, $\lambda_{sulf.@cal.}$ can be calculated from the equation 5.4 where, m_i are the weights of the samples at particular points i in the TGA curve and M_x are the molecular weights of the components x. The degree of sulfation achieved in the carbonator conditions, $\lambda_{sulf.@car.}$ in mol-%, at 650°C can be determined from the equation 5.5. Finally, the degree of carbonation achieved CaO mol-% to $CaCO_3$, $\lambda_{carb.}$, in the carbonator is given by the equation 5.6. m_{cal}/M_{CaO} is the initial number of CaO mols in the sample. m_{cal} is the sample's weight after first calcination which can be calculated by deducting the ($m_1^{'}$ - $m_2^{'}$) from initial sample weight, m_0. $(m_3^{'} - m_2^{'})/((M_{CaSO_4} - M_{CaO}) \times 1000)$ is the number of $CaSO_4$ mols formed at calciner conditions, $(m_5^{'} - m_3^{'})/((M_{CaSO_4} - M_{CaO}) \times 1000)$ is the number of $CaSO_4$ mols formed

at carbonator conditions and $(m_4^{'} - m_5^{'})/((M_{CO_2}) \times 1000)$ is the number of $CaCO_3$ mols formed.

$$\lambda_{sulf.@cal.} = \left[\frac{(m_3^{'} - m_2^{'})/(M_{CaSO_4} - M_{CaO})}{(m_{cal}/M_{CaO})}\right] \times 100 \tag{5.4}$$

$$\lambda_{sulf.@car.} = \left[\frac{(m_5^{'} - m_3^{'})/(M_{CaSO_4} - M_{CaO})}{(m_{cal}/M_{CaO})}\right] \times 100 \tag{5.5}$$

$$\lambda_{carb.} = \left[\frac{(m_4^{'} - m_5^{'})/(M_{CO_2})}{(m_{cal}/M_{CaO})}\right] \times 100 \tag{5.6}$$

5.2.4 Influence of sulfation occurring at a calciner

Sulfation in a calciner affects the CO_2 capture potential of the sorbents since it consumes the active CaO meant for CO_2 capture in the carbonator. In order to quantify this effect, samples were first calcined at 900°C in N_2 atmosphere and sulfated for 20 minutes at the same temperature with 3000 ppm SO_2, 5%-vol O_2 and N_2. Then they were cooled down to 650°C for carbonation in 15mol-% CO_2 and N_2 for another 20 minutes. The same procedure was repeated for four times. The tests were carried out with one variant of sample type. The degree of sulfation achieved by the sample in the calciner conditions will be discussed first. Figure 5.4 shows the comparison of sulfation achieved by limestone 1 and 2 in 20 minutes at a typical calciner condition for each of the four cycles. Both samples show similar degrees of conversion in the first two cycles while in the 3^{rd} and 4^{th} cycle the difference begins to widen. The difference in conversion also increases with increasing the number of cycles. It can be observed that the degree of sulfation at the second cycle is higher than at the first cycle.

Figure 5.5 compares limestone 1, DFB and the hydrated DFB samples for the sulfation achieved in each of the four cycles, once again at the same calciner conditions. It is worth to mention that the DFB and the hydrated DFB are also derivatives of the limestone 1 and contain no sulfur. The same procedure as explained in section 4.2.4 was followed to hydrate the DFB sample. As can be seen in the same figure 5.5, the DFB sample shows the lowest sulfation while the hydrated DFB is the highest and the limestone 1 lies in-between. The DFB sample's lowest sulfation which also decreases with cycle number, could have been caused by the loss of surface area at the DFB test facility due to the repetitive carbonations and calcinations, rapid heating and physical attrition of the particles. However the hydrated DFB achieved the highest suflation. It can be deduced from this observation that the hydration seems to enhance the CaO availability by causing cracks on the sorbent granules which opens up more fresh material to the reactive gases. However the effect of hydration on particle morphology is also important and needs to be further investigated. More on hydration for sorbent particle reactivation and enhanced CO_2 capture is discussed in section 4.2.4 of chapter 4.

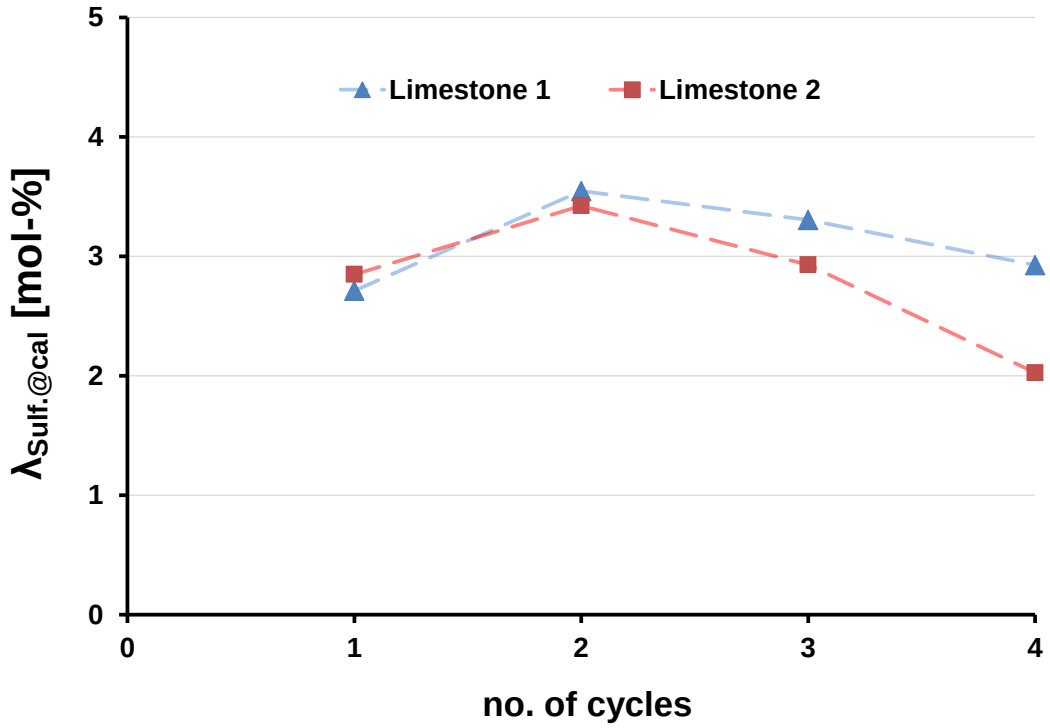

Figure 5.4: CaO mol-% conversion to $CaSO_4$ for limestone 1 & 2

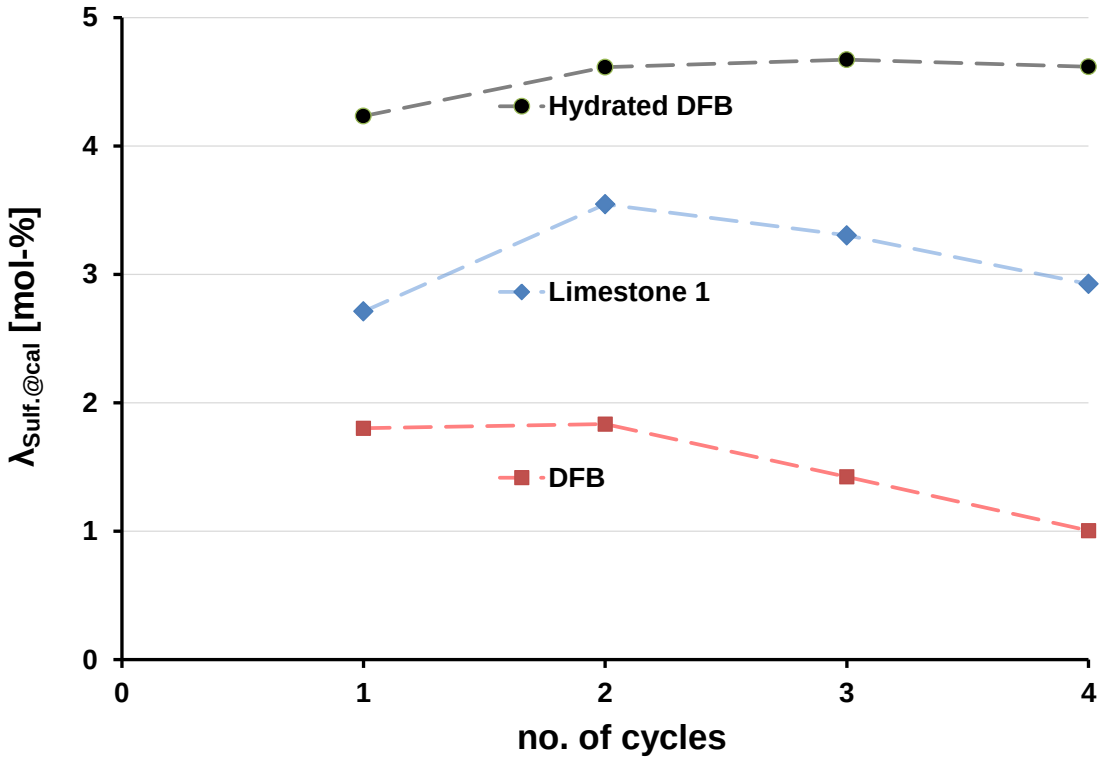

Figure 5.5: CaO mol-% conversion to $CaSO_4$ for limestone 1, DFB and Hydrated DFB sample

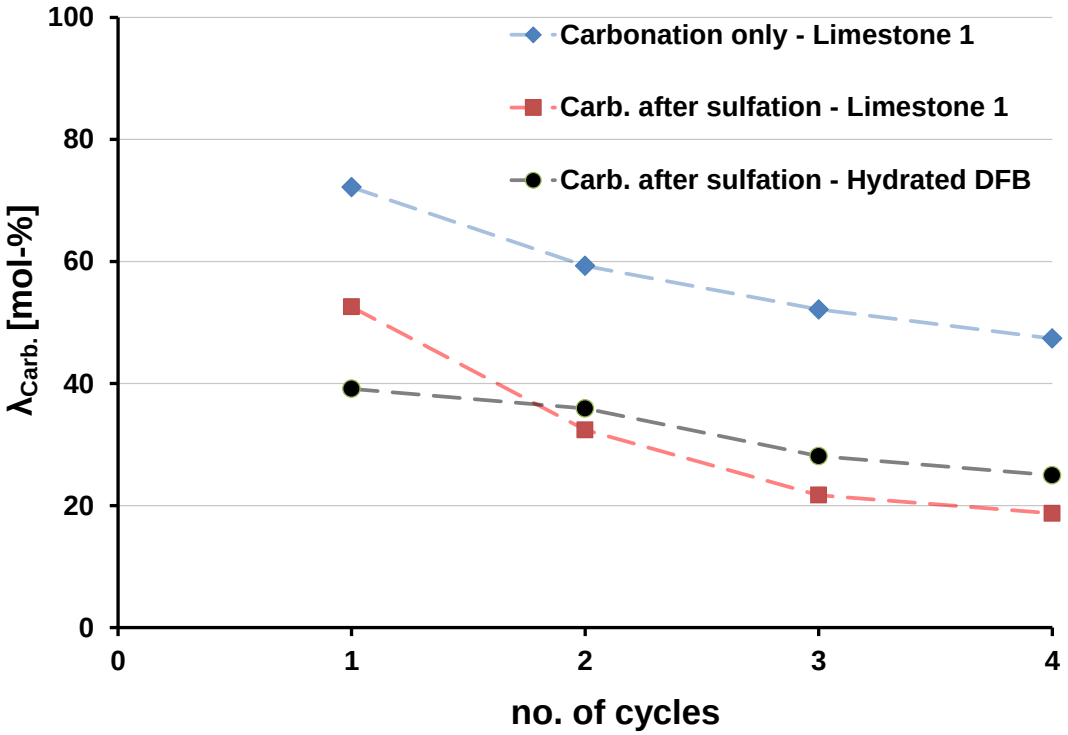

Figure 5.6: CaO mol-% conversion to $CaCO_3$ after subjected to sulfation in calciner conditions for limestone 1, DFB & hydrated DFB samples

Figure 5.6 plots the $\lambda_{carb.}$ of limestone 1 and hydrated DFB with number of cycles, after subjected to sulfation in calciner operating conditions. In order quantify the effect of sulfation on carbonation, one test run was conducted without sulfation and plotted on the same figure. It is a well-reported fact that the carbonation conversion decreases with increasing number of cycles due to the loss of surface area. In addition to this, the sulfation offers an added adverse effect on carbonation conversion of limestone particles as can be seen in figure 5.6. The conversion difference between the carbonation only line and the carbonation after subjected to sulfation lines are considerably large (more than 20mol-%). It can be attributed to the fact that the $CaSO_4$ produced by sulfation 1 reaction equation 5.2 remained in the particle during the carbonation. The $CaSO_4$ remained in the sorbent particle not only reduces the available CaO for the carbonation but also effectively blocks the pore structures of the CaO. The effect of pore blockage by the $CaSO_4$ product layer can be realized by comparing the $\lambda_{carb.}$ of limestone 1's 1^{st} cycle between carbonation only (72mol-%) and the carbonation after the sulfation (52mol-%). The sum of $\lambda_{carb.}$ (52mol-%) and $\lambda_{sulf.@cal.}$ (3mol-%) in the latter case (55 mol-%) is much less than the $\lambda_{carb.}$ of the former case without sulfation(72mol-%). That means, apart form the CaO that was converted to $CaSO_4$(3mol-%), some more CaO (17mol-%) remained as inert material or is unable to get converted during the following carbonation. Thus the sulfation at calciner significantly hindered the carbonation.

The $\lambda_{carb.}$ shows the decreasing trend with the cycle number in all three cases in fig-

ure 5.6. However, the gap between the cases of limestone 1 carbonation only and the carbonation after sulfation, increases with number of cycles. This seemed to suggest the accumulation of $CaSO_4$ in the sorbent particles during each cycle. It can also be noted that the deactivation of the hydrated sample occurs at a slower rate than limestone 1 as the $\lambda_{carb.}$ of the former is more than the latter except for the 1^{st} cycle. This means that the hydrated samples achieved higher sulfation as well as carbonation.

5.2.5 Influence of sulfation occurring at a carbonator

As discussed in section 5.2.4, sulfation at calciner reduced the CO_2 capture capacity of the sorbents due to the formation of $CaSO_4$ which remained stable with number of cycles. When it comes to the CaL carbonator, the sulfation and carbonation take place simultaneously. The sulfation 2, concerning the $CaCO_3$ sulfation according to the reaction equation 5.3, occurs in carbonators in addition to the sulfation of CaO. This part of experiments is to quantify the extent of sulfation and carbonation during the simultaneous reactions at the carbonator temperatures of 650°C and 700°C. The trend in the ratio of carbonation to sulfation as a function of residence time has also been determined and compared against the number of cycles.

The samples were calcined at 850°C in 100% N_2 atmosphere and subjected to simultaneous carbonation and sulfation at two different temperatures (700°C & 650°C) in 2700 ppm SO_2, 10%-vol CO_2(100 000 ppm) and N_2. Since the CO_2 concentration is more than 30 times higher than that of SO_2, a higher rate of carbonation is expected. However, a higher free energy change of sulfation reaction thermodynamically favors it over carbonation. In order to shed light on simultaneous carbonation and sulfation reactions kinetics, the residence times were varied as 5, 10, 30 and 50 minutes. Altogether there were four experiments conducted at each carbonation temperature and each of the four residence times. All the TGA runs were conducted for four number of cycles.

Figures 5.7 and 5.8 respectively show the limestone 1's CaO mol-% to $CaSO_4$ and CaO mol-% to $CaCO_3$ conversions, occurred simultaneously at 650°C, versus the residence times of 5, 10, 30 and 50 minutes in 10%-vol CO_2, 2700 ppm SO_2 and N_2 gas mixture for four cycles. With regards to the sulfation, the rate and the value of $\lambda_{sulf.@carb.}$ for the first two cycles steadily increase with increasing residence time. In the third cycle the $\lambda_{sulf.@carb.}$ rate slightly falls at 50 minutes while it gets even slower in the 4th cycle, reaching a lower value than at 30 minutes. This could have been caused by the combined effect of sorbent sintering and the thickening of $CaSO_4$ product layer due to the prolonged residence time of 50 minutes for four consecutive cycles. Sintering leads to loss of specific surface area which causes reactivity loss.

In the case of $\lambda_{carb.}$ in figure 5.8, the rate and the values do not change significantly up to 10 minutes residence time, which corresponds to the initial kinetically controlled fast reaction phase, for all the four investigated cycles. The $\lambda_{carb.}$ for 20 minutes residence time showed around 50mol-% conversion compared to the carbonation without any sulfation of

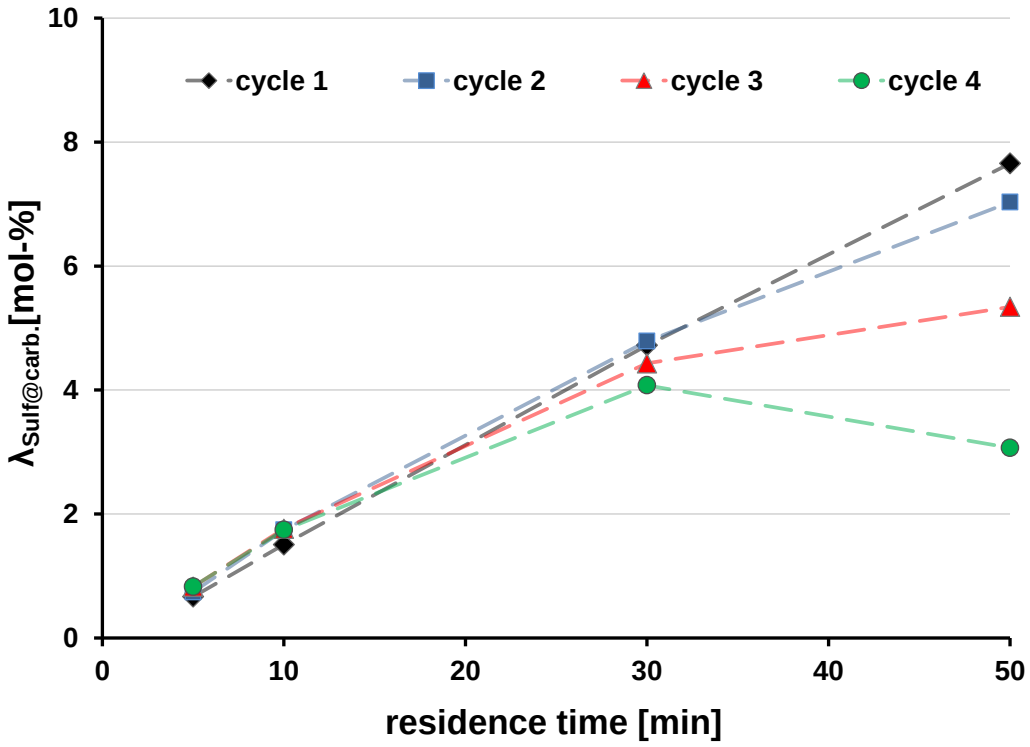

Figure 5.7: Limestone 1's CaO mol-% conversion to $CaSO_4$ during the simultaneous carbonation & sulfation in carbonator conditions at 650°C

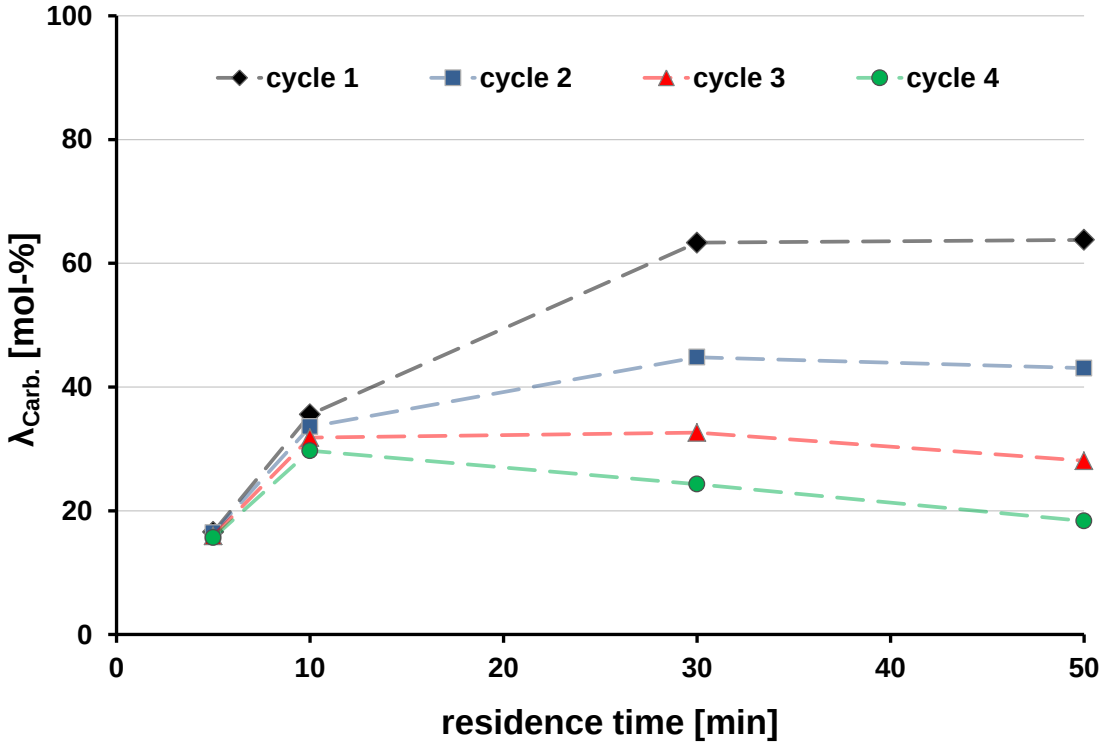

Figure 5.8: Limestone 1's CaO mol-% conversion to $CaCO_3$ during the simultaneous carbonation & sulfation in carbonator conditions at 650°C

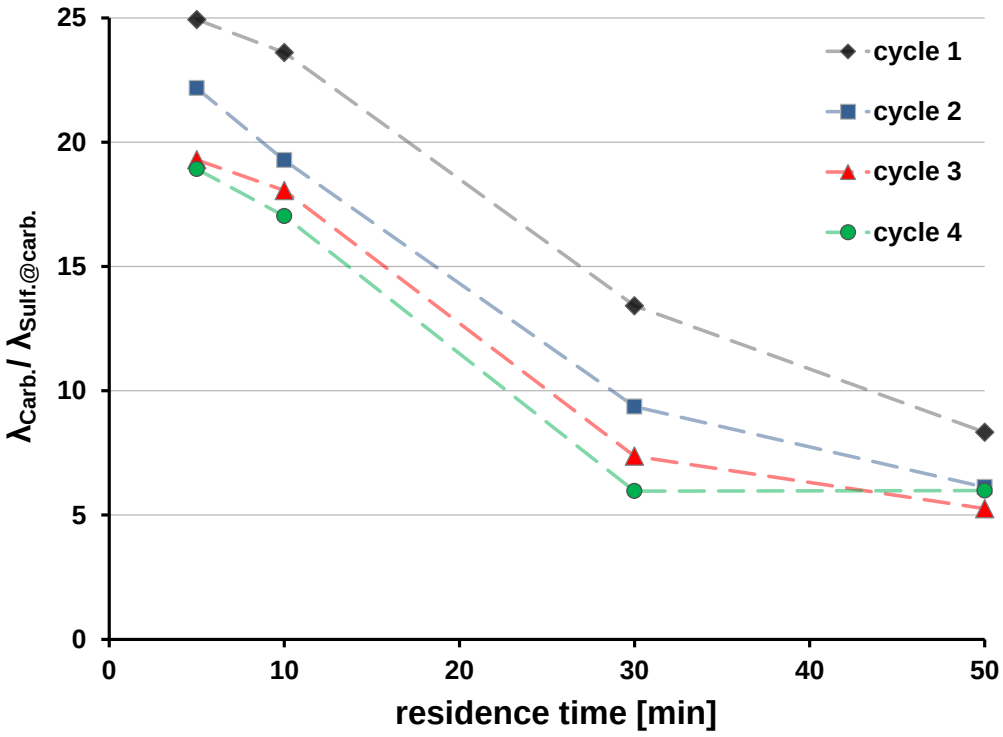

Figure 5.9: The ratio of $\lambda_{carb.}/\lambda_{sulf.@carb.}$ for the simultaneous carbonation & sulfation in carbonator conditions at 650°C

72mol-% in figure 5.6. It can be seen that the $\lambda_{carb.}$ also reduces with increasing number of cycles in each of the four residence times. In case of the first two cycles, the value of $\lambda_{carb.}$ remains the same for the 30 and 50 minutes residence time. However, the corresponding $\lambda_{sulf.@carb.}$ keeps increasing (figure 5.7). This observation suggests that the sulfation 2 reaction (reaction equation 5.3) could have occurred and converted the $CaCO_3$ formed during the carbonation to $CaSO_4$.

Figure 5.9 plots the ratio of $\lambda_{carb.}/\lambda_{sulf.@carb.}$ versus the residence time for all the four cycles of limestone 1 at 650°C. The aim of the CaL process is to capture as much CO_2 as possible from the flue gas with a minimum amount of sorbent circulating between the reactors. The amount of sorbent circulation required for CaL process depends on the ratio of active sorbent material present in the circulating stream as explained in section 4.1. However it was found out that the accumulation of $CaSO_4$, the product of sulfation, deactivates the sorbents. Hence, finding an optimum residence time which maximises $\lambda_{carb.}$ and minimising the $\lambda_{sulf.@carb.}$ is very important. Moreover, the average residence time of sorbent particles in a CFB carbonator will be in the range of a couple of minutes. The figure 5.9 plot apparently shows that the lower residence time favours the carbonation than its competing sulfation. That means, when comparing 5 and 10 minutes residence time, the former will fit the criteria for a CFB carbonator. Apart from that the number of cycles also has a significant effect on $\lambda_{carb.}$ and $\lambda_{sulf.@carb.}$ according to figures 5.7 and 5.8. In a real CaL plant the sorbent particles will undergo several dozens of cycles, thus to

Table 5.1: The ratio of $\lambda_{carb.}/\lambda_{sulf.@carb.}$ for 5 min carbonation at 650°C & 700°C

Carb. temp.	**Ratio of $\lambda_{carb.}/\lambda_{sulf.@carb.}$**			
	n=1	**n=2**	**n=3**	**n=4**
650°C	24.9	22.2	19.3	18.9
700°C	10.0	8.1	7.0	6.6

calculate the optimum residence time, one has to consider the average characteristics of the sorbent population. It is necessary to analyse tens of cycles in the same manner to find out the residence time suitable for a real CaL plant. In this case the maximum residence time can be limited to 10 minutes and the frequency of the points can be increased to get more accurate results.

Carbonation temperature is also to be optimised in order to get the maximum CO_2 separation in the presence of SO_2. Table 5.1 lists the ratio of $\lambda_{carb.}/\lambda_{sulf.@carb.}$ for the carbonation temperatures of 650°C and 700°C and for 5 minutes residence time. It is apparent that the ratio is much higher at 650°C throughout all the for cycles. The individual $\lambda_{carb.}$ values have also been found to be higher at this temperature than 700°C. Hence, comparing 700°C and 650°C, the latter can be suggested as the optimum carbonator temperature to maximise the CO_2 separation in the presence of SO_2.

5.2.6 Sulfation rate analysis

It was observed in section 5.2.5 that the sulfation occurred much slower than the carbonation at CaL reactor operating conditions. It can be attributed to the lower SO_2 concentration than the CO_2 in the carbonator. It has also been observed that the sulfation adversely affected the carbonation capacity of the sorbents. A set of experiments were conducted to analyse the rate of pure sulfation (without the presence of CO_2) at typical calciner and carbonator temperatures for extended periods. Figure 5.10 shows the rate of sulfation of calcined limestone 1 (CaO) at 900°C and 650°C in 3000 ppm SO_2, 5%-vol O_2 & N_2 for more than 2 hours. The rates are almost the same up to 80 minutes and then the 900°C sulfation begins to slow down. The reason could have been the sintering of the particles due to the exposure to high temperatures for a long period of time, which reduces the specific surface area directly linked to the reactivity. However at 650°C, sulfation seems to occur at a consistent rate as it is not significantly affected by the sintering.

Sulfation 2 reaction (reaction equation 5.3) occurs mostly in the carbonator due to the availability of $CaCO_3$, while the sulfation 1 reaction with CaO (reaction equation 5.2) takes place in both reactors. Figure 5.11 shows a comparison of sulfation rates of limestone 1, calcined limestone (CaO) and once carbonated limestone 1 ($CaCO_3$) at 650°C in 2700 ppm SO_2, 4.5 %-vol O_2 & N_2 for 60 minutes. The sulfation rate of the calcined limestone 1 (CaO) and once carbonated limestone are comparable up until 15 minutes time and then

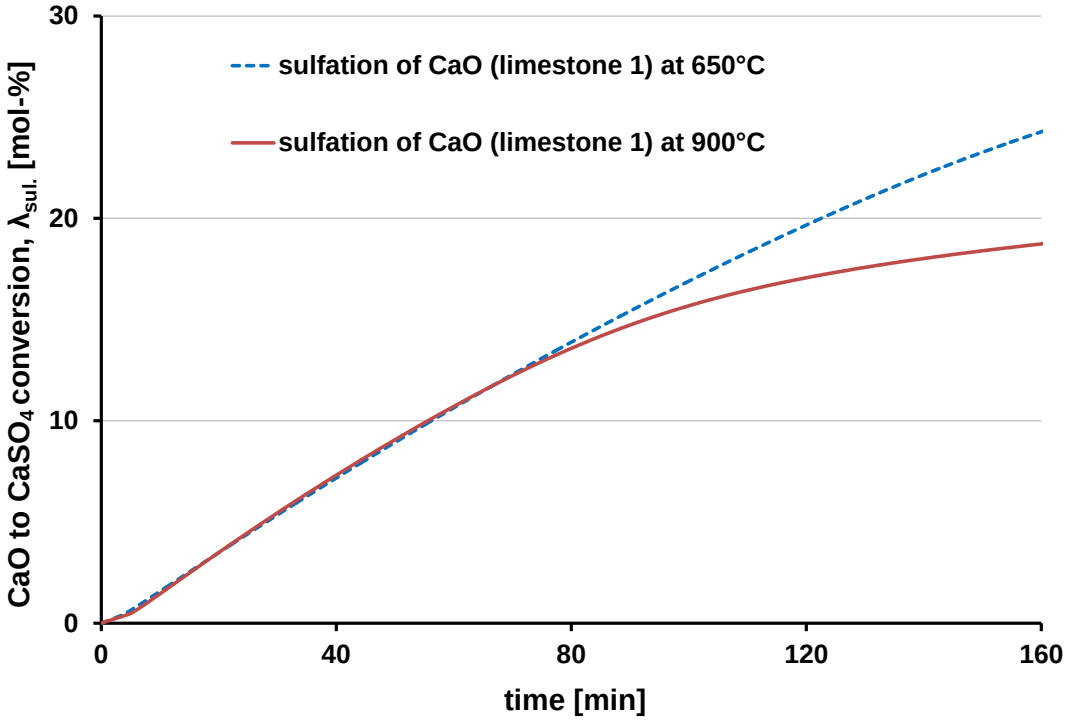

Figure 5.10: Sulfation of calcined limestone 1 at 650°C and 900°C

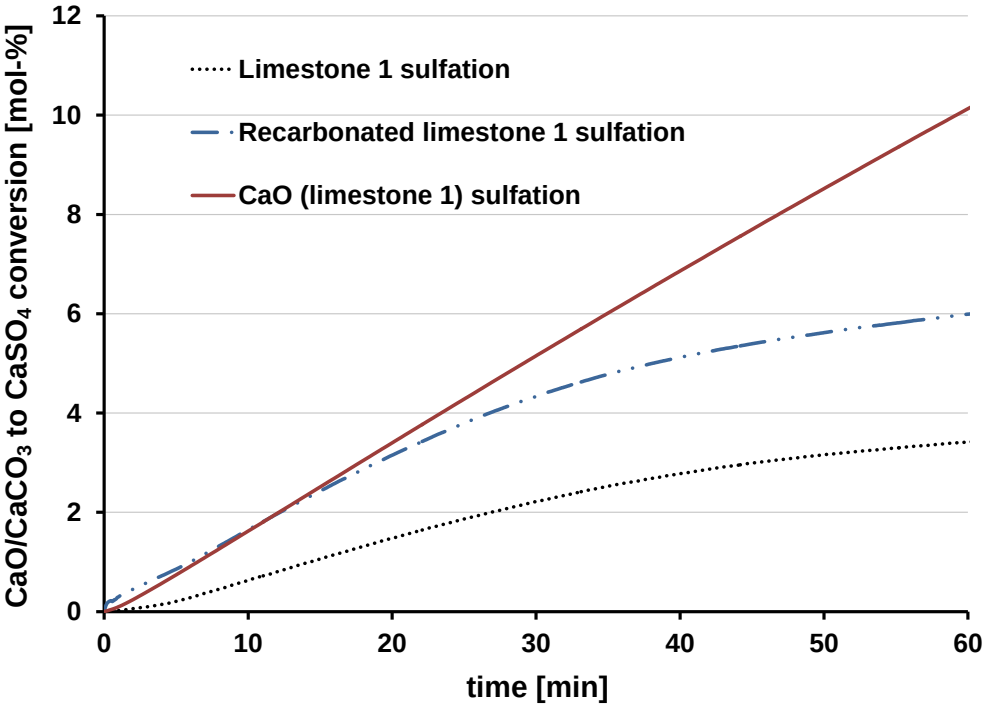

Figure 5.11: Sulfation of various forms of limestone 1 at 650°C

they fall apart. That means, at the beginning the sulfation 1 and the sulfation 2 reactions occurred at comparable rates. Therefore it can be stated that the newly formed $CaCO_3$ is more reactive to SO_2 than the original limestone which showed the lowest sulfation.

5.3 Conclusion

Sulfation and carbonation experiments were conducted in a TGA at typical calciner and carbonator operating conditions of a CaL process. It was witnessed in both the calciner and carbonator reactor operating conditions that the $CaSO_4$ formed as a result of sulfation which got accumulated in the sample over the number of cycles. The $CaSO_4$ accumulation in the sorbents will reduce the amount of CaO available for CO_2 capture and hence will undermine sorbents' CO_2 capture potential. After subjected to hydration, the DFB sample was found to be highly reactive as almost equal as a fresh limestone towards both SO_2 and CO_2. Analysis of carbonation to sulfation ratio against the residence time revealed that the smaller the residence time the better the CO_2 capture efficiency is as the formation of $CaSO_4$ is reduced that blocks the CaO. Out of the two tested carbonation temperatures of 650°C and 700°C, the former one was found to be more favorable for CO_2 separation at atmospheric conditions. No significant sulfation rate difference was observed in sulfation-only tests at both reactor operating temperatures of 650°C and 900°C. However the sulfation rate of once carbonated limestone(subjected to one cycle) was faster than the fresh limestone at 650°C.

Chapter 6

Calcium looping for partial oxidation processes

A detailed description of calcium looping(CaL) based CO_2 capture for partial oxidation processes (pre-combustion capture) and its process configuration are given in section 1.2.1. This chapter comprises of three sections. The first section deals with the TGA experiments in a reducing synthetic syngas atmosphere at elevated pressure conditions. Three parameters are studied by varying the limestone type, carbonation temperature and CO_2 concentrations. The second section is to investigate the sintering that occurs at high temperatures, especially during the particle regeneration/calcination phase. The calcination temperatures of fresh limestone samples are varied from 900°C to 1100°C and the following carbonations are quantified and compared. The last section deals with the influence of incomplete carbonations on particle decay with increasing number of calcination and carbonation reaction(CCR) cycles. TGA experiments are carried out for several number of CCR cycles with the carbonation time of one minute. The sorbant decay as a result of several CCR cycles with a short carbonation time is compared with that of a regular CCR cycles.

6.1 TGA experiments with synthetic syngas

TGA experiments were carried out with two limestone samples 1 & 2 at gasification conditions to study the in situ CO_2 capture of an Absorption Enhanced Gasification of Solids(AEGS) process. The test procedure as described in section 4.1.4 was followed for the atmospheric pressure conditions. In case of pressurised TGA experiments, firstly the sample was placed into the reaction chamber and then it was filled with N_2 to 5 bar gauge pressure. Once a steady state weight signal was obtained, the gas supply was switched on followed by heating. All the calcinations were at 900°C in 100% N_2 for 5 minutes. The carbonations were carried out with a synthetic syngas mixture containing 43%-vol H_2, 23%-vol CO_2, 17%-vol CO, 7%-vol CH_4 and N_2. The carbonation temperatures were also varied from 700°C to 800°C with 25°C steps. The duration of the carbonations were 20 minutes and the experiments were conducted for 7 CCR cycles. The results and the discussions follow in the next sections.

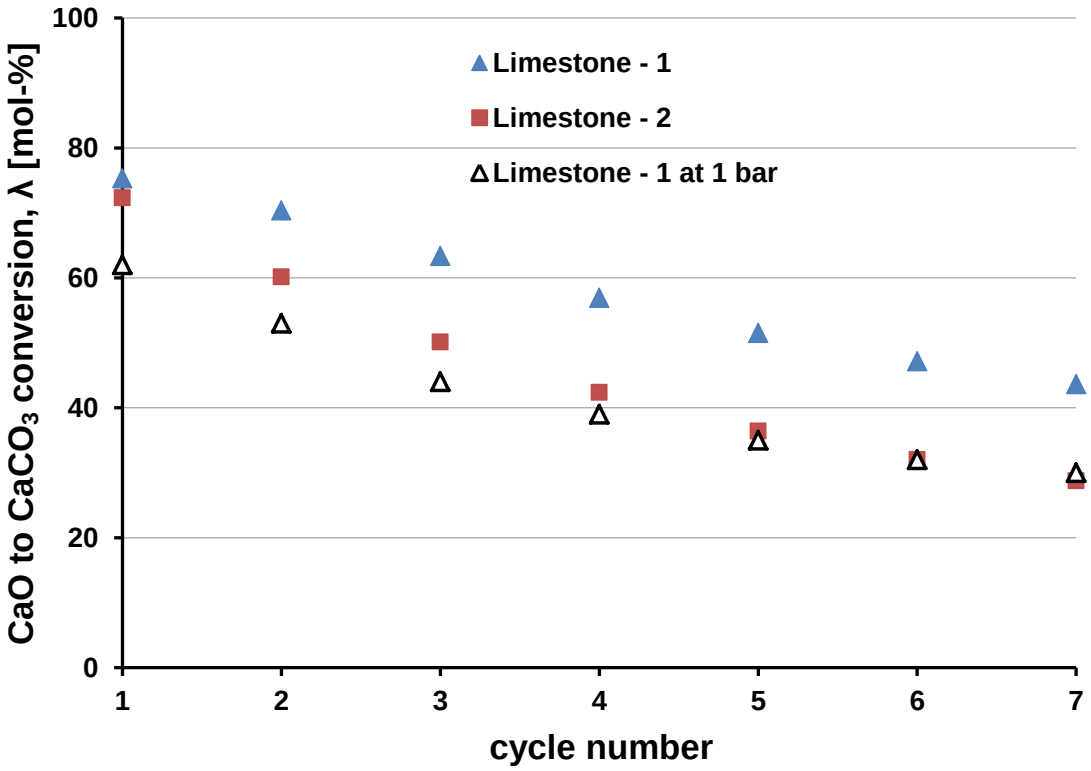

Figure 6.1: CaO mol-% conversion to $CaCO_3$ of limestone 1&2 at 6 bars

6.1.1 Influence of limestone types on CaO conversion at high pressure

Figure 6.1 plots the CaO mol-% conversion to $CaCO_3$ of limestone 1 & 2 at 6 bar in synthetic syngas mixture at 750°C for 7 CCR cycles. In order to compare the carbonations with the atmospheric conditions, the limestone 1's CaO mol-% conversion also was plotted on the same diagram, at the same carbonation conditions. As one can expect, the CaO conversions decline with increasing number of CCR cycles for both of the limestones. Although the 1^{st} CCR cycle's conversions of limestone 1 & 2 are nearly equal (~75 mol-%) at 6 bar, the latter decreases faster than the former and at the end of 7^{th} CCR cycle the conversions are 44 and 30 mol-% CaO respectively. When it comes to the atmospheric conditions, the conversions of limestone 1 is lower than the limestone 1 and limestone 2 which are carbonated at 6 bar pressure however with the same synthetic syngas mixture for 20 minutes. For the carbonation temperature of 750°C, the corresponding equilibrium CO_2 concentration is nearly 10%-vol. The CO_2 concentration difference between the gas phase and the equilibrium is higher for the pressurised case than the atmospheric case. As discussed in section 4.2.2 of chapter 4 that the higher the CO_2 concentration difference the higher is the reaction rate. Therefore, at 6 bar case the CO_2 concentration difference is higher and leads to the higher reaction rate (than at the atmospheric conditions) and higher conversions for the carbonation duration of 20 minutes. The decay coefficients(k)

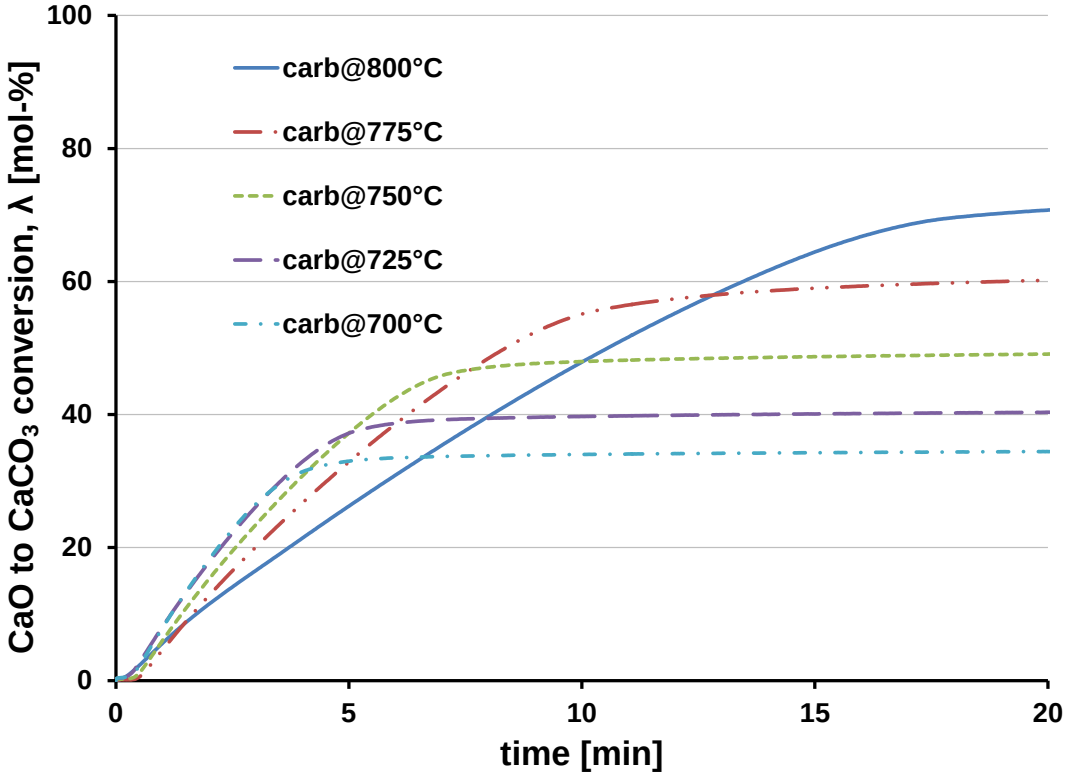

Figure 6.2: CaO mol-% conversion to $CaCO_3$ of limestone 2 at 6 bars with varying carb. temperatures

were also calculated for all three cases by the equation 3.4 as explained in section 3.2.3. The k values are 0.21 and 0.28 for limestone 1 & 2 respectively at 6 bar and 0.22 for the limestone 1 at 1 bar. These values are also in line with the observation that the limestone 1 is better than limestone 2 for CO_2 separation as the decay coefficient k is smaller for the former.

6.1.2 Influence of the carbonation temperature on CaO conversion at high pressure

One of the main reasons to increase the reactor pressure in an AEGS process is to increase the CO_2 partial pressure. The increased CO_2 partial pressure will enable the CO_2 capture at higher temperatures at which a higher solid fuel conversion (char conversion) is ensured. The relationship between the equilibrium CO_2 partial pressure and the temperature is plotted in figure 2.1 in chapter 2 and this relationship can also be expressed by the equation 2.1.

Figure 6.2 plots the CaO mol-% conversion of limestone 2 in synthetic syngas mixture at temperatures of 700°C, 725°C, 750°C, 775°C and 800°C for 20 minutes at 6 bar. The 1^{st} carbonation was performed at 800°C and then the carbonation temperatures were reduced util 700°C with the consecutive CCR cycles. CaO mol-% conversions in 20 minutes are

reducing with decreasing carbonation temperatures and also with increasing number of CCR cycles. However the main cause of the reduction is definitely due to the increasing number of CCR cycles since the 20 minutes residence time is relatively long enough to offset any reaction rate variations occurred during the initial fast reaction phase. If one considers a 5 minutes residence time, the conversions are not influenced by the number of CCR cycles but the carbonation temperature, according to the figure 6.2.The CaO conversions in 5 minutes residence time are the lowest for the 800°C case despite being at the 1^{st} CCR cycle. However its conversion later became the highest in 20 minutes residence time.

The sample was subjected to consecutive carbonation cycles at varying temperatures instead of having fresh samples for each of the carbonation temperature. This is because the initial fast carbonation reaction phase is important in a CaL process and it is not influenced by the number of CCR cycles (when the number of CCR cycles are less than 10). However the initial fast phase conversion is highly influenced by the carbonation temperature. The reaction rates at fast reaction phase follow a descending order; 700°C $>$ 725°C $>$ 750°C $>$ 775°C $>$ 800°C. This can be explained by looking at the the CO_2 concentration difference between the TGA gas phase and the equilibrium concentration which corresponds to that particular temperature, a parameter directly proportional to reaction rate. Equilibrium CO_2 concentration decreases with reducing temperature while the TGA gas phase CO_2 concentration is kept constant, thus the difference increases. This phenomenon was also explained in a reaction rate comparison between fresh limestone samples and DFB samples in section 4.2.3. In order to achieve an optimised conversion in 10 minutes, a 775°C carbonation can be recommended as it achieved more than 50%-mol conversion with reasonably high conversion rate. Similarly for a 5 minutes residence time, 750°C carbonation is advantageous as it has not only achieved a high conversion but also remained in the fast phase.

6.1.3 Influence of the CO_2 concentration on the CaO conversion at high pressure

The syngas CO_2 concentration of an AEGS process after the CO shift reaction would be much higher than the flue gas concentration from a conventional coal combustion(∼15%-vol) process. However the CO_2 concentration of an AEGS gasifier varies as the capture occurs simultaneously in the same reactor. TGA experiments were conducted to analyse the reaction rates with varying CO_2 concentration at AEGS process conditions. Limestone 2 was carbonated at 6 bar and 750°C with varying CO_2 concentrations as 15%-vol, 25%-vol, 35%-vol and 40%-vol for 20 minutes while the calcination conditions were kept the same as 950°C, in pure N_2 and 5 minutes duration. The CO_2 concentrations were varied from 15%-vol and up to 40%-vol with consecutive CCR cycles.

Figure 6.3 plots the 20 minutes CaO mol-% conversions for varying CO_2 concentrations. The conversions decrease with the increasing CO_2 concentration and number of

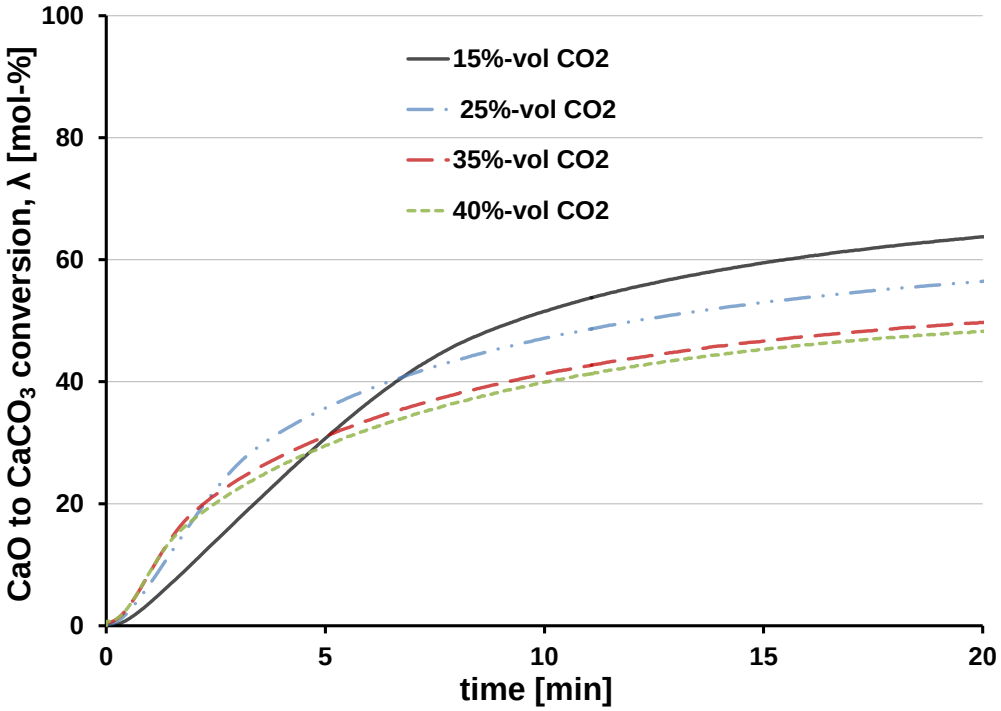

Figure 6.3: CaO mol-% conversion to $CaCO_3$ of limestone 2 at 6 bars with varying CO_2 concentration

CCR cycles. The main reason for the reduction in conversion is definitely due to the increasing CCR cycle number, because the effect on CaO conversion due to the varying CO_2 concentrations during the fast reaction phase were offset in 20 minutes residence time. As mentioned in section 6.1.2 the fast phase conversion is of importance for the CaL process. That means the conversions in 5-10 minutes are relevant. When it comes to the 5 minutes conversions, 25%-vol CO_2 case achieved the highest value and for the 10 minutes case the 15%-vol CO_2 case was the highest. The latter case shows a low rate of conversion during the fast phase than the other cases with higher CO_2 concentrations. The reason is that the CO_2 concentration difference of the gas phase and equilibrium is directly proportional to the reaction rate in the fast reaction phase and it is given by the formula 4.1. The higher the CO_2 concentration in the gas phase, the higher is the difference and thus the conversion rate. One can also visually observe that the duration of the fast reaction phase is getting smaller with increasing CO_2 concentrations. Higher CO_2 concentrations shorten the fast reaction phase which means that the carbonator space time (τ_{active}) as discussed in section 4.1 of chapter 4, is getting smaller. The τ_{active} can be increased by adding more fresh material(as makeup flow), to achieve required CO_2 capture in a particular carbonator.

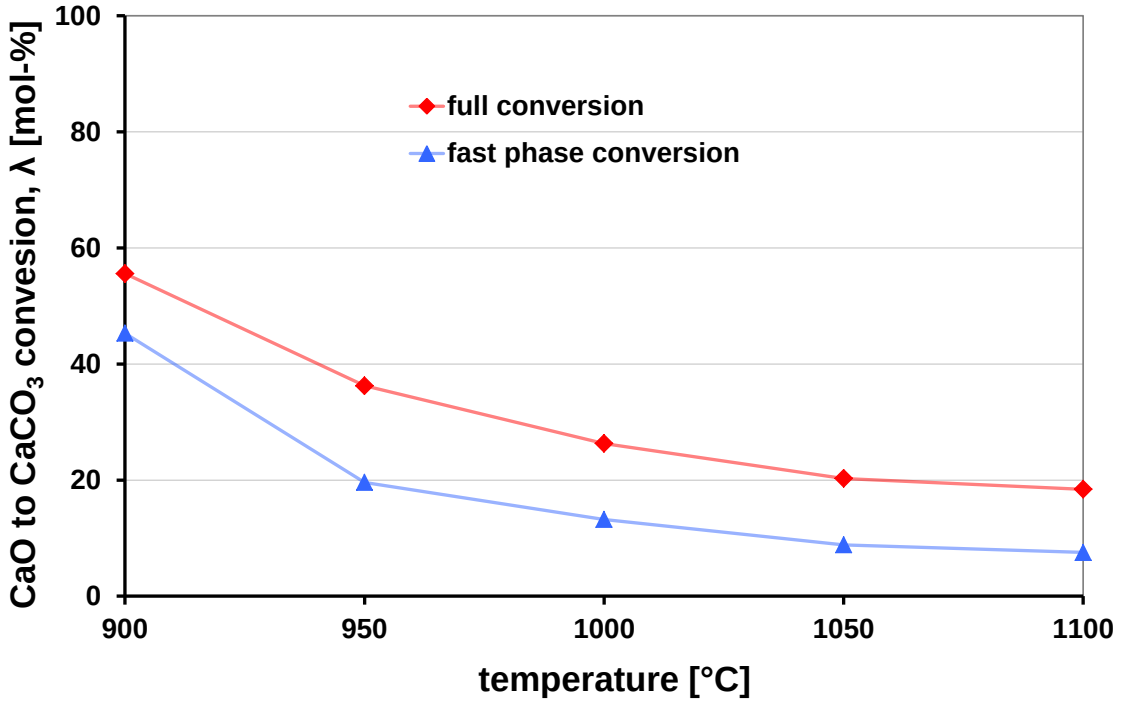

Figure 6.4: CaO mol-% conversion to $CaCO_3$ of limestone 2 with varying calcination temperatures

6.2 High temperature sintering

The total pressure of the AEGS gasifier cum carbonator should be higher for enabling the in situ CO_2 capture and enhanced fuel conversion. However the calciner should be kept at atmospheric conditions. In this case the CO_2 partial pressure in the calciner will not exceed one bar so that the calcinations can still be performed at about 900°C. If the calciner is to be operated at high pressures, the calcination temperature should also be increased to induce the calcination reaction. Increasing the calcination temperature causes not only a huge exergy loss but also intense sintering of particles and surface area losses. The effect of high temperature calcinations was studied in a TGA environment by measuring the corresponding carbonation conversions.

Effect of calcination temperature on CaO conversions was discussed in section 3.2.2 and it was concluded that the higher the calcination temperature the lower the conversion. However in this study the calcination temperatures were higher(1100°C) than the previous study(930°C) and the calcinations were performed at 1 bar in 90%-vol CO_2 environment as in a real CaL process. The carbonations were conducted at 650°C, 15%-vol CO_2 & N_2 for 30 minutes. The calcination temperatures were varied as 900°C, 950°C, 1000°C, 1050°C and 1100°C. At every temperature a fresh sample was used to avoid the influence of CCR cycle number. At each calcination temperatures the CaO mol-% conversion of the 1^{st} CCR cycles was measured.

Figure 6.4 plots the CaO mol-% conversions of the limestone 2 at varying calcination temperatures. The fast phase conversion for each case was calculated by a procedure explained in section 4.1.4 and plotted in the same figure. As one can expect the CaO conversions decrease with increasing calcination temperatures. The conversion at 900°C calcination is 55 mol-% and it decreases to just 18 mol-% at 1100°C calcination. When it comes to the fast phase conversion, it decreases from 45 mol-% to 7 mol-% for the same calcination(carbonation temperature is kept constant) temperatures. However the fast phase conversion matters for the CaL process and it reduced by almost 6 times at 1100°C calcination. The calcination rates also were analysed separately. The rates were relatively high despite the high CO_2 concentration(90%-vol) which would hinder the release of CO_2 from the $CaCO_3$ crystals. However, complete calcinations were achieved in 6 minutes at temperatures 950°C to 1100°C. The calcination was slow at 900°C due to the CO_2 presence (90%-vol) and it took more than 20 minutes to achieve a complete calcination. By comparing the effect of calcination temperatures discussed in section 3.2.2, it can be concluded that the high temperature calcinations induced intense sintering of CaO and caused drastic reductions in CaO mol-% conversions. Therefore, high temperature calcinations should be avoided in a CaL process with naturally occurring sorbents.

6.3 Impact of incomplete carbonation on sorbent decay

Concerning all the TGA analysis so far, the carbonations were carried out for more than 20 minutes. However in case of a real CaL process, the residence time of a sorbent particle is in the range of a couple of minutes, depending on the degree of fluidisation and the carbonator-to-calciner sorbent split fraction. In this circumstances the particle can only be partially carbonated. It is interesting to find out the behavior of partially carbonated particle in consecutive CCR cycles. Some important aspects to be looked at are how fast it will be carbonated in the following cycle and how the carbonation capacity is affected with regard to the number of partial carbonation calcination reactions(PCCR) cycles.

At first, 19 PCCR cycles were carried out in the TGA. All the carbonations and calcinations were conducted at the same adiabatic temperature of 800°C. The reaction gas flows were switched alternatively, such that the carbonation and calcination reactions can take place at the adiabatic conditions. The calcinations and the partial carbonations were conducted in 100% N_2 for 10 minutes and in 100% CO_2 for 1 minute respectively. The reason for using pure CO_2 for the carbonations was to make sure that it happens at 800°C. The 20^{th} carbonation was allowed to happen for 20 minutes so that it can be compared with that of a full carbonation calcination reaction(FCCR) cycles.

Figure 6.5 shows the carbonations of nineteen PCCR cycles. One can observe the bumps in the temperature curve which correspond to each carbonation. It is almost certain that it is caused by the highly exothermic carbonation reaction. When it comes to the sorbent

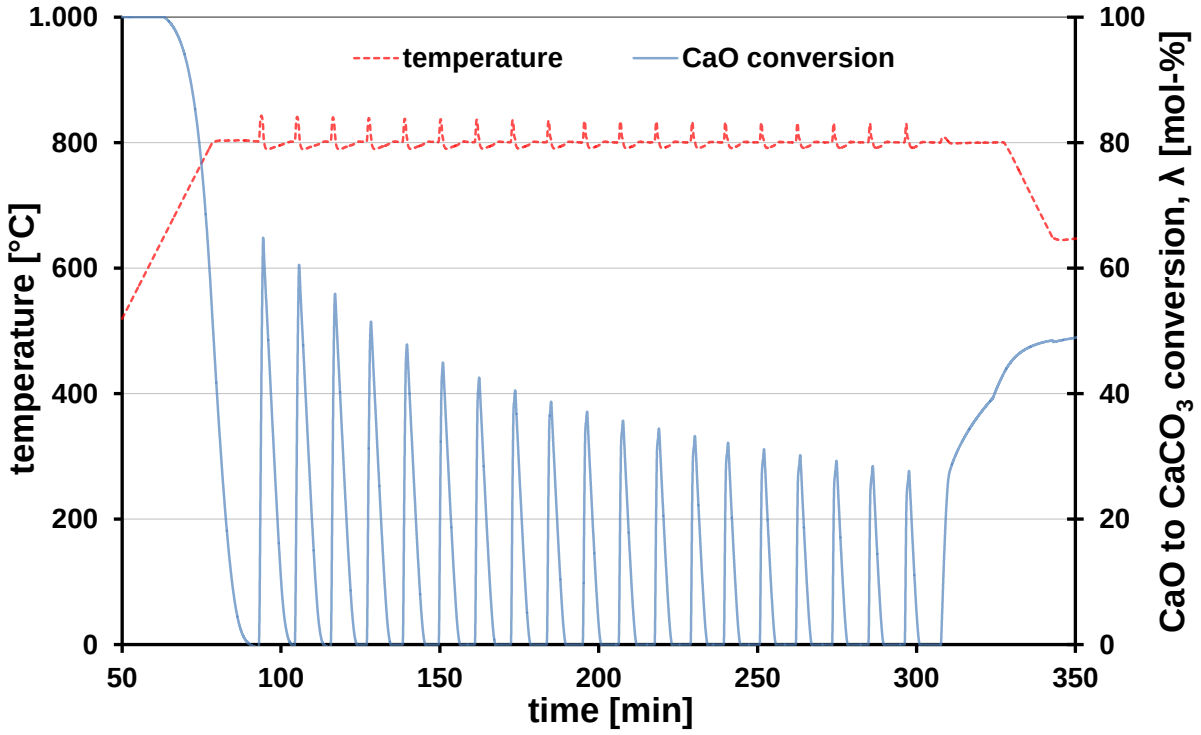

Figure 6.5: TGA curve of incomplete carbonation of limestone 1

decay pattern, it follows the same trend as of full carbonations with increasing CCR cycles. The CaO mol-% conversions of the PCCR's 1^{st} and 19^{th} cycles are 64.3 and 26.2 respectively. On the other hand, FCCR's CaO mol-% conversions of the same limestone for the 1^{st} and 19^{th} cycles were 67.4 and 22.4 respectively (full carbonation values obtained from the experiments described in section 4.2.1). It is clear that the PCCR's CaO mol-% conversion at the 19^{th} cycle is higher than that of FCCR. Moreover, the 20^{th} cycle conversion of the PCCR's full carbonation and that of the FCCR's are respectively 49.5 and 22.9. That means after 20 CCR cycles, the CO_2 capture potential of the partially carbonated sample was more than double the fully carbonated ones. So it seems that the partial carbonations helped to sustain the reactivity of the natural limestone. However the carbonation and calcination conditions of the full carbonation experiments were totally different, which could adversely affect the sorbent reactivity by inducing particle sintering, especially due to the calcinations at 900°C (it is much higher than the PCCR's 800°C). It is hard to draw a concrete conclusion on the effect of partial carbonations over the sorbent decay in a real CaL process conditions, only based on this set of experiments. More data with the same experimental conditions for the full and partial carbonations are required.

6.4 Conclusion

TGA experiments depicting CO_2 capture at reducing conditions were carried out for two limestone samples at 6 bar pressure. As one can expect that neither the reducing atmosphere nor the presence of H_2 and CH_4 had a negative influence on the reactivity of CO_2 and CaO. However, the temperature influenced the fast phase carbonation in such a way that the lower the temperature the higher is the conversion. Moreover, the higher the concentration of CO_2 the higher the conversion rate as observed in atmospheric pressure conditions. Limestone 1's reactivity with CCR number was better than the limestone 2 as the calculated decay coefficient(k) was smaller(0.21) for the former than the latter(0.28). Sintering intensified with increasing calcination temperatures. Specially between 900°C and 950°C a drastic drop in fast phase reactivity was observed where the sorbet lost more than 50% reactivity. It is desirable to operate the calciner at no more than 900°C in order to avoid a drastic loss in reactivity. Incomplete carbonations seemed to sustain the reactivity with increasing number of CCR cycles, since the CO_2 capture potential of the partially carbonated sample was more than the double of the fully carbonated sample after 20 CCR cycles.

Chapter 7

Summary and recommendations

This chapter summarises the conclusions drawn from this research work. Recommendations are given for further investigations and process development.

7.1 Summary

Commercial CO_2 separation technologies for fossil fueled power generation processes are energy intensive and incur heavy costs. In contrast, an emerging CaL scheme offers cost benefits by utilising cheap and abundant sorbents and separates the CO_2 from full and partial fuel oxidation based power generation processes. Since the separation technology is in the early developmental stage, research works are required in many aspects. This research work contributes to the development of the CaL process by exploring different approaches in process modeling, sorbent research and process parametric studies.

The fundamental aspects along with detailed descriptions of CaL process for full (post-combustion) and partial (pre-combustion) fuel oxidation based power generation processes are explained. A three reactor concept for pre-combustion with an entrained flow gasifier, carbonator cum water gas shift reactor and the calciner is modeled in ASPEN plus with hard coal feed. This pre-combustion CO_2 capture scheme shows net electricity and hydrogen production efficiencies of 12.6%(η_{El}) & 46.8%,(η_{H_2}) respectively. In case of CaL for post-combustion capture, the calculated electrical efficiency,(η_{El}) is 38.6%. According to the calculations, the efficiency penalty of the CaL process is between 6-7% points (when compared to an advanced coal power plant efficiency of 45%). Moreover, the efficiency penalties reported for CaL looping is 6-8%, MEA based process is 10-12%, oxy-fuel is 11-12% and the IGCC is 8-10%.

Major focus is given to the sorbent reactivity studies. A wide range of sorbent samples have been studied in a differential thermal analyser(DTA), a thermogravimetric analyser(TGA), a scanning electron microscope(SEM) and a specific surface area analyser to determine the CaO content, reactivity with CO_2, texture& pore structure and specific surface area. The unique data gathered on these specific set of limestone/dolomite samples would be useful in future designs of CaL processes. Sorbent reactivity plays a vital role in achieving high efficiencies in any CaL based CO_2 capture system. The effect on sorbent reactivity due to the following three parameters; geographical origin,

calcination temperature and number of calcination and carbonation reaction(CCR) cycles have experimentally been determined. It is revealed that all three parameters affect the sorbent reactivity. However, the number of CCR cycles and the calcination temperature become relevant for a given sorbent. If that sorbent is used for a particular number of CCR cycles, the only parameter that affects the reactivity is the calcination temperature. The higher the calcination temperature the higher is the rate of sorbent deactivation. Specific surface area measurements showed that the sample which is calcined at lower temperature(750°C) produced higher specific surface area than at higher calcination temperature(850°C). Moreover the scanning electron microscopic(SEM) images showed plenty of sharp edges on the surface of the sample calcined at 750°, that consolidated the specific surface area measurements. The specific surface area measurements and SEM analysis have revealed that the high calcination temperature reduces the specific surface area of CaO and thus decreases the carbonation conversion. A calciner design aims to reduce the sorbent deactivation is proposed in this thesis by lowering its operating temperature via steam injection. Operating temperatures above 900°C should be avoided to safeguard the reactivity of CaO.

A parametric study has been carried out at IFK's semi-pilot scale 10 kW_{th} DFB CaL test facility. A crucial parameter is the 'active space time(τ_{active})' which defines the CO_2 capture efficiency of a carbonator and is determined by analysing the sorbent samples collected at steady state operation. A TGA experimental procedure has been designed and applied for this parametric study. In a separate study, reactivities of spent samples from the IFK's DFB CaL test facility and corresponding fresh ones have been compared with respect to the number of CCR cycles, carbonation temperature and CO_2 concentration. DFB samples show very low CaO conversions($\sim$10%) which are no longer affected with increasing number of CCR cycles. Further on, a successful method has been found out to restore the lost CO_2 capture capacity of spent sorbents. The reactivation is performed by spraying distilled water over the samples. The resulting hydrated sample's reactivity is almost equal to a fresh one. A modified CaL scheme incorporating a unit for partial hydration is proposed to enhance the CO_2 capture efficiency. However, the morphological changes due to hydration are not taken into account.

The flue gas from a coal power plant contains small amounts(ppm level) of SO_2 which can react with calcium sorbents in a CaL process. Limestone samples have been analysed in a TGA at calciner and carbonator operating conditions for CO_2 capture in the presence of SO_2. Simultaneous carbonation and sulfation tests have been performed, depicting the carbonator operating conditions, to optimise the CO_2 capture in the presence of SO_2. A comparison of carbonation to sulfation ratio against the residence time provides a clear indication to minimise the adverse effect of sulfation in a CaL process for CO_2 separation. The lower the residence time the higher is the carbonation to sulfation ratio. Therefore short residence times(1-10 minutes) are favorable for the carbonation conversion over sulfation. Moreover, no significant sulfation rate differences are observed in sulfation-only

tests at carbonator and calciner operating temperatures of 650°C and 900°C. However the sulfation rate of once carbonated limestone(subjected to one cycle) is faster than the original limestone.

Pressurised TGA experiments in the context of CaL for partial oxidation processes have been carried out with synthetic syngas. As one can expect, neither the reducing atmosphere nor the presence of H_2 and CH_4 have a negative influence on the reactivity of CaO. However, the temperature influenced the fast phase carbonation in such a way that the lower the temperature the higher is the conversion. Moreover, the higher the concentration of CO_2 the higher the conversion rate is in atmospheric pressure conditions. TGA investigations on high temperature sintering, which tends to occur during the particle regeneration/calcination phase have been carried out. Sintering got intensified with increasing calcination temperatures. Specially between 900°C and 950°C which is the likely calciner operating temperature range, a drastic drop in fast phase reactivity is observed. The effect of incomplete carbonations on particle reactivity with CCR cycle number has also been studied separately. It is reveled that the partial carbonation helps to sustain the sorbent reactivity to some extend. After 20 CCR cycles, the CO_2 capture potential of the partially carbonated sample is more than the double of the fully carbonated sample. However this needs be further investigated with identical test conditions.

7.2 Recommendations

As a process in development, research is still required in many aspects from thermodynamic modeling to experimental studies. Process calculations of novel concepts integrating the CaL need to be explored. A three reactor gasifier concept has been modeled in this thesis and it shows a substantial efficiency potential in comparison to competing technologies. Further steam cycle optimisation studies are required with regard to this process concept.

The loss of reactivity with the CCR cycle number is to be studied further, probably by modifying (pretreating) the natural sorbents. Moreover, calcium sorbents can also be produced by chemical synthesis. There are only a few studies so far on this topic. It is the essence of the CaL process that it uses the natural sorbents, however it makes sense to explore various synthesis methods to economically produce sorbents that sustain reactivity for hundreds of CCR cycles.

Process parametric study with a circulating fluidised bed calciner and a bubbling fluidised bed carbonator have been carried out in a collaborative work with the Institut für Feuerungs- und Kraftwerkstechnik(IFK) in Stuttgart. In this context, a dual circulating fluidised bed reactor configuration is to be studied for process parameter optimisation. Sorbent circulation rate, sorbent split fraction between the carbonator and the calciner, sorbent particle attrition and the frictional losses are some of the important parameters to be investigated in this regard. Last but not least, in the near future, large scale demon-

strations of the CaL are necessary to rigorously prove the technology and to compete with other mature CO_2 capture technologies such as Amine scrubbing.

Bibliography

D. Aaron and C. Tsouris. Separation of CO_2 from flue gas : A review. *Separation Science and Technology*, 40:321–348, 2005. 4, 31

J.C. Abanades and D. Alvarey. Conversion limits in the reaction of CO_2 with lime. *Energy & Fuels*, 17:308–315, 2003. 7, 8

J.C. Abanades, E.S. Rubin, and E.J. Anthony. Sorbent cost and performance in CO_2 capture systems. *Ind. Eng. Chem. Res.*, 43:3462–3466, 2004. 8, 13, 60

J.C. Abanades, E.J. Anthony, J. Wang, and J.E. Oakey. Fluidized bed combustion systems integrating CO_2 capture with CaO. *Environmental Science & Technology*, 39:2861–2866, 2005. XI, 14, 23, 24

J.C. Abanades, G. Grasa, L. Alonso, N. Rodriguez, E.J. Anthony, and L.M. Romeo. Cost structure of a post-combustion CO_2 capture system using CaO. *Environmental Science & Technology*, 41:5523–5527, 2007. 8, 27

J.C. Abanades, M. Alonso, N. Rodrigues, B. Gonzalez, G. Grasa, and R. Murillo. Capturing CO_2 from combustion flue gases with a carbonation calcination loop; experimental results and process development. *Energy Procedia*, 1:1147–1154, 2009. 22, 27

M. Aihara, T. Nagai, J. Matsushita, Y. Negishi, and H. Ohya. Development of porous solid reactant for thermal energy storage and temperature upgrade using carbonation decarbonation reaction. *Applied Energy*, 69:225–238, 2001. 51

D. Alvarez and J.C. Abanades. Pore-size and shape effects on the recarbonation performance of calcium oxide submitted to repeated calcination recarbonation cycles. *Energy & Fuels*, 19:270–278, 2005a. 8

D. Alvarez and J.C. Abanades. Determination of the critical product layer thickness in the reaction of CaO with CO_2. *Ind. Eng. Chem. Res.*, 44:5608–5615, 2005b. 44, 70

D. Alvarez, M. Pena, and A.G. Borrego. Behavior of different calcium-based sorbents in a calcination/ carbonation cycle for CO_2 capture. *Energy & Fuels*, 21:1534–1542, 2007. 25

M. Anheden and G. Svedberg. Exergy analysis of chemical looping combustion systems. *Energ Conversion and Management*, 39:1967–1980, 1998. 5

E.H. Baker. The calcium oxide-carbon dioxide system in the pressure range 1-300 atmospheres. *Journal of the Chem. Soc.*, 70:464–470, 1962. 14

S.K. Bhatia and D.D. Perlmutter. Effect of product layer on the kinetics of the CO_2 - lime reaction. *AIChE Journal*, 29:79–86, 1983. 59

R.H. Borgwardt. Calcination kinetics and surface area of dispersed limestone particles. *A.I.C.H.E. Journal*, 31:104–111, 1985. 25

R.H. Borgwardt. Calcium oxide sintering in atmospheres containing water and carbon dioxide. *Ind. Eng. Chem. Res.*, 28:493–500, 1989. 25

B.J.P. Buhre, L.K. Elliott, C.D. Sheng, , R.P. Gupta, and T.F. Wall. Oxy-fuel combustion technology for coal-fired power generation. *Progress in Energy and Combustion Science*, 31:283–307, 2005. 5, 33

A. Charitos, C. Hawthorne, A.R. Bidwe, S. Sivalingam, A. Schuster, H. Spliethoff, and G. Scheffknecht. Parametric investigation of the calcium looping process for CO_2 capture in a 10 kW_{th} dual fluidized bed. *Int. J. of Greenhouse Gas Control*, 4:776 – 784, 2010a. 8, 12, 61, 62, 67

A. Charitos, C. Hawthorne, A.R. Bidwea, L. Korovesis, A. Schuster, and G. Scheffknecht. Hydrodynamic analysis of a 10 kW_{th} calcium looping dual fluidized bed for post-combustion CO_2 capture. *Power Technology*, 200:117–127, 2010b. 8

K. Damen, M.V. Troost, A. Faaij, and W. Turkenburg. A comparison of electricity and hydrogen production systems with CO_2 capture and storage. part a: Review and selection of promising conversion and capture technologies. *Progress in Energy and Combustion Science*, 32:215–246, 2006. 4

M. Davidson and S. Santos, editors. *Oxyfuel combustion of pulverised coal*. IEA Greenhouse Gas R&D Programme, 2010. 33

J. Davison. Performance and costs of power plants with capture and storage of CO_2. *Energy*, 32:1163 – 1176, 2007. 3, 8

L.S. Fan. *Chemical looping systems for fossil energy conversions*. John Wiley & sons Inc., 2010. 5, 19

P.H.M. Feron and C.A. Hendriks. CO_2 capture process principles and costs. *Oil & Gas Science and Technology*, 60:451–459, 2005. 4

N.H. Florin and P. Fennell. Review of advanced carbon capture technologies. Technical report, Work stream 2, Report 5A of the AVOID programme, Available online at www.avoid.uk.net, 2010. 14, 32

N.H. Florin and A.T. Harris. Review:Enhanced hydrogen production from biomass with in situ carbon dioxide capture using calcium oxide sorbents. *Chemical Engineering Science*, 63:287–316, 2008. 17

G. Grasa and J.C. Abanades. CO_2 capture capacity of CaO in long series of carbonation/calcination cycles. *Ind. Eng. Chem. Res.*, 45:8846–8851, 2006. 47, 68, 70, 74

G. Grasa, M. Alonso, and J.C. Abanades. Sulfation of CaO particles in a carbonation/calcination loop to capture CO_2. *Ind. Eng. Chem. Res.*, 47:1630–1635, 2008. 79

D. Gray, S. Salerno, and G. Tomlinson. Current and future igcc technologies: Bituminous coal to power. Technical report, Year Mitretek Systems, 2004. 34

H. Gupta and L.S. Fan. Carbonation-calcination cycle using high reactivity calcium oxide for carbon dioxide separation from flue gas. *Ind. Eng. Chem. Res.*, 41:4035–4042, 2002. 8, 13

C. Hawthorne, A. Charitos, C.A. Perez-Pulido, Z. Bing, and G. Scheffknecht. Design of a dual fluidized bed system for the post-combustion removal of CO_2 using CaO:Part I. CFB carbonator model. In *Proceedings of the 9th International Conference on Circulating Fluidized Beds, Hamburg, Germany.*, 2008. 60

C. Hawthorne, M. Trossmann, C.P. Galindo, A. Schuster, and G. Scheffknecht. Simulation of the carbonate looping power cycle. *Energy Procedia*, 1:1387–1394, 2009. 8, 27

H. Herzog. What future for carbon capture and sequestration? *Environmental Science & Technology*, 4:148A–153A, 2001. 2

H. Herzog. Scaling up carbon dioxide capture and storage: From megatons to gigatons. *Energy economics*, 33:597–604, 2011. 2

M.V. Iyer, H. Gupta, B.B. Sakadjian, and L.S. Fan. Multicyclic study on the simultaneous carbonation and sulfation of high-reactivity CaO. *Ind. Eng. Chem. Res.*, 43:3939–3947, 2004. IX, X, 79, 80, 81

C. Kunze, D. Sudipta, and H. Spliethoff. A novel IGCC plant with membrane oxygen separation and carbon capture by carbonation calcinations loop. *Int. J. of Greenhouse Gas Control*, 5:1176–1183, 2011. 36

Y. Li, S. Buchi, J.R. Grace, and C. Jim Lim. SO_2 removal and CO_2 capture by limestone resulting from calcination/sulfation/carbonation cycles. *Energy & Fuels*, 19:1927–1934, 2005. 79

S. Lin, M. Harada, Y. Suzuki, and H. Hatano. Hydrogen production from coal by separating carbon dioxide during gasification. *Fuel*, 81:2079–2085, 2002. 5

E. Martelli, T. Kreutz, and S. Consonni. Comparison of coal IGCC with and without CO_2 capture and storage: Shell gasification with standard vs. partial water quench. *Energy Procedia*, 1:607–614, 2009. 36

D Martinsen, J. Linssen, P. Markewitz, and S. Voegele. CCS: A future CO_2 mitigation option for Germany?-A bottom-up approach. *Energy Policy*, 35:2110–2120, 2007. 2

N.R. McGlashan. Chemical-looping combustion-a thermodynamic study. *J. Mechanical Engineering Science*, 222:1005–1018, 2008. 5

R. Notz, I. Toennies, N. McCann, G. Scheffknecht, and H. Hasse. CO_2 capture for fossil fuel-fired power plants. *Chemical Engineering Technology*, 34:163–172, 2011. 32

N. Nsakala, F. Kluger, G.N. Liljedahl, S. Suraniti, and R. Chamberland. Development of oxyfuel firing to enable CO_2 capture. In *32nd International Technical Conference on Coal Utilization & Fuel System, June 10-15, Clearwater, Florida, USA*, 2007. 33

F.G. Penea and P. Coca. Elcogas: R&D activities forwards zero emissions IGCC plants. Technical report, ELCOGAS S.A., 2009. 34

C. Pfeifer, B. Puchner, and H. Hofbauer. In-situ CO_2-absorption in a dual fluidized bed biomass steam gasifier to produce a hydrogen rich syngas. *International Journal of Chemical Reactor Engineering*, 5:A9, 2007. 4

A. Ponzio, S. Sivalingam, W. Yang, W. Blasiak, and O. Eriksson. Ignition of single coal particles in high-temperature oxidizers with various oxygen concentrations. *Fuel*, 87: 974 – 987, 2008. 33

A. Ponzio, S. Sivalingam, W. Yang, W. Blasiak, and O. Eriksson. Nitrogen release during thermochemical conversion of single coal pellets in highly preheated mixtures of oxygen and nitrogen. *Fuel*, 88:1127 – 1134, 2009. 33

M. Prins, R. Ploeg, R. Berg, C. Patil, E. Dorst, F. Geuzebroek, and D. Paul. Technology advances in IGCC with CCS. In *4th International Conference on Clean Coal Technologies, May 18-21, Dresden, Germany*, 2009. 36

R. Quadrelli and S. Peterson. The energy–climate challenge: Recent trends in CO_2 emissions from fuel combustion. *Energy Policy*, 35:5938–5952, 2007. 2, 3

R. Rhudy and S. Black. Chilled ammonia process update. In *10th International Network for CO_2 Capture, Lyon, France, 24-25 May*, 2007. 32

G. Scheffknecht, J. Maier, R. Berger, and Thorwarth. An overview on CO_2 capture technologies and current R&D activities at IVD. In *10th International Conference on Boiler Technology, Szczyrk, Orle Gniazdo, Poland., 17-20 October.*, 2006. 18

T. Shimizu, T. Hirama, H. Hosoda, K. Kitano, M. Inagaki, and K. Tejima. A twin fluid-bed reactor for removal of CO_2 from combustion processes. *Trans IChemE*, 77 Part A: 62–68, 1999. 7

S. Sivalingam, S. Gleis, H. Spliethoff, P. Yrjas, and M. Hupa. Cyclic carbonation calcination studies of limestone and dolomite for CO_2 separation from combustion flue gases. *Journal of Engineering for Gas Turbines and Power*, 131:0118011(8 pages), 2009. doi: 10.1115/1.2969090. 7, 12, 14, 58

S. Sivalingam, S. Gleis, and H. Spliethoff. Sorbent reactivity studies for CO_2 and SO_2 co-capture by calcium looping process. In *Proceedings of ASME Turbo Expo 2011*, Vancouver, Canada., 6-10 June 2011a. 12

S. Sivalingam, S. Gleis, H. Spliethoff, C. Hawthorne, A. Charitos, and G. Scheffknecht. Analysis and comparison of reactivity and CO_2 capture capacity of fresh calcium-based sorbents and samples from a lab-scale dual fluidized bed calcium looping facility. *Journal of Engineering for Gas Turbines and Power*, 133:071705(6 pages), 2011b. doi: 10.1115/1.4002683. 8, 12, 22

H. Spliethoff. *Power Generation from Solid Fuels*. Springer Verlag Berlin Heidelberg, 2010. VIII, 3, 31, 34, 35, 36

H. Spliethoff. Oxy-coal combustion for power generation. In *9^{th} European Conference on Industrial Furnaces and Boilers (INFUB-9), Estoril, Portugal.*, 2011. 3, 33, 34

P. Sun, J.R. Grace, C.J. Lim, and E.J. Anthony. Removal of CO_2 by calcium-based sorbents in the presence of SO_2. *Energy & Fuels*, 21:163–170, 2007. 79

P. Sun, J.R. Grace, C.J. Lim, and E.J. Anthony. Investigation of attempts to improve cyclic CO_2 capture by sorbent hydration and modification. *Ind. Eng. Chem. Res.*, 47: 2024–2032, 2008. 75

M.B. Toftegaard, J. Brix, P.A. Jensen, P. Glarborg, and A.D. Jensen. Oxy-fuel combustion of solid fuels. *Progress in Energy and Combustion Science*, 36:581–625, 2010. 3, 4, 5

T.F. Wall. Combustion process for carbon capture. *Proceedings of the Combustion Institute*, 31:31–47, 2007. 34

T.F. Wall, Y. Liua, C. Sperob, L. Elliott, S. Kharea, R. Rathnama, F. Zeenathala, B. Moghtaderia, B. Buhred, C. Shenge, R. Guptaf, T. Yamadac, K. Makinoc, and J. Yua. An overview on oxyfuel coal combustion -state of the art research and technology development. *Chemical engineering research and design*, 87:1003–1016, 2009. 5

J. Wang and E.J. Anthony. On the decay behavior of the CO_2 absorption capacity of CaO-based sorbents. *Ind. Eng. Chem. Res.*, 44:627–629, 2005. 48

T. Weimer, R. Berger, C. Hawthorne, and J.C. Abanades. Lime enhanced gasification of solid fuels: Examination of a process for simultaneous hydrogen production and CO_2 capture. *Fuel*, 87:1678–1686, 2008. 4, 18